ABSTRACT

Title of Dissertation: **Biomimetic Polymer Capsules: Novel Architecture and Properties**

So Hyun Ahn, Doctor of Philosophy, 2021

Directed By: Professor Srinivasa R. Raghavan,
Department of Chemical and Biomolecular Engineering

Professor William E. Bentley,
Fischell Department of Bioengineering

This study focuses on polymer capsules made from biocompatible, water-soluble polymers. Typically, the capsule core is a hydrogel in which proteins, nanoparticles, or biological cells can be encapsulated, while the capsule shell is permeable to small, but not large molecules. We explore two new designs or architectures for such capsules. One is a *multi-compartment capsule* (MCC) where a capsule has several distinct compartments inside it. A second design is a *multilayer capsule*, where concentric layers of different chemistries surround a core. These new designs mimic structures commonly found in nature such as a eukaryotic cell or an onion. Our goal is to exploit these novel capsule architectures to achieve new or improved properties.

In our first study, we introduce a new kind of multilayer capsule, wherein a protective shell of covalently crosslinked polymer (acrylate) surrounds a core formed by physical crosslinking (alginate). Alginate capsules are widely used for cell-encapsulation, but they are quite weak. We show that a covalent acrylate shell can be added to these capsules in a single step under mild conditions. The shell protects the core from degradation while allowing the encapsulated cells to remain viable and functional. A variation of the

synthesis technique yields capsules with two concentric shells (alginate, then acrylate) surrounding a liquid core.

Next, we create MCCs in which microbes from two different kingdoms, i.e., bacteria (*Pseudomonas aeruginosa*) and fungi (*Candida albicans*), are placed next to each other in distinct inner compartments. This MCC platform holds advantages over traditional co-culture as it eliminates physical contact between the two microbes and allows for real-time monitoring of cell growth in 3D. Using this platform, we study the effects of both physical variables (e.g., pH) as well as chemical additives (e.g., surfactants) on the growth of the two populations. We also detect crosstalk between the bacteria and fungi, i.e., as the bacteria grow, they inhibit the formation of hyphal filaments by the fungi, which make the fungi less invasive.

Lastly, we create MCCs with 'smart' inner compartments, which are sensitive to various stimuli. An analogy is drawn to different organelles in a cell, which have different constituents and unique functions. We select the chemistry or architecture of each inner compartment of the MCC such that their responses are distinct and orthogonal. For example, one compartment alone breaks apart when the MCC is contacted with an enzyme, while another gets degraded by the introduction of hydrogen peroxide (H_2O_2), and a third is disrupted by ultraviolet (UV) light. Another concept is shown where the degradation of one compartment induces the degradation of another. We believe these new designs will make the MCC platform more attractive for various biological applications.

BIOMIMETIC POLYMER CAPSULES: NOVEL ARCHITECTURE AND PROPERTIES

by

So Hyun Ahn

Dissertation submitted to the Faculty of the Graduate School of the
University of Maryland, College Park, in partial fulfillment
of the requirements for the degree of
Doctor of Philosophy
2021

Advisory Committee:

Professor Srinivasa R. Raghavan, University of Maryland, Co-Chair
Professor William E. Bentley, University of Maryland, Co-Chair
Professor Amy J. Karlsson, University of Maryland
Professor Taylor J. Woehl, University of Maryland
Professor Don L. DeVoe, University of Maryland, Dean's Representative

Acknowledgements

I would first like to express my sincere appreciation to Dr. Raghavan and Dr. Bentley for their guidance, mentorship, and unwavering support throughout my doctoral study. Had it not for the faith my advisors placed in me, I would not have succeeded in completing the new chapter of my life as a graduate student. Your knowledge, wisdom and stimulating discussion have been the most valuable tools for my research. You always encouraged me to think outside the box and push my abilities to the limit. I will keep all the lessons I learned from you as I move forward.

I would like to thank my committee members, Professor Don DeVoe, Professor Taylor Woehl and Professor Amy Karlsson for serving on my committee and providing insightful comments. It was a pleasure to have a chance to work with Amy and her students and I truly appreciate her advice and generosity for offering me resources form her lab.

Many thanks go to all my colleagues and friends whom I had a pleasure to work with from both groups. Niti Agrawal, Nikhil Subraveti, Hema Choudhary, Leah Borden, Medha Rath, Eric VanArsdale, Sally Wang, Chen-Yu Chen, Chen-Yu Tsao, Dana Motabar, and Jinyang Li. Thank you so much for all your constructive advice, help and friendship. Support from everyone one of you has been invaluable part of my time here and I will always cherish all the fun memories I had with you.

Last but not least, I would like to acknowledge the most important people in my life, my amazing family, for all their support and love throughout this process. Thank you all for always being there for me and waiting for me to get on my feet again when I fell. I could not have asked for a better family and would not have made it here without you. I am especially thankful for my parents, Chul Young An and Kyung Suk Kim, for their boundless love and encouragement. You are the best mom and dad I could have asked for.

Table of Contents

List of Figures

List of Abbreviations

AAm	Acrylamide
PEGDA	Polyethylene(glycol) diacrylate
BIS	Methylenebis(acrylamide)
TEMED	N,N,N',N'-Tetramethylethylenediamine
APS	Ammonium persulfate
DI	deionized
LB	Luria broth
PBS	Phosphate buffered Saline
EDTA	Ethylenediaminetetraacetic acid
PEG	Polyethylene glycol
IPTG	Isopropyl β-D-1-thiogalactopyranoside
MCC	Multi-compartment capsules
FITC	Fluorescein Isothiocyanate
EDC	1-ethyl-3-(3-dimethyl-aminopropyl) carbodiimide
NHS	N-Hydroxy succinimide
LAP	lithium phenyl-2,4,6-trimethyl-benzoylphosphinate
UV	Ultraviolet
OD	Optical density
DMEM	Dulbecco's modified eagle medium
FBS	Fetal bovine serum

YPD	Yeast peptone dextrose
AI-1	Autoinducer-1
QS	Quorum sensing
CTAB	Cetyltrimethylammonium romide
CB-NPs	Carbon black nanoparticles
IO-NPs	Iron oxide nanoparticles
GF-NPs	Green fluorescent nanoparticles
GOx	Glucose oxidase
SLac	Sodium lactate

Chapter 1
Introduction and Overview

1.1 Problem Description and Motivation

Throughout history, humans have looked to nature to discover solutions to new challenges. Even today, interesting phenomena and structures in nature are under scrutiny by scientists in attempts to improve existing products or make new inventions.[1] The act of mimicking pre-existing systems in nature to create new synthetic structures with novel design or properties has been termed "biomimetics".[2] One natural structure that has inspired researchers is the cell itself. In its simplest form, the cell is a container in which all the ingredients for life are present, including proteins, DNA, RNA, and lipids.[3] The sizes of cells range from around 1 μm for prokaryotic cells to between 5 and 100 μm for eukaryotic cells, including human cells. The core of the cell is the cytoplasm, which has a gel-like nature due to its being a network of the cytoskeletal filaments.[4] This gel is enveloped by the cell membrane, made from lipids and proteins.[3]

In attempting to mimic a primitive cell, the construct that comes to mind is a *capsule*, as shown in Figure 1.1A. Here, the capsule is depicted as a spherical container, with a distinct core enclosed by a shell. The core can be formed by polymer chains, and if these chains were connected into a network, the core would have gel-like character, similar to the cytoplasm. The shell could be formed by a different polymer, or it could be made from lipids, similar to a cell membrane. Alternatively, the shell and core could be formed

from the same polymer, but could differ in some way: e.g., the shell could be stiffer or denser compared to the core.

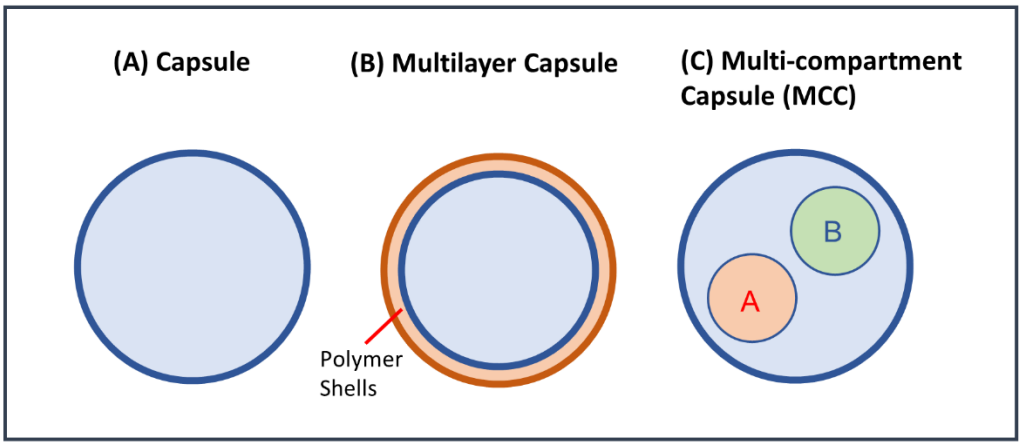

Figure 1.1 Schematics of polymer capsules with different architectures. (A) The simplest capsule with a core surrounded by a single, thin shell; (B) A *multilayer* capsule (onion-like) with multiple concentric shells; (C) A *multi-compartment* capsule (MCC) with distinct inner compartments.

Recently, many researchers have recognized that the simplest design for a capsule (Figure 1.1A) does not have the right architecture compared to natural counterparts.[4,5] For example, various structures in nature exhibit a capsule-like (core-shell) architecture, but often have *multiple* concentric layers. Examples include fruits and vegetables like the onion, eggs and embryos, as well as seeds. Thus, one enhancement to the simple capsule is to introduce multiple concentric layers, and such a *multilayer capsule* is depicted in Figure 1.1B. Each layer could be made from different materials or could encapsulate distinct molecules or particles.[6-20] Another key aspect is compartmentalization.[4,5] In this regard, the eukaryotic cell provides the inspiration because it is a container with many smaller containers (compartments, i.e., organelles) within it. Thus, another way to enhance capsules is to create multiple inner compartments, each with a different payload.[21-31] Such

a *multi-compartment capsule* (MCC) is shown in Figure 1.1C. Because MCCs resemble eukaryotic cells, these structures are also termed 'artificial cells' or 'protocells' in the literature.[13,14,24,32]

1.2 Proposed Approach

In this dissertation, we explore the novel capsule designs shown in Figures 1.1B and 1.1C in the context of biological applications. Thereby, this research attempts to bridge approaches from the Raghavan and Bentley labs. Our labs have previously reported simple, yet versatile routes to make both MCCs[23] and multilayer capsules.[33] We have adapted these routes to make capsules with novel attributes (either in their architecture or in their properties or functions). Three such capsules are reported here:

1.2.1 Capsules with a Physical Core and a Covalent Shell

In Chapter 3, we introduce a new method for synthesizing capsules with two or three concentric layers. Importantly, the entire (microscale) capsule is synthesized in a single step using a microfluidic device. In the 2-layer capsule (Figure 1.2A), the core is a gel of the biopolymer alginate that is physically crosslinked with multivalent cations. The shell is a thin layer of covalently crosslinked acrylate, which is polymerized around the alginate gel by either heat or ultraviolet (UV) light. In the 3-layer capsule (Figure 1.2B), the core is just water, and this is covered by a shell of alginate, followed by an outer shell of acrylate. In both cases, the outer acrylate shell is very stable and protects the capsule from degradation. Our synthesis method is gentle enough to allow encapsulation of both

bacteria and mammalian cells in the above capsules. The cells remain viable and proliferate in the capsules while the covalent shell provides mechanical and chemical stability.

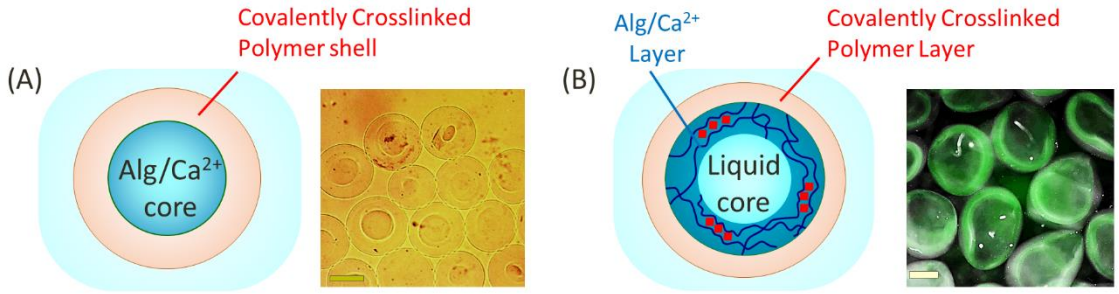

Figure 1.2. Multilayer microcapsules synthesized in Chapter 3. (A) 2-layer capsules with an alginate-gel core (physically crosslinked by multivalent cations) and a gelled shell of covalently-crosslinked acrylate derivative. (B) 3-layer capsules with a liquid core, a shell of alginate gel, and then a shell of acrylate gel. (Scale bars: 200 μm)

1.2.2 MCCs with Fungi and Bacteria in Separate Compartments

Our method to synthesize MCCs allows for encapsulation of different payloads in each compartment. In Chapter 4, we encapsulate microbes from different kingdoms (fungi and bacteria) in compartments within an MCC. This MCC platform offers advantages over traditional co-culture as it keeps the two sets of microbes separate and allows for real-time monitoring of cell growth in 3D. Using this platform, we study the effects of different external stresses on cell growth. Also, the microbes in the two adjacent compartments can still communicate with each other through small molecules, which can pass through the shells of the compartments. In this regard, we find in one case that, as bacteria grow, they secrete molecules that inhibit the formation of hyphal filaments by the fungi, which make the fungi less invasive.

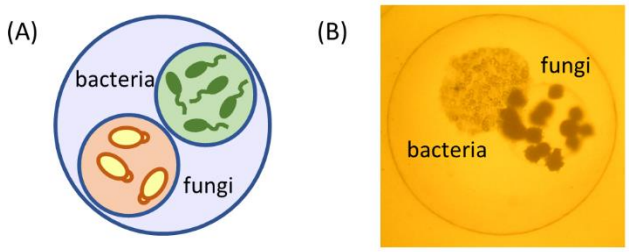

Figure 1.3. Multi-compartment capsules (MCCs) with fungi and bacteria in separate compartments (Chapter 4). A schematic (A) and micrograph (B) of such an MCC are shown. This construct allows us to study the comparative growth of the cells and their interaction in real time.

1.2.3 MCCs with 'Smart' Compartments that Respond to Various Stimuli

The same MCC construct is also used in Chapter 5 to create MCCs with 'smart' inner compartments, which are sensitive to various stimuli. In a cell, there are organelles with different constituents, which in turn dictate their specific functions. For example, in lysosomes the environment is acidic while in peroxisomes the environment is oxidative. Similarly, for our smart compartments, we select different chemistry or architecture for each of them such that their responses are distinct and orthogonal. As shown schematically in Figure 1.4, only Compartment A breaks apart when the MCC is contacted with Stimulus 1 (e.g., an enzyme), while only Compartment B gets degraded by Stimulus 2 (e.g., ultraviolet light, or hydrogen peroxide). Another concept is shown in this Chapter where the degradation of one compartment thereafter triggers the degradation of another in a cascade process. We believe these new designs will make the MCC platform more attractive and suitable for various biological or cell-mimicking applications.

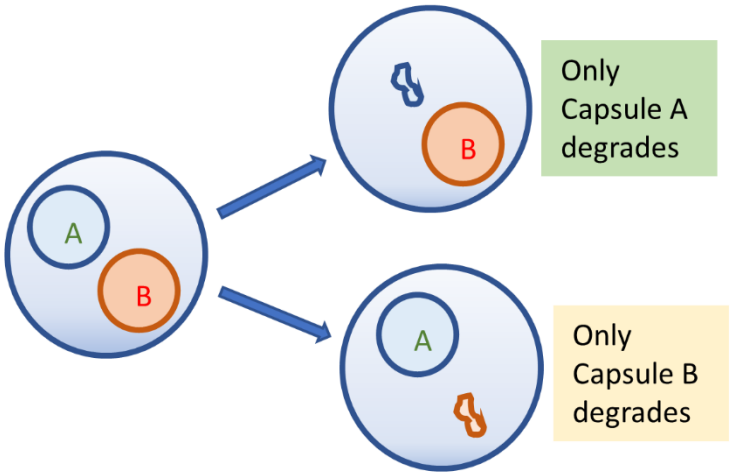

Figure 1.4. Multi-compartment capsules (MCCs) with 'smart' compartments, described in Chapter 5. Compartments A and B have distinct features, which make them sensitive to different stimuli. As shown by the schematic, when Stimulus 1 (e.g., an enzyme, or reductant, or light) is applied, only compartment A is degraded. Conversely, when Stimulus 2 is applied, only compartment B is degraded. Thus, the compartments exhibit orthogonal responses to the stimuli.

1.3 Significance of This Work

The capsules presented in this dissertation hold significance in many aspects, both fundamental and application-oriented. Broadly, we are advancing the use of capsules in biological and biomedical contexts. Notably, all our capsules are constructed using biocompatible materials under mild, aqueous conditions. Thus, our systems are compatible with cells of different kinds as well as with all kinds of biomolecules. With regard to the specific studies in Chapters 3-5:

- The multilayer capsules from Chapter 3 could be a useful platform for cell encapsulation. While conventional alginate capsules degrade easily, the presence of a covalent shell prevents degradation and thereby protects encapsulated cells. Stable

capsules with cells could also be used for oral delivery of probiotic bacteria to the gut, and they could also serve as sentinels to monitor the health of the gut.

- Next, the MCCs from Chapter 4 could be used for understanding the interactions between microbes of different kingdoms. Such studies could enhance our understanding of pathogenic microbes and suggest ways to mitigate their pathogenicity. The MCC platform could also be used for drug-discovery, e.g., in identifying drugs that kill one type of microbe while sparing others.

- Lastly, the MCCs with 'smart' compartments from Chapter 5 could serve as a toolbox for exploring studies with artificial cells/protocells. The ability to selectively degrade one compartment ('organelle') on-demand is crucial to facilitating such studies. These MCCs with responsive capabilities could also find use in controlled release or drug-delivery.

Chapter 2

Background

2.1 Alginate and its Capsules/Gels

Sodium alginate is an anionic polysaccharide derived from brown algae.[34] It is a copolymer composed of (1,4)-linked β-D mannuronic (M) and α-L guluronic (G) residues. The residues occur in blocks and the ratio of M to G blocks varies depending on the source of alginate.[35,36] Alginate forms gels when a solution of the polymer is combined with a solution of multivalent cations such as those of calcium (Ca^{2+}), barium (Ba^{2+}), copper (Cu^{2+}), aluminum (Al^{3+}) or iron (Fe^{3+}).[34,37] The gels arise when the cations bind with the carboxylate groups in the G blocks on adjacent alginate chains to form "egg-box junctions" (Figure 2.1), thereby crosslinking the chains into a sample-spanning 3-D network. Hydrogels exhibit solid-like mechanical properties, and the gel stiffness increases with cation and alginate concentrations, and it is also higher in alginates with a higher G:M ratio.[34,37]

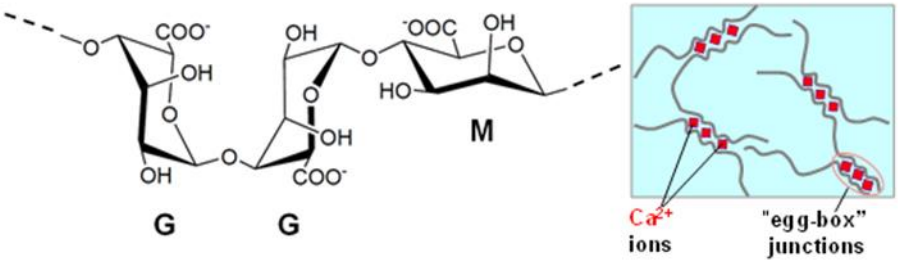

Figure 2.1. Structure of alginate and its gels. The alginate molecule (left) has G and M blocks randomly arranged along the chain. The G blocks form "egg-box" junctions with multivalent ions such as calcium, which crosslink the chains into a 3D network. Images adapted from Reference 38.

Gelation of alginate can also be accomplished in droplet form, i.e., by dropping a solution of alginate into a solution of cations like Ca^{2+}. If the gelation is uniform throughout the droplet, it is converted into a solid gel, which is also called a bead or gel-bead. More typically, gelation of the droplet is non-uniform, with the outer shell being more crosslinked than the inner core. In that case, the final structure is termed a 'capsule', and we will use the latter term as it is more general. Gels and capsules of alginate can also be formed by dropping the alginate solution into a solution of a positively charged biopolymer such as chitosan.[38] In that case, electrostatic complexation occurs at the surface of the droplet between the two polymer chains, which leads to a gelled shell surrounding a liquid core. It is worth noting that in both alginate-cation and alginate-chitosan capsules, the crosslinks or bonds involved are weak, physical ones. Capsules are widely used in the pharmaceutical, agricultural, and food industries as containers to store and/or release encapsulated moieties.[39-49]

Alginate is used extensively in biomaterials, drug delivery and cell-encapsulation studies due to its biocompatibility, abundance, low cost, and its ease of crosslinking.[34,37] In particular, biological payloads (i.e., various types of cells as well as biomolecules like proteins and DNA) can be easily encapsulated in alginate gels and capsules. For this, one simply needs to mix the material to be encapsulated in an alginate solution and add this dropwise into a reservoir containing the cation of choice.[34,36] The cells or biomolecules will then be entrapped in the 3D network of alginate chains. The mesh or pore size of such a network will be ~ 5 nm, and so while the network can entrap proteins (which have sizes ~ 5 nm or larger), it cannot entrap small molecules like drugs or salt ions. This is beneficial

for cell culture because it ensures that cells can exchange oxygen, nutrients, and waste with the external medium.[35,36,50,51] The hydrogel matrix also mimics the extracellular matrix that exists around cells in biological tissues. Many types of cells, both mammalian as well as microbial, have been encapsulated in polymer capsules.[39-46,52-57]

The physical bonds involved in forming alginate capsules (and gels) can be reversed in many ways. Focusing on alginate-Ca^{2+} systems, the divalent cations can be extracted from their egg-box junctions by molecules present in the external solution, including simple monovalent ions (e.g., Na^{+}) present in buffers.[58-60] Ca^{2+} can also be removed by chelating agents such as ethylene diamine tetracetic acid (EDTA) or sodium citrate.[34,58] Another way to degrade alginate capsules is by the use of an enzyme called alginate lyase,[61-63] which cuts alginate chains into oligomers through β-elimination of the glycosidic linkage.[61] Several studies have reported release of encapsulated cells from alginate capsules by the action of alginate lyase.[48,49,64,65] An example in this regard is shown in Figure 2.2A.

Degradation of alginate capsules crosslinked with Fe^{3+} can also be done in a different way. It is known that Fe^{3+} can be reduced to Fe^{2+} by various agents.[66-71] The carboxylates on alginate chains have a weaker affinity for Fe^{2+}. Therefore, the reduction of Fe^{3+} will weaken the alginate network, and the gel or capsule can get degraded.[67,69] In a related manner, the reduction of Fe^{3+} to Fe^{2+} has also been reported to be induced by irradiation with ultraviolet (UV) light, as shown in Figure 2.2B.[67,69,71] Furthermore,

reducing agents such as hydrogen peroxide and ascorbic acid can also have an effect on alginate gels and capsules, depending on the crosslinking cation used.[66,70]

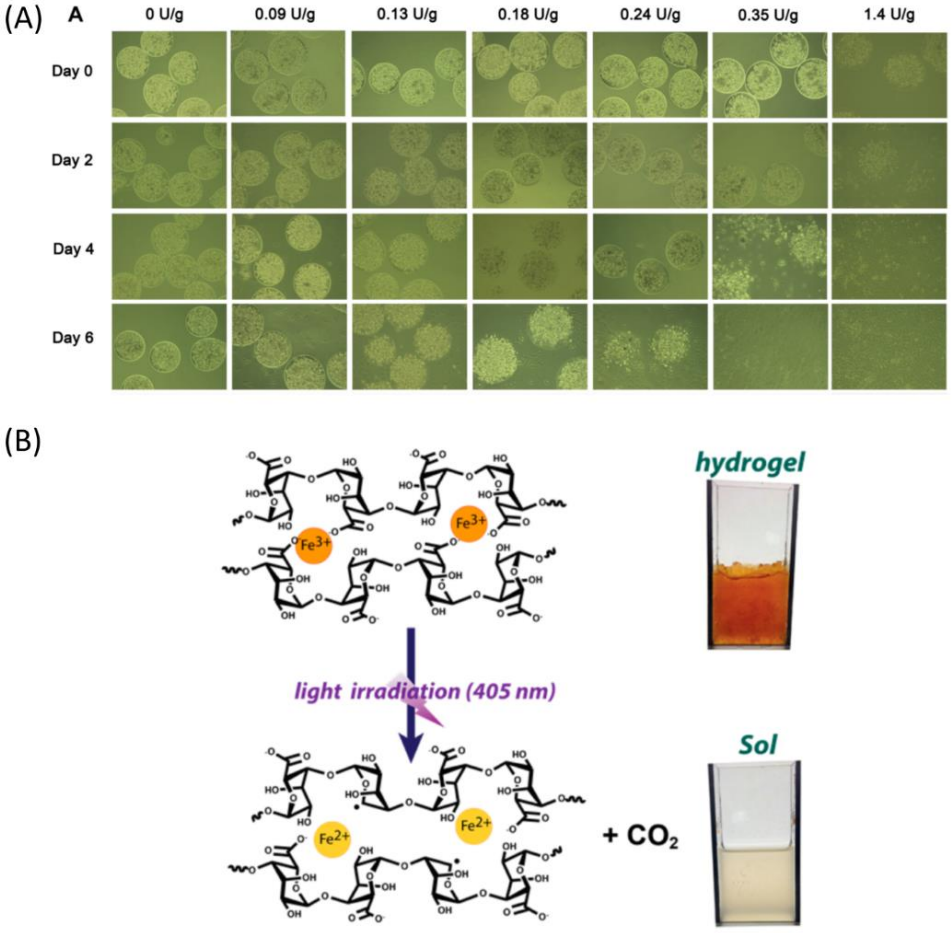

Figure 2.2 Different methods to degrade alginate gels or capsules. (A) Enzymatic degradation using alginate lyase. The figure shows that adipose derived stem cells encapsulated in alginate capsules degrade upon exposure to enzyme lyase thereby releasing adipose stem cells from the gel. (B) Alginate crosslinked by Fe^{3+} ions can be degraded by light-assisted reduction of the ions. Alginate crosslinked with Fe^{3+} ions is degraded and turn to a solution upon exposure to light at 405 nm due to reduction of the crosslinking ion. Images adapted from References 49 and 72.

2.2 Capsules with Multiple Layers

Capsules with multiple polymer layers (see Chapter 1) present advantages over single-layered polymer capsules – the multiple layers bring in different functionalities in terms of mechanical behavior, permeability, and responses to different stimuli.[6,7] In the 1990s, a technique for depositing multilayered films onto a solid surface was introduced using oppositely charged polyelectrolytes and it is now referred to as the layer-by-layer (LbL) technique.[72] This technique has also been used to make multilayer capsules by various researchers.[16-18,20,26] However, LbL is cumbersome and takes a long time; moreover, each layer is only a few nanometers thick. Multilayer microcapsules with better control of layer thickness and properties have been synthesized by other techniques including emulsification, electro-spraying and multiphase microfluidics.[8-11]

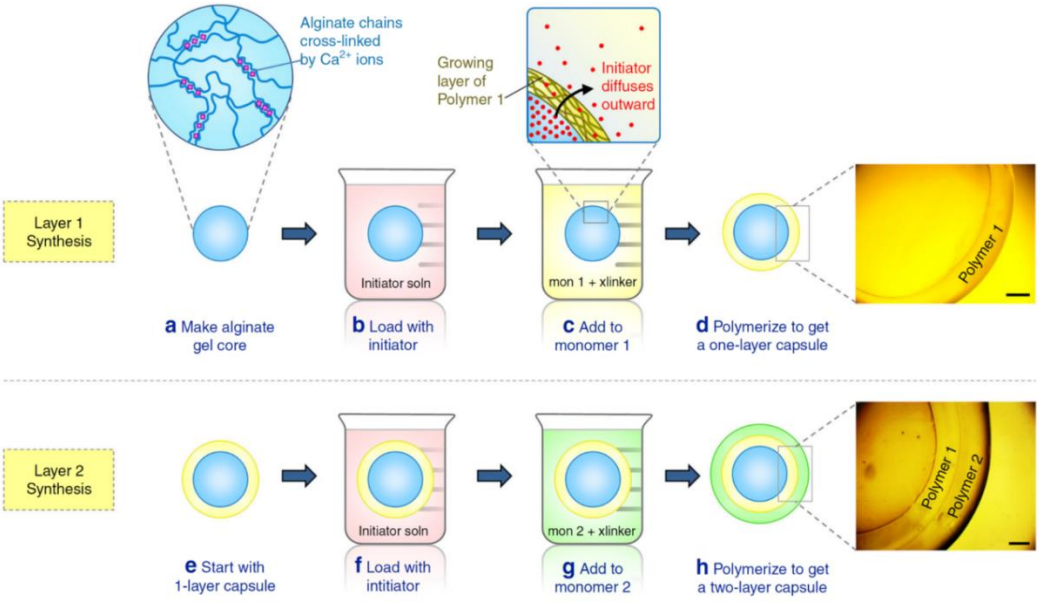

Figure 2.3 Synthesis of multilayer capsules using an inside-out method. An alginate core is loaded with initiator and transferred to a monomer solution to initiate free-radical polymerization. This creates a Layer 1 of Polymer 1 (top). The step is repeated to form a Layer 2 of Polymer 2 (bottom). (Scale bars: 500 μm.) Images adapted from Reference 34.

Our lab has recently has developed a technique where a shell of covalently crosslinked polymer can be formed around a core of physically crosslinked alginate.[33] This technique is shown in Figure 2.2 and will be used in Chapters 3 and 5. An alginate core is first loaded with initiator and then transferred to a solution containing monomer, crosslinker and accelerant. As the initiator diffuses out from the core, free-radical polymerization occurs which results in formation of a thin polymer layer around the core. These steps can be repeated multiple times to create additional layers around the core, which can be of the same or different polymers. The technique is called 'inside-out polymerization' because each layer grows outward from the surface.

2.3 Capsules with Multiple Inner Compartments

A eukaryotic cell contains organelles, each of which is bound by a membrane. Inspired by this architecture, many researchers have attempted to create 'artificial cells' or 'protocells', which have a similar multi-compartment structure with multiple small compartments ('organelles') within an overall capsule.[12-15,24,25,32,73] Towards this end, in our labs, we have developed multi-compartment capsules (MCCs) based on biopolymers like alginate.[23] The inner compartments are alginate microcapsules, formed in a microfluidic device (see further details below) by contacting alginate with a reservoir of Ca^{2+} ions and chitosan. To synthesize MCCs, preformed microcapsules are then resuspended in alginate solution, fed through a larger capillary, and dropped into the same reservoir solution (Figure 2.4a). A population of MCCs is formed, where one or more inner compartments are contained within a larger capsule. The number of inner compartments can be varied from 0 to 1 to 2 to more by varying the number density of microcapsules in

the alginate feed (Figure 2.4b). Different payloads such as bacteria, nanoparticles, or proteins, can be encapsulated in each of the inner compartments (Figure 2.4c). This technique to form MCCs will be utilized in Chapters 4 and 5.

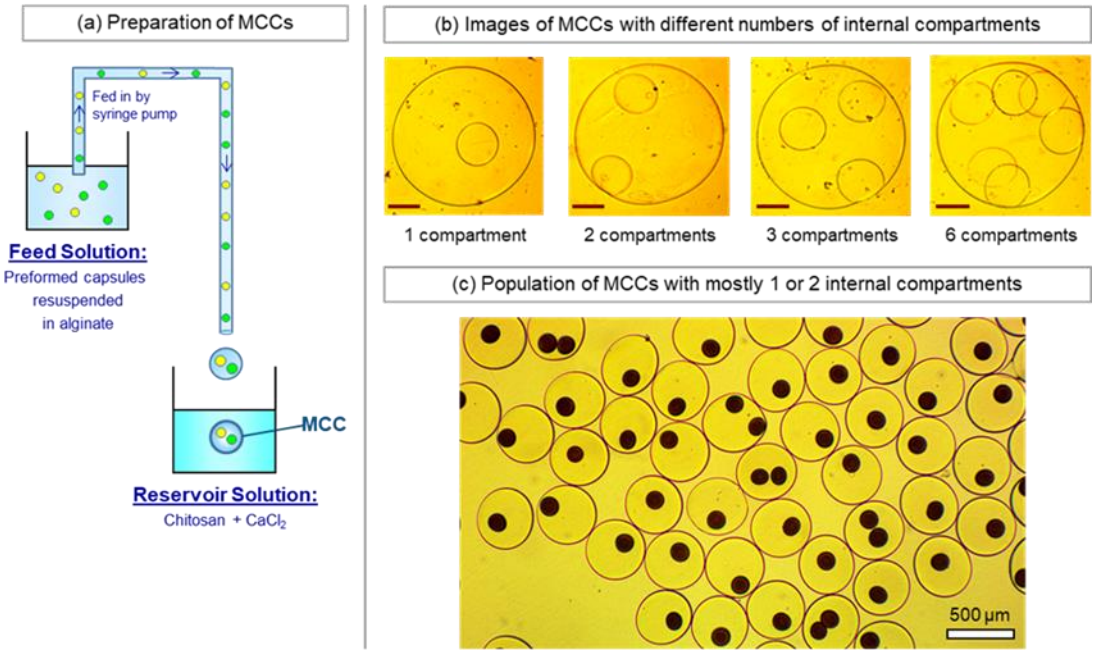

Figure 2.4 Synthesis of multi-compartment capsules (MCCs). (a) A suspension of preformed capsules in alginate solution is fed through a glass capillary. Gas pulses shear off droplets from the tip of the capillary, and the droplets enter a reservoir solution containing chitosan and Ca^{2+}. This results in MCCs. (b) Optical micrographs of individual MCCs with different numbers of inner compartments. (c) Optical micrographs of MCCs having either one or two inner compartments that contain magnetic Fe_3O_4 nanoparticles. Images adapted from Reference 23.

2.4 Capsule Synthesis by Microfluidics

Microfluidics refers to the control and manipulation of small volumes of fluids (from nano to pico liters), typically within channels whose dimensions are on the order of 10 to 100 μm.[74] Droplet microfluidics is a category of microfluidics involving generation of discrete droplets with controlled volume and composition.[75-77] Typically, in droplet microfluidics, monodisperse aqueous droplets are generated by the use of two phases: the dispersed aqueous phase and another immiscible liquid (i.e., an oil) as the continuous phase.[78,79] The oil phase either flows around the aqueous flow (this is termed flow-focusing) or in a perpendicular direction (i.e., at a T-junction), with the net result being the generation of aqueous droplets in a continuous oil phase. Droplet sizes are typically around 100 to 500 μm and their size is controlled by the flow rates of the two phases.

Once the droplets are formed within microchannels, they can be converted into solid capsules or beads by collecting the droplets in a reservoir that contains crosslinkers.[78] Crosslinking can also be done *in situ* by using UV light as the droplets are flowing through a microchannel.[78] Droplet microfluidics using water and oil phases can be used for creating capsules with cells: in that case, the cells are suspended in the aqueous phase, which is then converted to droplets and then to capsules. However, the collected capsules have to be washed extensively to remove all traces oil before further use.[9,57] Such washing steps can be time consuming and damaging to the encapsulated cells.

To avoid the issues noted above, our labs have devised a microfluidic system that uses only water and gas and completely avoids the use of an oil phase.[23] This water/gas

system has been used to make regular capsules as well as MCCs. The typical setup uses alginate as the polymer, which is mixed with payloads and fed through a glass capillary using a syringe pump (Figure 2.5A). At the tip of the capillary, droplets are sheared off by pulses of gas (air or nitrogen), with the pulse rate controlled by a function generator. The droplets then enter a reservoir solution (that contains Ca^{2+} and/or chitosan), where they are converted to capsules. Control of droplet and thereby capsule size is done through two parameters: flow rate of the feed solution and the frequency of the gas pulses. At higher frequencies and lower flow rates, smaller capsules are generated, as shown in Figure 5.2B. The micrographs of the generated capsules (Figure 5.2C) show that they are quite monodisperse with < 3% polydispersity. Most importantly, this is a simple yet gentle technique that is highly conducive for the encapsulation of biological cells in the capsules.

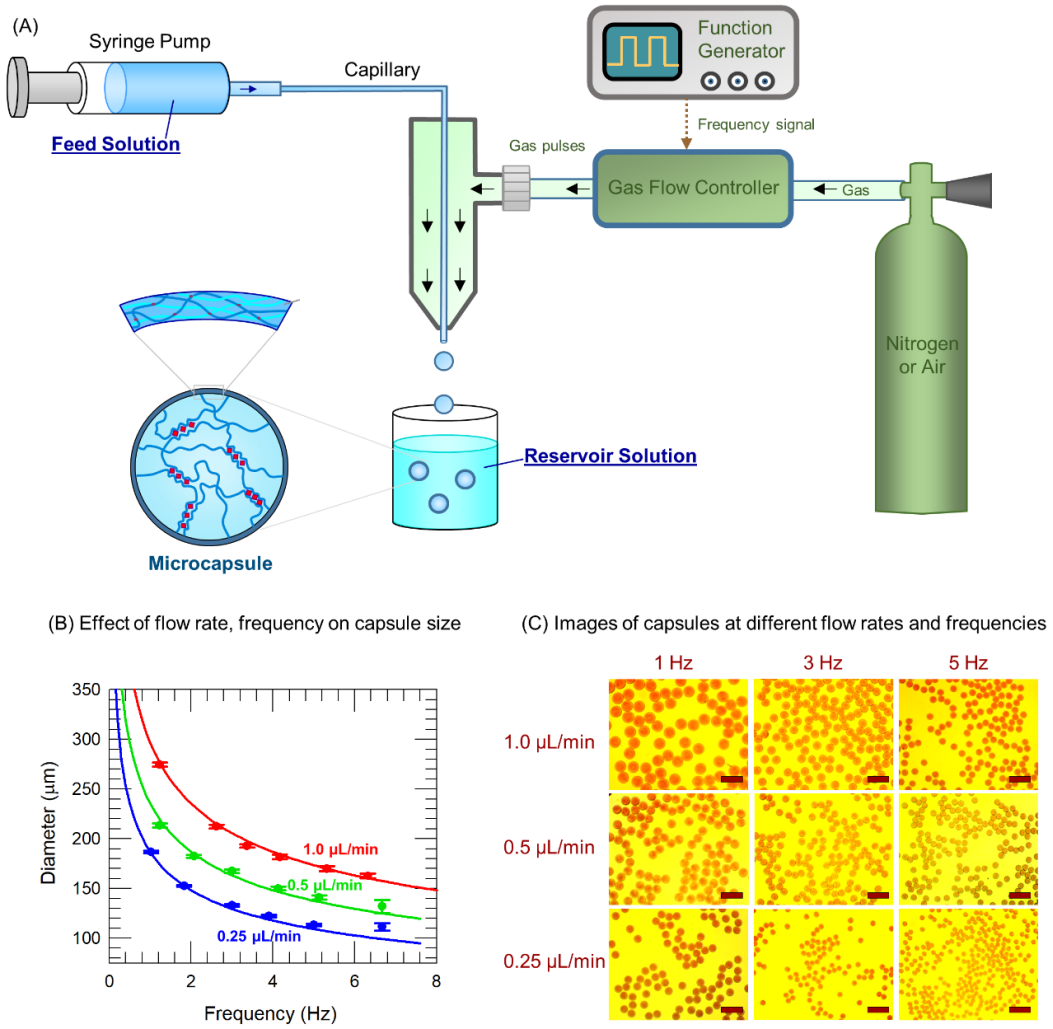

Figure 2.5. Synthesis of microcapsules by a water–gas microfluidic technique. (A) A schematic of the set-up. A feed solution containing polymers is sent through a capillary and droplets are sheared off at the tip by pulses of gas (nitrogen or air). The frequency of the pulses is controlled by the function generator. The droplets then enter the reservoir solution containing crosslinking agents (other polymers or multivalent ions), whereupon the droplets and converted into microcapsules. (B) A plot of capsule diameter vs. pulse frequency at three flow rates. (C) Optical micrographs of typical capsules generated at different flow rates and frequencies. Scale bars in the images are 500 μm. Images adapted from Reference 23.

Chapter 3

Multilayer Capsules with a Covalent Outer Shell

The results presented in this chapter have been published in the following journal article: S. H. Ahn, M. Rath, C.-Y. Tsao, W. E. Bentley and S. R. Raghavan, "Single-step synthesis of alginate microgels enveloped with a covalent polymeric shell: A simple way to protect encapsulated cells." *ACS Applied Materials & Interfaces*, 13, 18432-18442 (**2021**).

3.1 Introduction

Cell encapsulation refers to the entrapment of live cells in polymeric scaffolds, with conditions tailored to ensure that the cells remain viable and functional.[35,36,50,51] This technique has found increasing application across various fields, particularly in tissue engineering.[50,51] For cell encapsulation to be successful, both the type of polymer as well as the physical properties of the final scaffold are important. Typically, the polymers form a hydrogel, i.e., a three-dimensional (3-D) network of cross-linked chains, with the cells entrapped in this network.[35,36,50,51] Hydrogels exhibit solid-like mechanical properties, which are important for keeping the cells protected and immobilized, while the large water content and porous nature of the gel network ensures that cells can exchange oxygen, nutrients and waste with the external medium. It is important for cell encapsulation in gels to be performed under mild, physiological conditions to ensure cell survival. The polymer backbone must also be nontoxic and compatible with the cells. The above requirements are commonly met by naturally derived biopolymers such as polysaccharides (e.g. alginate, chitosan, agar, hyaluronic acid) or proteins (e.g. gelatin or collagen).[36,51] Gels of the above biopolymers have been used to encapsulate various mammalian cell types such as pancreatic islets,[42] hepatocytes,[41] osteoblasts,[44] Jurkat cells,[45] and stem cells.[39] Gels have

also been used to encapsulate microbial cells such as yeast or bacteria for soil fertilization,[40] removal of urea and ammonia,[43] or the delivery of probiotics to the gut.[46]

Among the polymers mentioned above, the one that is most widely used for cell encapsulation is alginate due to its abundance, low cost, biocompatibility, and non-immunogenicity.[34,37] Alginate is an anionic polysaccharide derived from brown algae. It forms gels when combined with divalent cations such as calcium (Ca^{2+}) under mild conditions at physiological pH.[34,37] The gels arise because the Ca^{2+} cations bind with the carboxylate anions on adjacent alginate chains, thereby cross-linking the chains into a sample-spanning 3-D network.[34] To encapsulate cells in such a gel, one simply has to suspend the cells in an alginate solution and add this dropwise into a reservoir containing Ca^{2+}. The cell-bearing droplets then become converted into gels, and the sizes of these gels can be controlled by modulating the droplet size. Microscale gels (10 to 1000 μm), termed microgels or microbeads, are commonly used in applications.

Despite the many advantages of alginate for cell encapsulation, however, one major drawback is that alginate gels tend to degrade easily, i.e., they are chemically and mechanically weak.[58-60] For example, when these gels are stored in a buffer containing univalent cations such as sodium (Na^{+}), the Ca^{2+} cations get exchanged with the Na^{+}. This means a loss of cross-links from the alginate gels, which makes the gels weaker (i.e., decreases their elastic modulus). Moreover, a loosely cross-linked gel will tend to swell more in water, and if cross-links continue to be eliminated, the gel will completely degrade, i.e., the alginate will be solubilized. During this degradation process, cells encapsulated in

the gel will be released into the external solution. Removal of Ca^{2+} cross-links from an alginate gel can also be induced by anions in the solution like citrate that can chelate (competitively bind and remove) the Ca^{2+}. For this reason, cell-bearing alginate gels cannot be stored in citrate buffers as an example. The problem of premature degradation in cell-bearing alginate gels has been noted in numerous studies.[58-60] An underlying reason for the easy degradability of alginate gels is that they are formed by physical (ionic) bonds rather than by covalent bonds.

To address the above problem, many attempts have been made to increase the chemical and mechanical durability of alginate gels. One approach has been to coat the anionic alginate gels with cationic polymers such as chitosan.[38,56] However, coating procedures can be time consuming due to multiple steps, and cationic polymers also tend to be toxic to cells.[56] Another approach is to blend alginate with other natural biopolymers such as agarose or gelatin.[54,55] More recently, interpenetrating networks (IPNs) of alginate and one or more biocompatible synthetic polymers have been synthesized. For example, an IPN of alginate and acrylamide (AAm) has been reported for encapsulation of stem cells.[52,53] In another example, an IPN of polyethylene glycol-diacrylate (PEGDA) and alginate was used to encapsulate bacteria.[57] Lastly, alginate derivatives bearing covalently cross-linkable groups have been used to form gels.[80,81] The presence of strong covalent bonds can ensure that a gel remains intact even if the ionic bonds degrade. However, there are several problems with existing approaches. First, if a covalent network coexists with the alginate, the former could impair the growth of encapsulated cells. Second, the degradation of ionic bonds in an alginate gel will still induce the gel to swell appreciably

(even if covalent bonds are also present) and cells in the gel can be released. Also, to form a second network, additional steps are usually required, which makes the encapsulation procedure more complex. Likewise, synthesizing alginate derivatives can be complex and laborious. In short, a simple and straightforward way to strengthen alginate gels has proved elusive.

In this Chapter, we describe a simple technique for the protection of alginate microgels, which involves enveloping the microgel in a layer of covalently cross-linked polymer gel. Importantly, the synthesis of such 'microcapsules' is accomplished in a single step that is completed in a matter of minutes from start to finish. Briefly, our approach involves sending a feed solution of alginate and either a thermal or a photoinitiator through a microcapillary into a reservoir containing both Ca^{2+} and monomers (e.g., AAm). This results in a core-shell structure with a core of alginate cross-linked by Ca^{2+} and a thin shell of cross-linked AAm formed by free-radical polymerization that occurs either by ambient heat or by short exposure to UV light. The thin polymer shell around the alginate core stabilizes the overall microcapsule. Even if the alginate core were to get degraded due to ion-exchange or chelation, the microcapsule remains intact because of its covalently cross-linked shell. The presence of such a robust shell differentiates our approach from other core-shell capsules that have involved alginate.[8-11] Using the above procedure, we encapsulate bacteria and mammalian cells in the core of the capsules and show that the cells remain viable. The thickness and chemistry of the polymer shell as well as the microstructure of the overall capsule can be varied systematically. We believe the

simplicity and versatility of our technique will allow it to be widely adopted to improve the properties of alginate microgels in myriad applications.

3.2 Experimental Section

Materials. The following chemicals were obtained from Sigma-Aldrich: alginate (medium viscosity alginic acid, sodium salt from brown algae), acrylamide (AAm), N,N'-methylenebis(acrylamide) (BIS), calcium chloride dihydrate (CaCl2), ammonium persulfate (APS), tetramethylethylene diamine (TEMED), polyethyleneglycol diacrylate (PEGDA, MW 575), lithium phenyl-2,4,6-trimethyl-benzoylphosphinate (LAP), 1X phosphate buffered saline (PBS), glycerol, sodium citrate, and ethylenediaminetetraacetic acid (EDTA). Deionized (DI) water was used in all experiments. Luria Broth (LB) was obtained from Life Technologies. Dulbecco's modified eagle medium (DMEM), Dulbecco's PBS (DPBS), 0.25 % trypsin-EDTA, fetal bovine serum (FBS), live/dead kit for mammalian cells, and isopropyl β-d-1-thiogalactopyranoside (IPTG) were obtained from ThermoFisher.

Capillary Device for Microcapsule Synthesis. The device for microcapsule synthesis was fabricated in a manner similar to that from our earlier work.[23] Briefly, a capillary with a 200 μm inner diameter (ID) (Vitrocom 8320, 5 cm long) was inserted into the center barrel of a multibarrel glass capillary (from World Precision Instrument) and was fixed with epoxy glue. A P1000 plastic pipette-tip was cut and placed around the multibarrel capillary, leaving 3 mm of the 200-μm capillary extruding out from the pipette casing. The pipette-tip was glued to a male Luer adapter tee (Cole-Parmer, UX-45508-00) with epoxy glue.

Next, a female Luer hose-barb adapter (Cole-Parmer, UX-45508-00) was inserted to one end of Tygon tubing (15 cm, ID 3/16'') and joined with epoxy glue. The part of the capillary protruding from the male Luer adapter tee was inserted to the other end of the Tygon tubing to connect the tubing with the assembled capillary. The rest of the setup, including a syringe pump, a function generator, and a gas flow regulator were identical to those from our previous study. Before each experiment, the 3-mm capillary tip was immersed in a hydrophobic coating (Rainex from Home Depot). To form droplets of the feed solution, nitrogen gas was flowed through the Tygon tubing around the capillary tip (Figure 1). The nitrogen pressure was kept at 5 psi, and pulses of gas were sent at a frequency of 0.5 Hz.

Synthesis of Microcapsules (Thermal Polymerization). The feed solution was made in DI water containing varying amount of APS initiator and 2 wt% alginate. The reservoir solution in the case of alginate-AAm microcapsules was made by dissolving 10 wt% AAm, 0.034 wt% cross-linker (BIS), 1.5 wt% accelerant (TEMED), and 1.6 wt% (150 mM) of $CaCl_2$ in DI water. The feed was loaded into a syringe and fed through the capillary device mentioned above, with the feed flow rate typically being 25 μL/min. Droplets were sheared off from the capillary tip by pulses of nitrogen gas and these entered into an unstirred reservoir solution, whereupon they became capsules (Figure 1). Typically, collection was done for 5 min (yielding a total of 600 capsules), and the capsules were washed three times with DI water to remove residual chemicals. Capsules were then suspended in DI water for storage. For alginate-PEGDA microcapsules, the procedure was identical, but the reservoir solution was made with 20 wt% PEGDA instead of AAm and BIS.

Synthesis of Microcapsules (UV Polymerization). The feed solution was made in DI water with 1 wt% LAP initiator and 2 wt% alginate. The reservoir solution in the case of alginate-AAm microcapsules was identical to the above (10 wt% AAm, 0.034 wt% BIS and 1.6 wt% of $CaCl_2$ in DI water). The feed was loaded into a syringe and was fed through the capillary device at a flow rate ~ 30 µL/min. Droplets from the capillary tip entered into an unstirred reservoir solution, whereupon they were exposed to UV light from an Ionica 36 W UV lamp that generates wavelengths from 350 to 400 nm. The droplets are exposed to UV light for 60-90s, whereupon they are converted into capsules (Figure 1). The capsules were washed three times with DI water to remove residual chemicals and then suspended in DI water for storage.

Optical Microscopy. Brightfield images of the microcapsules were obtained using an inverted optical microscope (Zeiss Axiovert 135 TV) using a 2.5× objective. Images under brightfield and fluorescence of the microcapsules with encapsulated cells were obtained using an Olympus MVX10 microscope. To better visualize the shell, the capsules were observed under slight under-focus in some cases**.**

Scanning Electron Microscopy (SEM). 5 µL of a suspension of alginate-AAm microcapsules was pipetted onto a double-sided carbon tape that in turn was attached on an SEM stub. A drop (3.5 µL) of ionic liquid (Hilm IL 1000, Hitachi) was added and gently mixed using the micropipette. The sample was set to dry in air on a Petri dish for about 30 min. Excess liquid was then removed by a filter paper and the sample was then

dried overnight. The dried sample was examined on a Hitachi SEM (SU-70) with an accelerating voltage of 5 kV.

Mechanical Properties of Microcapsules. Alginate microgels and alginate-AAm microcapsules were compressed between parallel plates using a MicroSquisher (CellScale Inc.). A beam with a thickness of 0.3 mm, a length of 60 mm attached to a 2x2 mm2 metal plate was used for the compression. All samples were kept in PBS for 24 h prior to testing. Samples were compressed by 55% with a load time of 40 s, a 10 s hold, followed by a recovery time of 40 s. Data acquired was for the force required to compress the sample; this force was converted to stress by dividing by the cross-sectional area of the capsule.

Synthesis of Multilayer Microcapsules. The feed solution in this case contained 50 wt% glycerol, 1.6 wt% of $CaCl_2$, 1.5 wt% APS, and with the rest being DI water. The reservoir solution consisted of 10 wt% AAm, 0.3 wt% alginate, 0.034 wt% BIS, and 1.5 wt% TEMED dissolved in DI water. As above, droplets get sheared off from the capillary tip and fall into a reservoir solution that is stirred using a magnetic stir bar at 700 rpm. The droplets thereby transform into multilayer capsules, as discussed under Figure 8. Collection was again done for 5 min and the capsules were washed and stored as before.

Synthesis of Fluorescent Alginate. Fluorescent alginate conjugated with FITC was synthesized following a previous report.[82] Briefly, 120 mg of alginate was dissolved in 10 mL of sodium acetate buffer (pH 5). After 10 min, 50 mg of 1-ethyl-3-(3-dimethyl-aminopropyl) carbodiimide (EDC) and 30 mg of N-hydroxy succinimide (NHS) were

added and stirred at 700 rpm for 30 min at room temperature. The mixture was then precipitated by adding 100 mL of isopropanol. The precipitate was dissolved in 100 mL of sodium bicarbonate buffer (pH 8.5). After 10 min, 0.5 mg of FITC was added and the mixture was stirred for 4 h at room temperature. 100 mL of acetone was added under vacuum filtration to precipitate the alginate-FITC derivative. The resulting derivative was dried under vacuum. The alginate-FITC was combined with the regular alginate in a 1:100 ratio for studies involving fluorescence microscopy.

Bacterial Strain and Growth Conditions. The *E. coli* reporter strain BL21(DE3)-(pET-DsRed) was used for the cell encapsulation study.[83,84] These bacteria were grown in LB media overnight with 50 µg/mL kanamycin at 37°C with 250 rpm shaking, reinoculated by a 1:100 dilution, and grown to approximately an optical density (OD) of 0.4 at 600 nm.

Encapsulation of Bacteria in Microcapsules. After reinoculation, 15 mL of cell culture was spun down at 4°C, 2000 rpm for 20 min. Cell pellets were re-suspended in 400 µL of PBS and 100 µL of LB. For preparing cell-bearing capsules, the feed contained 500 µL of the cell culture, 500 µL of DI water and 1 mL of 2 wt% alginate that was dissolved in PBS. Droplets of this feed were introduced into the reservoir solution containing AAm to create alginate-AAm capsules with bacteria in the core. The capsules were first washed three times with PBS (pH 7.4) and kept on ice. Washed capsules were placed in 1 mL Eppendorf tubes to which 800 µL of PBS and 200 µL of LB and 1 µL of 1 M IPTG were added. The capsules were then cultured overnight (for 18 h) in the case of Figure 6. In both cases, culture was done at 37°C with 250 rpm shaking.

Encapsulation of Mammalian Cells in Microcapsules. Caco-2 cells were cultured in DMEM supplemented with 10% FBS, 1% penicillin (100 units/mL) and streptomycin (0.1 g/mL) in a 37°C incubator with 5% CO2 and passaged two times a week. Prior to encapsulation, cells were grown to 80% confluence, trypsinized and centrifuged at 300 rpm for 15 min at 4°C. Cell pellets were resuspended in 1 mL of DMEM and kept on ice. Cell density was checked using a hemocytometer and the density was adjusted by adding PBS until it reached $1x10^6$ cells/mL. Next, an initiator solution was made by dissolving 0.012g (1.2 wt%) of LAP and 0.2 g of sodium alginate in 1 mL of PBS. For cell encapsulation, 0.15 mL of the cell suspension was mixed with 0.85 mL of the initiator solution to make the feed. The rest of the procedure followed that described in the above section on capsule synthesis by UV polymerization.

Mammalian Cell Culture and Live/Dead Assay. Microcapsules containing Caco-2 cells were placed in a sterile 24-well Petri dish and cultured in a 37°C incubator with 5% CO_2 for 1 week. For live/dead staining, capsules from one well were transferred to a 1 mL Eppendorf tube. Capsules were washed with DPBS three times. After washing, capsules were transferred to 1 mL of DPBS containing 2 μM ethidium homodimer-1 (dead stain) and 1 μM calcein AM (live stain), incubated at room temperature for 15 min and washed with DPBS before imaging. The number of cells in the images were counted and normalized using ImageJ software.

3.3 Results and Discussion

3.3.1 Synthesis of Alginate-Polymer Microcapsules

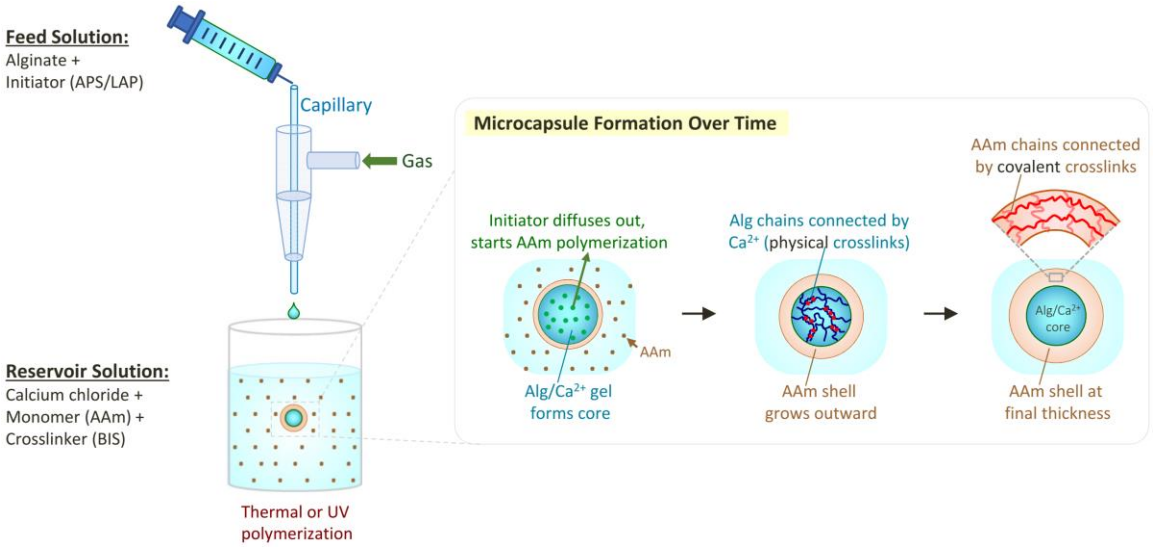

Figure 3.1. Schematic of the procedure used to synthesize alginate-polymer microcapsules. A feed of alginate (Alg) and initiator is sent through a capillary into a reservoir containing monomers and Ca^{2+}. Pulses of gas shear off aqueous droplets from the capillary tip. As the droplets enter the reservoir, the inset shows the progression towards the final microcapsule structure. First, the Alg in the droplets is gelled by Ca^{2+} and this forms the core of the structure. The initiator then diffuses out and, upon activation by ambient heat or UV light, polymerizes a shell of AAm around the Alg core. The AAm shell grows outward and reaches its final thickness in a few minutes.

The technique used to synthesize microcapsules with an alginate core and a covalent polymer shell is shown schematically in Figure 3.1. We use the concept of 'inside-out polymerization', which was developed recently by our lab. The idea is to include one component of a free-radical polymerization (the initiator) in a core structure while the remaining components (monomers) are added to the surrounding solution. In that case, the initiator would diffuse outward from the core, where it would encounter the dissolved monomers and induce polymerization. A covalently cross-linked polymer shell would thereby grow outward from the core.[33] Here, we couple such polymerization with the

gelation of alginate via ionic cross-links. To accomplish this at the microscale, we use a water-gas microfluidic device that employs pulses of gas to shear off aqueous droplets from the tip of a microcapillary.[23] Unlike other microfluidic approaches used for microcapsule synthesis,[57,60] this technique eliminates the use of oil or non-aqueous solvents. This is attractive because the technique is thereby more compatible with cell encapsulation.[11] Control of droplet size in the range between 80 to 500 μm is made possible by modulating the aqueous flow rate and the gas pressure.[11]

The single-step process in Figure 3.1 begins with a feed solution that contains both alginate (2 wt%) and a free-radical initiator. In the case of thermal polymerization, we use ammonium persulfate (APS), typically at 2 wt%. Any payload to be encapsulated in the final structure (such as cells) would also be included in this feed. The reservoir contains the rest of the chemicals needed for polymerization, which include a monomer (e.g., acrylamide, AAm, 10 wt%), a cross-linker (e.g., N,N'-methylene-bis-acryl-amide, BIS, 0.15 wt%), and an accelerant (tetramethyl ethylenediamine, TEMED, 1.5 wt%). In addition to the above, the reservoir also contains 1.6 wt% (150 mM) of calcium chloride. When the device is switched on, the feed solution flows through a capillary of diameter 200 μm at its tip. Pulses of gas (air or nitrogen) are sent around the tip of the capillary, and for each pulse of gas, a droplet of the feed is sheared off from the tip.[23] As this droplet enters the reservoir, the alginate in the droplet is cross-linked by Ca^{2+} ions almost instantaneously, thus converting the droplet into a gel. At the same time, the APS initiator diffuses out of this gel into the solution. The APS induces the polymerization of AAm monomer, resulting in a thin layer of poly(AAm) around the alginate gel.[33] Due to the use of the accelerant

TEMED, the entire polymerization is completed in about 5 min at room temperature. A variation of the above process is used in the case of UV polymerization. The thermal initiator is replaced with a photoinitiator such as lithium phenyl-2,4,6-trimethylbenzoylphosphinate (LAP), typically at 1 wt%. Otherwise, the feed is identical to the above. The reservoir solution is also identical, except that TEMED is omitted. As droplets from the feed are collected in the reservoir, UV light is shone around the reservoir for 60-90 s. This is sufficient to complete the formation of the covalent poly(AAm) shell around the alginate core. The LAP photoinitiator was particularly chosen because it is known to be relatively nontoxic to cells,[85,86] and this will be particularly useful in the encapsulation of mammalian cells in the above structures.

3.3.2 Microstructure and Mechanical Properties of the Microcapsules

Figure 3.2 shows optical (brightfield) micrographs of structures obtained by the above procedures via thermal or UV polymerization. All structures are microcapsules with a distinct core (a gel of alginate cross-linked by Ca^{2+}) and a thin shell (a gel of covalently cross-linked polymer). The reason we obtain core-shell structures is because the rate of alginate cross-linking by Ca^{2+} is much faster than the rate of AAm polymerization.[33] If the alginate were mixed with monomers prior to contact with Ca^{2+}, one would obtain a composite (IPN) of alginate and AAm rather than a core-shell structure.[52] Instead, in our case, the core contains only alginate, which is conducive for cell encapsulation. At the same time, the shell provides protection to the alginate core, as will be shown below. The technique presented here is simple, yet versatile. It allows the average sizes of the core and

shell to be varied independently. Moreover, instead of AAm, the shell can be made from other monomers with a C=C bond that can be cross-linked by free radicals.

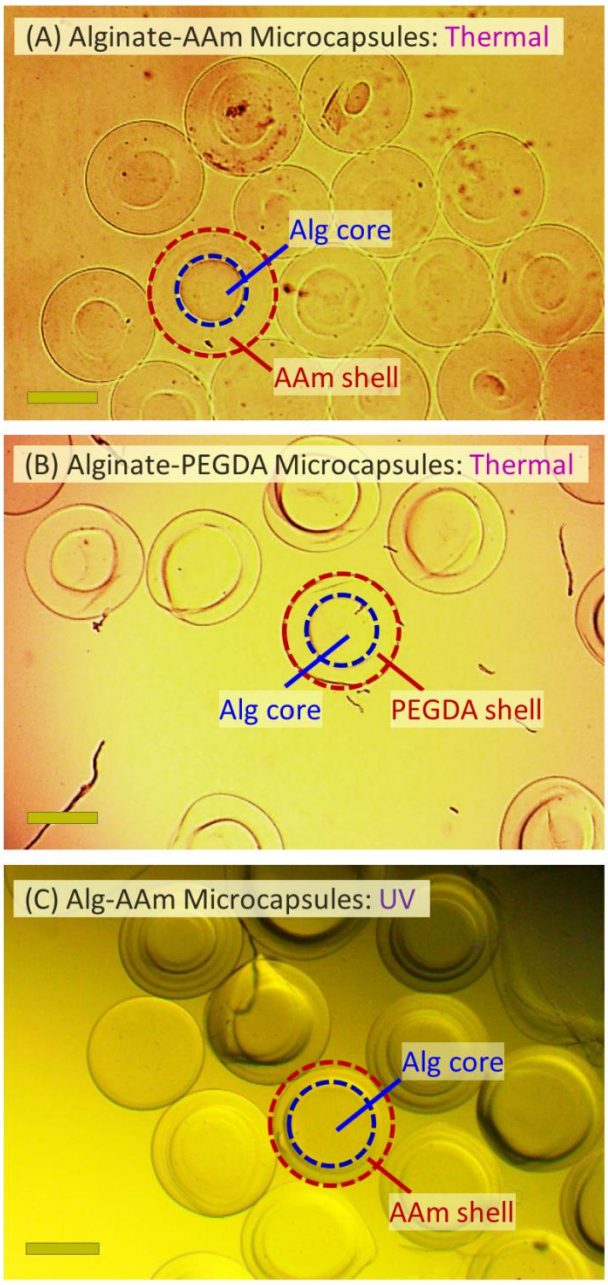

Figure 3.2. Images of microcapsules with a covalent polymer shell around an alginate core. (A) Shell of acrylamide (AAm) and (B) Shell of polyethylene glycol diacrylate (PEGDA), both via thermal polymerization. (C) Shell of AAm via UV polymerization. In all cases, the core and shell are distinctly visible and are marked around a specific capsule for clarity. Scale bars: 200 µm.

As an example, we have formed shells of polyethylene glycol diacrylate (PEGDA) around the alginate core, as shown in Figure 3.2(B). PEGDA, like AAm, is a monomer that is commonly used in biomedical applications.[51,57] In addition to optical microscopy, we have also used SEM to analyze the capsules. SEM images shown in Figure 3.3 confirm that there are two distinct layers to the capsules - an outer layer of covalent gel around a core of alginate gel for both (A) acrylamide and (B) PEGDA shell.

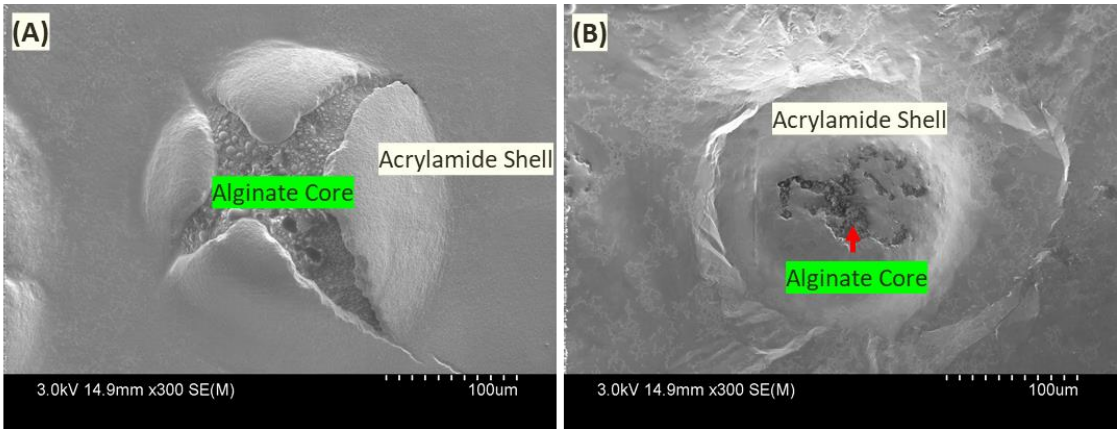

Figure 3.3. Scanning Electron Micrographs (SEM) of alginate-AAm microcapsules. (A) Microcapsule synthesized by thermal polymerization. (B) Microcapsule capsule synthesized by UV polymerization. In both images, the capsule is cracked open, thus revealing a distinct core (alginate microgel) and shell (AAm).

We have also compared the mechanical properties of alginate microgels versus microcapsules with an alginate core and a thin (~ 40 μm) covalent shell of AAm. The tests were performed under compression and the data (Figure 3) reveal that the the AAm shell makes the microcapsule significantly more robust than the microgel. When the alginate microgel (control) is compressed to about 50% strain, it is irreversibly squished from a sphere to a pancake shape and does not recover its original shape when the compression is stopped as shown in Figure 3.4A. On the other hand, when the alginate-AAm capsule is

compressed to a higher strain (~55%), the capsule recovers its original shape after compression (Figure 3.4B). Moreover, the peak stress measured during the compression of the alginate microgel is only around 13 kPa, which is much lower than that for the microcapsule (71 kPa). The data confirm the contribution of the thin polymer shell to the capsule elasticity and strength. Similar differences in mechanical properties have been reported in the case of macrosized (~ 5 mm) alginate gels with and without a polymer shell from our previous study.[33]

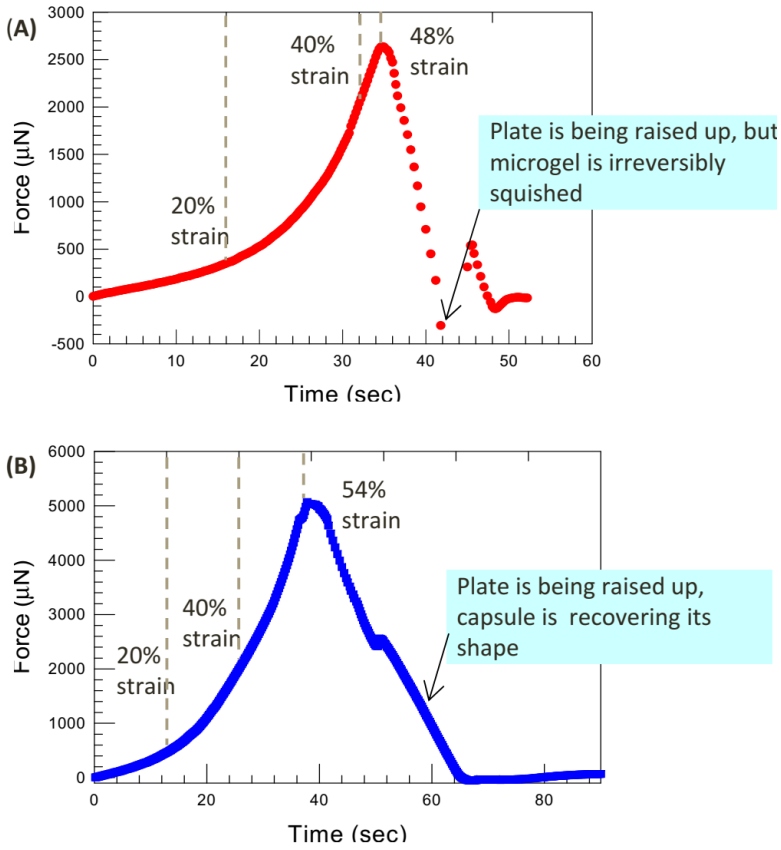

Figure 3.4. Results of compression tests on (A) alginate microgels and (B) alginate-AAm microcapsules. The graphs are plots of the force required for compression vs. time during steady compression. When compressed to 48% strain, alginate microgels fail to recover their shape whereas the alginate-AAm microcapsules can be compressed to 55% strain and still recover their original shape. The stress at the peak force is 13 kPa for alginate microgels and 71 kPa for Alg-AAm microcapsules. The compression tests thus show that the AAm shell improves the mechanical response of alginate microgels.

3.3.3 Tuning the Microcapsule Core and Shell Sizes

The growth of the polymer shell around the alginate core is controlled by the amount of initiator present in the core (i.e., in the feed solution). Once the droplets enter the reservoir, the shell grows over 1-2 min and reaches its final thickness. With longer incubation in the reservoir, there is no further growth of the shell, i.e., the growth is self-limiting. This is shown by Figure 3.5, where the concentration of initiator (APS) in the feed is varied. If the initiator is low (1 wt%), no visible shell of polymer (AAm) is found around any of the alginate cores (Figure 3.5A). Upon increasing the APS to 1.5 wt%, shells become visible around a few alginate cores (Figure 3.5B). Further increase of the APS to 2 wt% results in all alginate cores having uniform, discernible AAm shells (Figure 3.5C). However, when the APS is further increased to 3 wt%, the shell elongates into a tail in some cases, indicating that polymerization is not merely confined to the volume around the cores, but extends into the solution (Figure 3.5D). The tail may also reflect polymerization in the wake of the droplet as it falls in the reservoir. If the APS is increased above 3 wt%, soon after droplets of the feed enter the reservoir, the entire solution is gelled into a solid block. Overall, the results in Figure 3.5 imply that there is an optimal APS concentration around 2 wt% for forming polymer shells by thermal polymerization, and we have fixed this concentration for the studies below. In the case of 1 and 1.5 wt% APS, although shells are not visible, the structures do resist degradation by chelators, as discussed below. This means that thin shells are present in those cases too, and additionally, it implies that the shell thickness can be tuned by the initiator concentration.

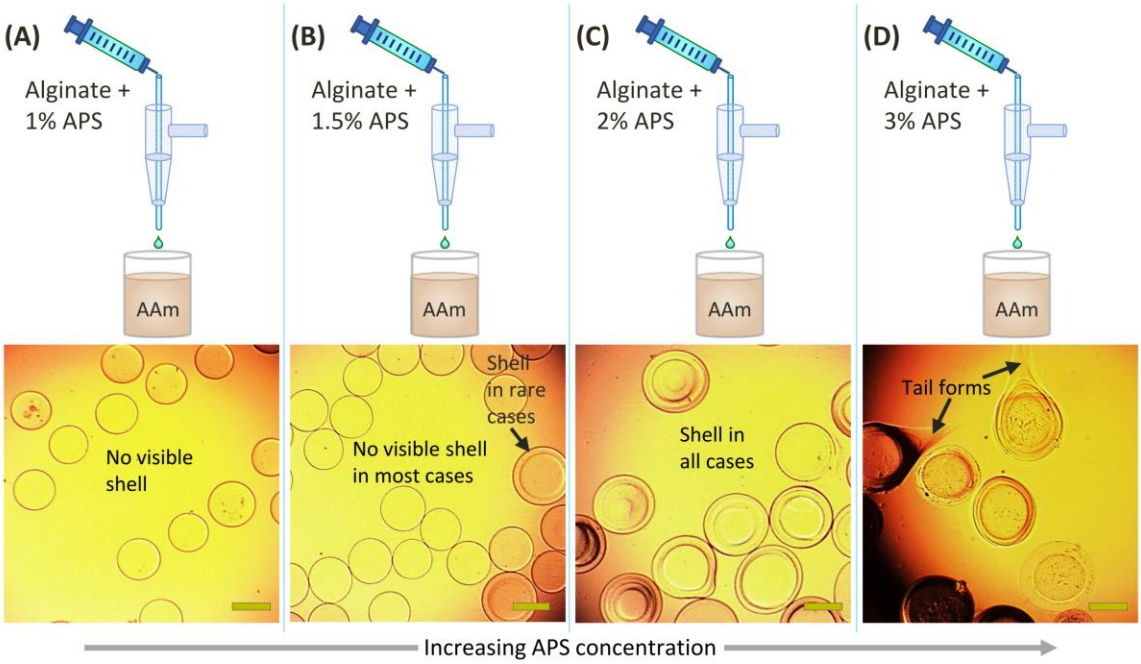

Figure 3.5. Effect of initiator (APS) concentration on the formation of alginate-AAm microcapsules by thermal polymerization. (A) 1 wt% APS: no AAm shells are visible; (B) 1.5 wt% APS: shells visible only around a few cores; (C) 2 wt% APS: visible shells around all cores; and (D) 3 wt% APS: tails around some cores, and the capsules clump together. Scale bars: 200 µm.

We can also vary the core diameter independent of the shell thickness. This can be done by changing the flow rate of the feed, which alters the droplet size (and thereby the core size), as shown in our previous study.[23] Here, we performed experiments at various flow rates with a feed of 2% alginate and 2% APS, with the reservoir containing AAm and 150 mM Ca^{2+}. At the lowest feed flow rate of 5 µL/min, the microcapsules have a core diameter of 88 µm and a shell thickness of 25 µm (Image 1 in Figure 3.6). If the flow rate is increased to 20 µL/min, the core diameter increases to 132 µm with the shell thickness being 28 µm (Image 2). With further increase of the flow rate to 40 µL/min, the core diameter reaches 142 µm and the shell thickness is 37 µm (Image 3). These data show that the main effect of increasing the flow rate is to increase the core

size, while the shell remains about the same thickness. Based on Figures 3.5 and 3.6, the core size can be controlled via the flow rate and the shell thickness via the initiator concentration.

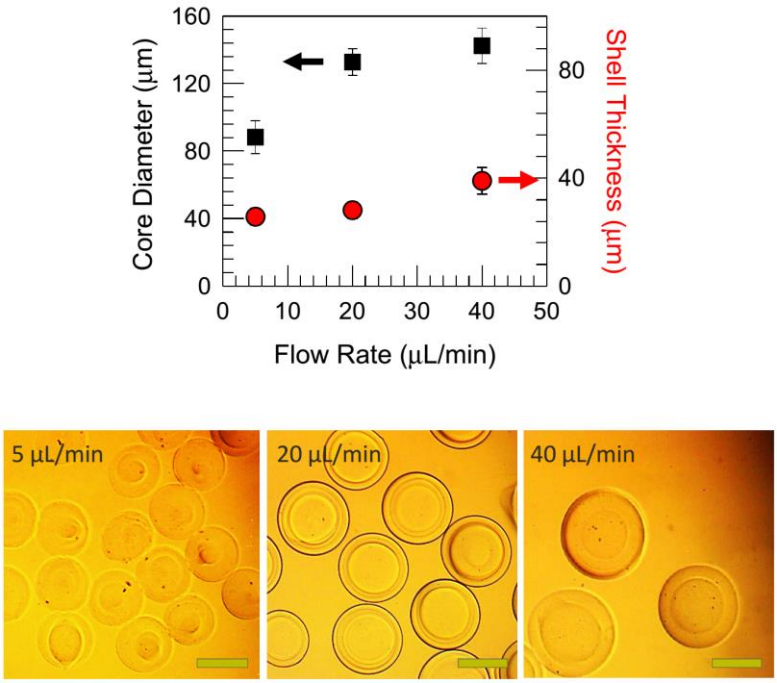

Figure 3.6. Effect of increasing the feed flow rate on microcapsule sizes. Increasing the flow rate increases the alginate core diameter while maintaining about the same AAm shell thickness (all structures made by thermal polymerization). This is shown by the plot above and the images below. Scale bars: 100 µm. The error bars represent the standard deviation of the distribution (n=3).

3.3.4 Microcapsule Stability and Swelling

Our main reason for adding a polymer shell around alginate gels was to prevent their degradation or swelling when contacted with certain ions or chelators. We now proceed to test these aspects. First, we placed bare alginate microgels and alginate-polymer microcapsules in 100 mM of ethylene diamine tetracetic acid (EDTA), a well-known

chelator of Ca^{2+} ions. As expected, the bare alginate microgels completely degrade within 30 min (Figure 3.7A).

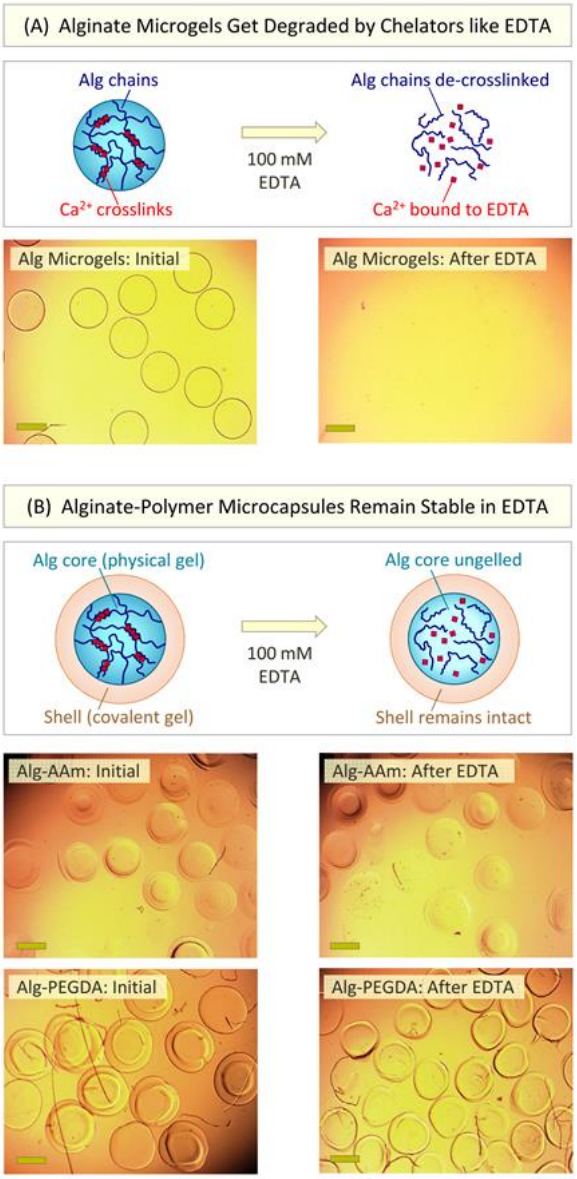

Figure 3.7. Stability of alginate-polymer microcapsules to chelation. (A) Alg microgels (control) are rapidly degraded within 30 min when placed in 100 mM EDTA. The schematics indicate that degradation is due to Ca^{2+} crosslinks being removed from the gels. (B) Alg-AAm and Alg-PEGDA microcapsules remain intact in 100 mM EDTA even after 24 h. The schematics indicate that degradation occurs in the cores of the capsules, but the polymer shells remain intact.

As per the schematics, the degradation is because Ca^{2+} cross-links are removed by EDTA, leaving behind linear alginate chains that are no longer part of a 3-D network. In contrast, alginate-AAm and alginate-PEGDA microcapsules both maintain their spherical shape even after 24 h in the EDTA solution (Figure 3.7B). In these cases, the alginate cores are expected to get degraded into linear alginate chains, but the polymer shells stay intact because they are held together by covalent bonds. Similar results are found if sodium citrate is used as the chelating agent instead of EDTA.

While chelators can cause complete degradation, alginate gels can also suffer partial degradation when placed in buffers. For example, when placed in phosphate buffered saline (PBS), some of the Ca^{2+} cross-links are exchanged with Na^{+}, which reduces the mechanical regidity of the gels. . In turn, a decrease in cross-link density will induce the gel to swell in water, which creates a vicious cycle because the swollen gel will be even weaker. If the gels are to be used for encapsulating biological payloads, their ability to maintain their mechanical integrity under physiological conditions will be crucial. To test the degree of swelling, we placed alginate microgels and alginate-polymer microcapsules in PBS (pH 7.4) and monitored their size over time up to 10 h. As expected, the alginate microgels (without any shell) show a 57% increase in size (data in Figure 3.8). In comparison, alginate-PEGDA microcapsules swell by 42% while the alginate-AAm microcapsules swell only by 28%. These results confirm that the presence of a polymer layer hinders swelling of the capsule. Among these two polymer shells, AAm appears to provide greater resistance to swelling, possibly indicating that the AAm network is more densely cross-linked than the PEGDA network. Note that AAm and PEGDA are both

nonionic polymers that will not be affected by the ionic strength or pH of the buffer solution. Thus, regardless of any loss of cross-links from the alginate core, the polymer shells will ensure that the microcapsules preserve their structural integrity.

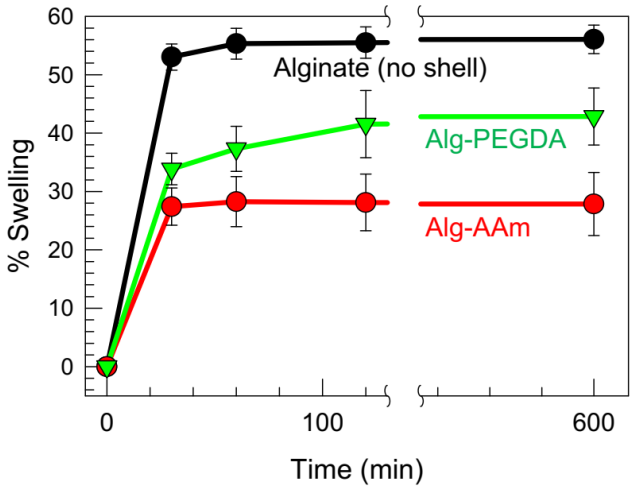

Figure 3.8. Swelling of microcapsules vs. microgels in PBS buffer. The extent of swelling over 10 h is plotted for Alg microgels (no shell), Alg-AAm microcapsules and Alg-PEGDA microcapsules. The presence of a polymer shell reduces the extent of swelling. The error bars represent the standard deviation (n=3).

3.3.5 Encapsulation of Cells in Microcapsules

We proceeded to study the encapsulation and culture of both bacteria and mammalian cells in the microcapsules. Culture of bacteria in alginate gels can be problematic because the gels can degrade either due to ion-exchange in growth media (similar to degradation in buffers, as discussed above) or because of rapid bacterial growth (bacteria often escape out of the gel matrix and spread to the outer solution).[58] In this regard, the polymer shell around the alginate core can protect the cells and also help maintain the cells in the core. Note that the polymer shell, being a porous gel, does allow diffusion of small molecules in and out of the core, which is essential for cell viability.

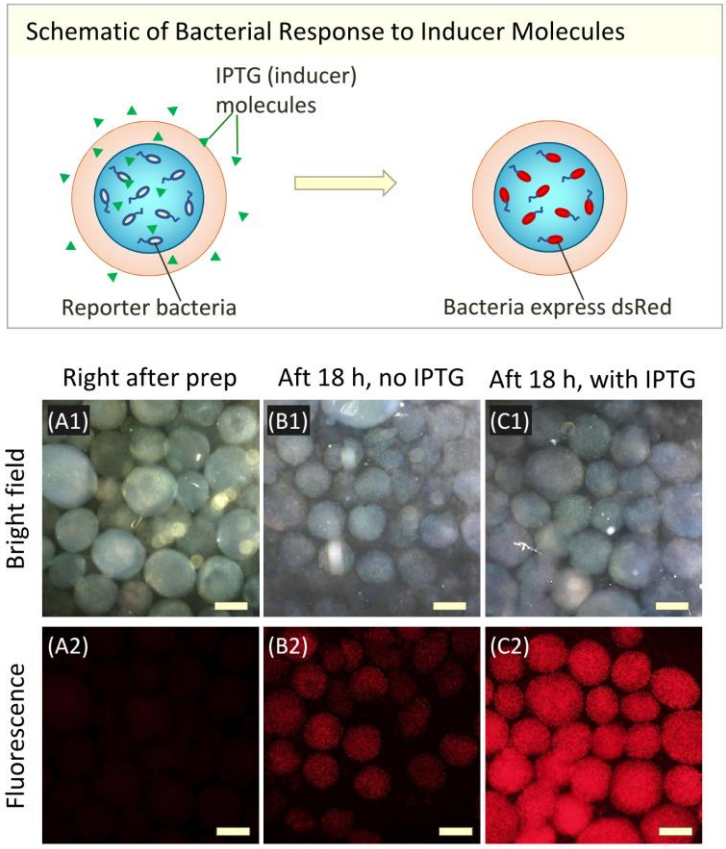

Figure 3.9. Culture of genetically engineered bacteria in alginate-AAm microcapsules and their response to an inducer. The bacteria (*E. coli*) are engineered to express a red fluorescent protein (DsRed) when exposed to a molecular inducer (IPTG), as indicated by the schematics. Brightfield and fluorescence micrographs are shown for the microcapsules: (A) Right after preparation; (B) Cultured without IPTG; and (C) Cultured with IPTG. Red fluorescence is higher in (C). Scale bars: 200 µm.

We conducted the encapsulation studies with a strain of *E. coli* that had been genetically engineered to express a red-fluorescent protein (DsRed) when isopropyl β-d-1-thiogalactopyranoside (IPTG), a small molecule 'inducer', is present in its environment.[83,84] The procedure for cell-encapsulation is that from Figure 3.1, with the feed containing both alginate/APS and the cells in a mixture of PBS and Luria Broth (LB) media. We used AAm as the monomer in the reservoir and after thermal polymerization, we obtained microcapsules with bacteria in the alginate core and

encased by an AAm shell (Figure 3.9). Following synthesis, the microcapsules were placed in culture media and incubated overnight (18 h) in a shaker at 37°C. Two culture conditions were explored: one without IPTG and the other in the presence of 1 mM IPTG. The images show that both non-induced and induced microcapsules maintain their structural integrity during the overnight incubation. Non-induced capsules show a low level of red fluorescence indicating low expression of DsRed (Figure 3.9B). In comparison, the induced capsules show significant red fluorescence, indicating that the presence of IPTG has indeed stimulated the cells to express the fluorescent DsRed protein (Figure 3.9C). Thus, the results confirm that the bacteria are viable and that they follow their genetically programmed response (i.e., they remain functional). Higher cell growth is observed in the UV-polymerized capsules, which is the mode we have employed for culture of mammalian cells as well.

Next, we explored the encapsulation and culture of mammalian cells, specifically those of the human epithelial cell line, Caco-2 (Figure 3.10). In this case, we used UV-polymerization to prepare the capsules for this a feed of alginate/LAP + cells in PBS was sent into a reservoir containing AAm and exposed to UV for 90 s, as shown under Figure 3.1. As mentioned earlier, the LAP photoinitiator was chosen because it is relatively nontoxic to cells.[85,86] The images in Figure 3.10 show that the capsules remain intact and maintain their spherical shape over the entire 7-day culture period. Moreover, we employed live/dead staining to infer the state of cells in the capsules, and the data were quantified using ImageJ. The cells are mostly live at all time points, as indicated by the predominantly green fluorescence in the images. Cell viability is calculated to be more than 85% after 4

days and more than 80% after 7 days. These results are very encouraging and show that our approach is suitable for encapsulation of both bacteria and mammalian cells. Note that the entire encapsulation of cells is done at room temperature without involving an immiscible oil phase, which is usually needed in other microfluidic approaches. Because mammalian cells grow at a slower rate than bacteria, maintenance of capsule integrity in growth media over a long period of time is arguably more important for these cells.

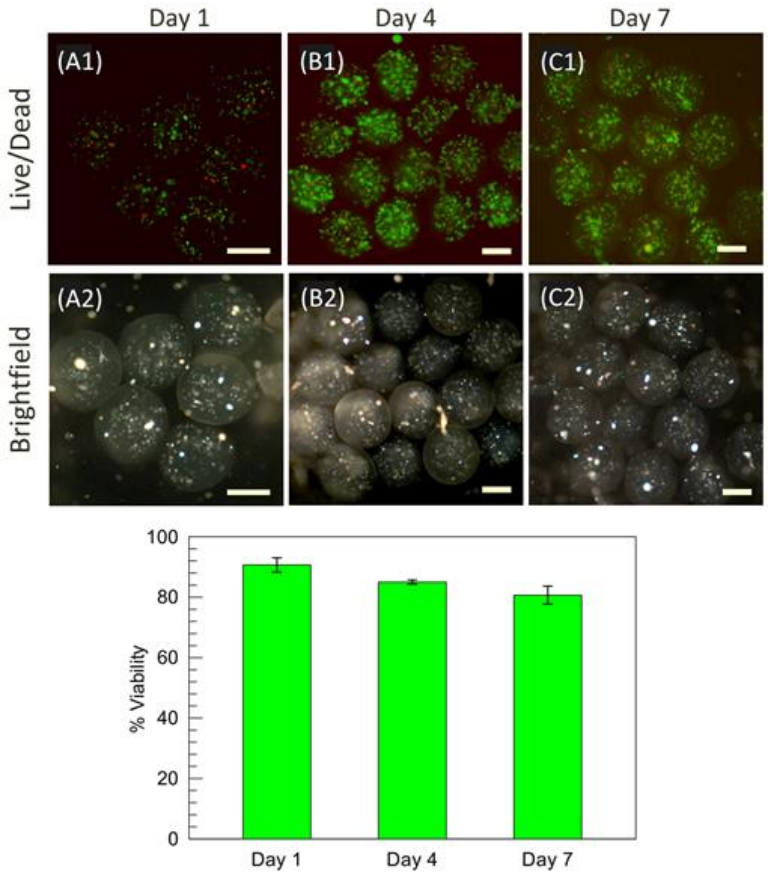

Figure 3.10. Encapsulation and culture of Caco-2 epithelial cells in UV-polymerized alginate-AAm microcapsules. Fluorescence and bright-field micrographs are shown over the 7-day culture, with live/dead staining (live = green and red = dead) indicating the state of the cells in the former. A bar graph of the cell viability at days 1, 4, and 7 is shown below the images, with the error bars representing the standard deviation from multiple (n = 3) experiments. Scale bars: 200 μm.

3.3.6 Multilayer Microcapsules with Liquid Cores

Lastly, we present a variation of our synthesis scheme that gives rise to a distinct structure for the microcapsules. In this case, rather than feeding a solution of alginate into Ca^{2+} to make gels or capsules, we reverse the order and use Ca^{2+} as the feed and alginate in the reservoir. Previous attempts using this scenario[87-89] have recognized that there are two problems. First, when a drop of Ca^{2+} solution encounters the alginate solution, the drop rapidly loses its spherical shape and dissolves away. In that case, there would be insufficient time to gel the droplet. To prevent this problem, researchers have added sucrose,[88] methyl cellulose[87] or xanthan gum[89] to increase the viscosity of the Ca^{2+} solution. Even with a viscosity increase, a second problem is that structures formed by adding Ca^{2+} to alginate are weaker mechanically compared to structures made by the 'normal' route of adding alginate to Ca^{2+}.

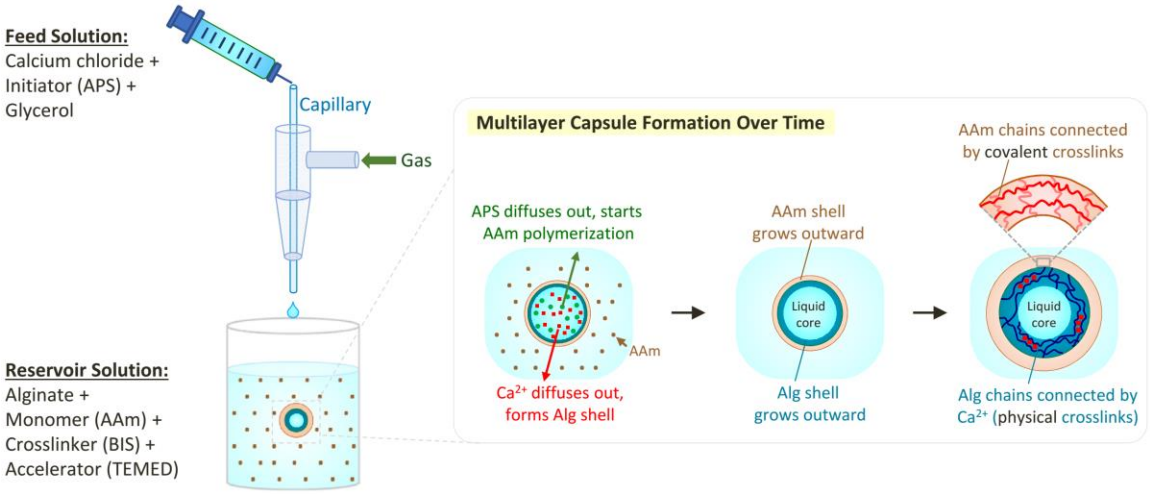

Figure 3.11. Schematic of the procedure used to synthesize multilayer capsules. A feed of Ca2+, initiator (APS), and glycerol is sent through a capillary into a reservoir containing alginate (Alg), monomers (AAm and BIS), and accelerator. Pulses of gas shear off aqueous droplets from the capillary tip. As the droplets enter the reservoir, the inset shows the progression towards the final multilayer capsule structure. First, the Ca2+ diffuses out and an Alg/Ca2+ shell forms around the liquid core. The APS then diffuses out and polymerizes a shell of AAm around the Alg shell. The final structure thus has two layers (Alg and AAm) and a liquid core.

Our approach (Figure 3.11) avoids both the above problems. Here, the feed is a solution of 1.6 wt% Ca^{2+} combined with the initiator (2 wt% APS) and with glycerol (50 wt%) as the thickener. The reservoir contains 0.3 wt% alginate and the monomers (AAm and BIS). In this case, when the feed droplet enters the reservoir, the Ca^{2+} and alginate will immediately come into contact, resulting in a shell of alginate gel around the liquid droplet.[87-89] Next, the APS will diffuse out and polymerize the monomer, resulting in a second shell of AAm. Thus, the final structure will be a multilayer microcapsule with an outer shell of AAm, an inner shell of alginate, and a liquid core. If capsules with a liquid core (rather than a gelled core) are desired, this approach provides a convenient way towards that end. Note that, the glycerol, being a small molecule, will diffuse out of the core over time into the external solution. Also, note that we use a much lower alginate concentration in the reservoir as compared to the feed solution in Figure 3.1. The reason is to maintain a relatively low viscosity of the reservoir solution. If the reservoir is highly viscous, the droplets from the capillary tip tend to splatter as they hit the reservoir and capsules are not formed.

Figure 3.12 shows optical micrographs (under brightfield and fluorescence) of the resulting microcapsules. To confirm the location of the alginate relative to the AAm, we used a fluorescent derivative of alginate, which was synthesized by attaching fluorescein isothio-cyanate (FITC) to the alginate backbone.[82] The alginate thus appears green under fluorescence microscopy. From the combined images (Figures 3.12C and 3.12D), it is clear that the capsules do have a liquid core (which appears dark because alginate is not present) surrounded by a shell of alginate gel (green) and then a shell of AAm. The images thereby

confirm the structure to be consistent with the schematic in Figure 3.11. When the capsules are submerged in solutions of a chelator (100 mM of EDTA or 500 mM of sodium citrate) overnight, they remain intact, but the inner alginate shell disappears, and the green fluorescence is now observed in the core (Figure 3.12E). This finding implies that the alginate shell is degraded by chelating away the Ca^{2+} cross-links. The resulting alginate chains are large enough that they remain inside the capsule core rather than diffusing out through the AAm shell into the external solution.

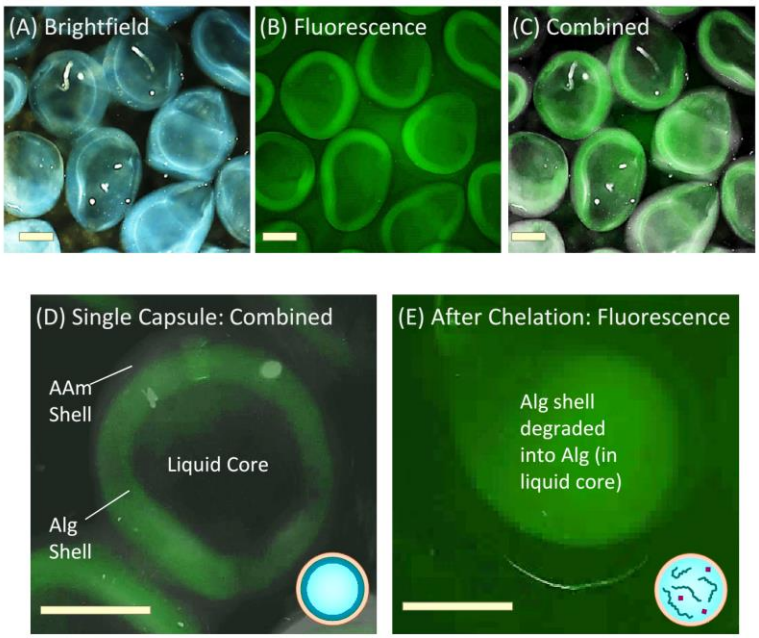

Figure 3.12. Images of multilayer microcapsules with concentric alginate and polymer layers around a liquid core. Images from brightfield (A) and fluorescence microscopy (B) are combined in (C). An enlargement of a single capsule from (C) is shown in (D). The green fluorescence is from alginate labeled with FITC. As indicated in (D), the capsules have a liquid core, followed by an alginate shell (green) and then a polymer (AAm) shell. (E) When these capsules are subjected to chelation using sodium citrate, the alginate shell degrades, and the fluorescent alginate is now found in the liquid core. Scale bars: 300 μm.

3.4 Conclusions

We have developed a new single-step technique to synthesize alginate microgels enveloped by a thin shell of covalently cross-linked polymer gel. The resulting microcapsules combine the attractive features of alginate (biocompatibility and suitability for cell growth) with those of covalent polymers (robustness and resistance to degradation due to chelators or ionic species). The polymer shell is formed by 'inside-out' polymerization, where an initiator in the core diffuses outward and reacts with monomers present externally. The thickness of the shell and the size of the core can be controlled by varying the concentration of initiator and the flow rate of the feed solution, respectively. Various monomers that can be cross-linked via free-radical polymerization using heat or UV light can be used to generate the shell. As the synthesis is done at room temperature in aqueous media, both bacterial and mammalian cells can be readily encapsulated in the microcapsules. Studies with cells show that the microcapsules remain intact over a culture period of up to 7 days, whereas alginate microgels without a shell disintegrate in less than a day over the same culture conditions. Lastly, we have also developed a variation of the synthesis method to generate microcapsules with multiple shells (alginate and polymer) around a liquid core. The simplicity and versatility of our approaches allow them to be broadly used as tools to enhance the properties of alginate microgels.

Chapter 4
Capsules with Bacteria and Fungi in Distinct Compartments

4.1 Introduction

Cells are the basic building blocks of all life forms on earth. From unicellular (e.g. bacteria) to multicellular (e.g. plants, animals), every living organism consists of cells. A defining characteristic of eukaryotic cells is the presence of many internal compartments (organelles).[4,5] Each organelle is covered by a membrane, which regulates the entry and exit of molecules.[3] Thus, each organelle has different contents and in turn serves different functions. In the last decade, researchers have attempted to capture this multi-organelle architecture in synthetic structures, which are termed 'artificial cells' or 'protocells'.[12-15,24,32,73] In this regard, our labs have recently reported cell-like structures that we refer to as *multi-compartment capsules* (MCCs).[23] These MCCs (sizes ~ 500 μm) are made from biopolymers like alginate, and our method allows us to encapsulate different payloads in each compartment (sizes ~ 100 μm). Payloads with sizes of 5 nm or larger (including enzymes and nanoparticles) remain sequestered in the hydrogel matrix within each compartment, but small molecules can enter or exit the compartments.

A crucial advantage of our approach to MCCs is that they are made by an oil-free microfluidic method, with gas being used to shear off aqueous droplets as the fluid exits out of a capillary tube. This facilitates the encapsulation of biological cells in the compartments. In our initial study, we encapsulated two strains of bacteria in adjacent compartments of MCCs and monitored communication between the cells. One producer

(P) strain received a chemical signal from the external medium and then secreted its own signaling molecules (autoinducer-2 or AI-2). AI-2 is one of a family of autoinducer molecules that mediate quorum sensing (QS) in bacteria.[90] QS is the phenomenon by which bacteria alter their gene expression when they reach a 'quorum', i.e., when their cell density becomes sufficiently high.[91-93] In our experiment, the AI-2 diffused from one compartment into the adjacent one, where it turned on QS in the reporter (R) cells present there – i.e., induced the cells to express a fluorescent protein.

In the present study, we extend the use of MCCs as a platform to study microbes from different kingdoms, specifically bacteria and fungi. Our chosen bacterial species is the gram-negative *Pseudomonas aeruginosa*, while the fungus is *Candida albicans*. Both microorganisms are known as opportunistic pathogens and are commonly found as part of the normal human microbiota.[94] Recent studies revealed that microorganism not only exist as free-floating cells but also exist as a community (i.e. mixed group of cells), embedded in an extra cellular matrix of polymeric material called biofilm.[95-97] *P. aeruginosa* are often found in mixed infections with the fungi, *C. albicans*, in more than 70% of infections involving biofilm formation such as cystic fibrosis.[95] Competition exists between the bacterium and the fungus inside biofilms which directly affects their virulence.[98-101] Therefore, study of cross-kingdom relationship between the pathogens can have direct impact on the patients. Co-cultures of *P. aeruginosa* and *C. albicans* are often studied in liquid culture or by plating on the same agar plate.[102-105] Both methods have their disadvantages. In liquid co-culture, cells come into physical contact during their growth, which can affect their growth rates, although it is difficult to pinpoint how they affect each

other.[104] On an agar plate, cells can grow in discrete 2-D layers, but this is not the 3-D environment they encounter in their natural habitat as cells are embedded inside a hydrogel matrix, not just colonizing the surface as on an agar plate.[102,103] MCCs with a hydrogel scaffold offer a 3-D environment for cell growth, and by encapsulating the cells in separate compartments, we can study their growth without physical contact (Figure 1). We are able to monitor cell growth in real-time by optical microscopy and thus elucidate how different chemicals (e.g., surfactants) or external conditions (e.g., pH) affect both kingdoms of cells. Scenarios where the fungi grow at the expense of bacteria (Figure 1A) or vice-versa (Figure 1B) are both reported in this Chapter.

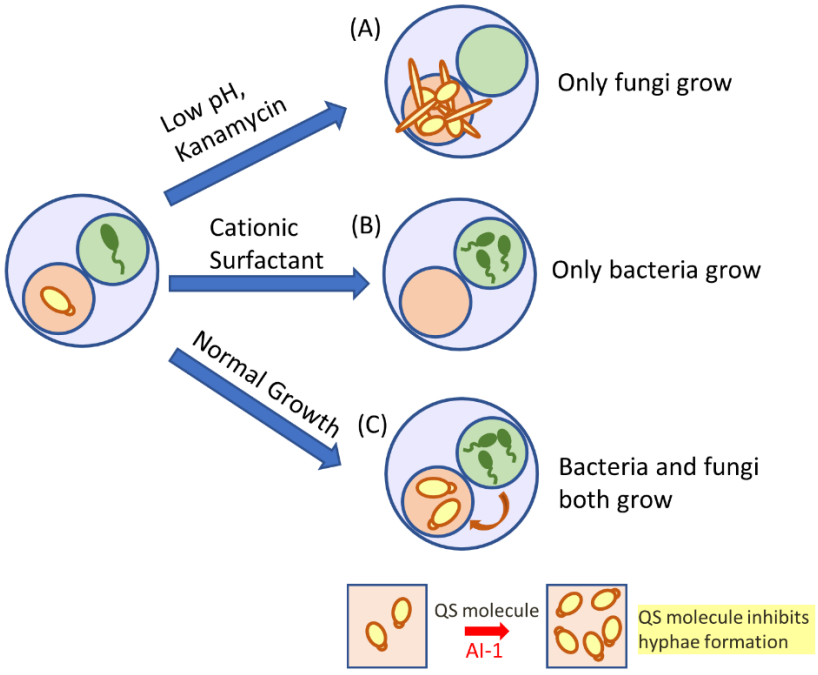

Figure 4.1 Schematic of studies done in this Chapter with multi-compartment capsules (MCCs) having fungi and bacteria cultured in separate compartments. (A) When certain chemicals (e.g., kanamycin) are added or when the pH is low, only fungi grow whereas the bacteria do not. (B) When other chemicals (e.g., cationic surfactants) are added, only the bacteria grow whereas the fungi do not. (C) Under normal growth conditions, inter-kingdom interaction is observed where signaling molecules produced by the bacteria affects the morphology of the fungi. The fungi remain in yeast, not hyphal form.

One further motivation for our studies is to explore inter-kingdom signaling between the microbes. QS molecules secreted by bacteria can affect cells from other kingdoms including fungi.[98-101] Such signaling is often observed in biofilms, which are a matrix of polysaccharides excreted by entrapped bacteria and can contain multiple types of microbes.[106] Biofilm formation in our body or on medical devices can often be a precursor to adverse effects on human health.[95-97] Thus, there is a need to understand and mitigate biofilm growth. *P. aeruginosa* and *C. albicans* in biofilms are believed to have an antagonistic relationship, i.e., one inhibits the other. This relationship is mediated by QS molecules: *P. aeruginosa* produces autoinducer-1 (AI-1), and in the presence of this molecule, *C. albicans* cells are expected to remain as 'yeast' (i.e., as spheroidal clusters) rather than as 'hyphae' (i.e., as long multicellular filaments).[98-101] The morphological transition from yeast to hyphae generally signifies that the fungi are becoming virulent, i.e., it serves as a measure of their pathogenicity.[107-109] In this study, we are able to monitor this morphological transition in real-time using our MCC construct (Figure 1C). The fungi transform from yeast to hyphae when the bacteria are absent while they remain in the yeast morphology when the bacteria are present. Our studies collectively show that the MCC is a simple, yet versatile platform for simultaneously examining various types of cells.

4.2 Experimental Section

Materials. The following chemicals were obtained from Sigma-Aldrich: alginate (medium viscosity alginic acid, sodium salt from brown algae), oligochitosan lactate, calcium chloride dihydrate ($CaCl_2$), sodium acetate, 1x phosphate buffered saline (PBS), glutaraldehyde (50% in water), N-(3-Oxododecanoyl)-L-homoserine lactone (AI-1), chitosan oligosaccharide lactate (MS <4000). Yeast extract peptone dextrose (YPD) was obtained from Life Technologies. Kanamycin, hexadecyltrimethylammonium bromide (CTAB) were obtained from ThermoFisher.

Strains and Growth Conditions. The experiments were performed with *P. aeruginosa* (PAO1) and *C. albicans* (SC5314) kindly provided by Bentley lab and Karlsson lab, respectively. All strains were cultured in a rotary shaker at 30°C in YPD broth at 250 rpm.

Preparation of Cell Bearing Microcapsules. *P. aeruginosa* and *C. albicans* were inoculated from frozen YPD and grown for 18 hrs in 30°C at 250 rpm. Next day, the cells were subcultured by a 1:100 dilution and grown to approximately an optical density (OD) of 0.4 at 600 nm. After reinoculation, 5 mL of each cell culture was spun down at 4°C, 2000 rpm for 20 min. Cell pellets were re-suspended in 800 µL of PBS and 200 µL of YPD to OD_{600} at 0.2. For preparing cell-bearing capsules, the feed contained 200 µL of the either *P. aeruginosa* or *C. albicans* cell culture, 2 mL of 2 wt% alginate that was dissolved in PBS. Droplets of this feed were introduced into the reservoir solution calcium chloride using a microfluidic setup as described in Chapter 3. The feed solution was flowed at a rate of 10 µL/min using 150 µm capillary while nitrogen gas was pulsed at 1 Hz and pressure

was kept at 7 psi. The capsules were then cultured separately for 12 hrs at 37°C with 250 rpm shaking. To observe inhibition of hyphae by *P. aeruginosa* QS molecule, 10-100 µM of AI-1 was added to the growth media from 10 mM stock in which microcapsules were cultured for 12 hrs.

Preparation of MCCs with Bacteria and Fungus. The microcapsules containing bacteria and fungus was mixed in 1:1 ratio after preparation in PBS and 500 µl of the mixture was added to 5 mL of 2 wt% sodium alginate dissolved in PBS. Then the solution was fed through a glass capillary whose diameter was 400 µm as described previously. The flow rate was 40 µL/min at a pressure of 10 psi, pulsed at 1 Hz. The droplets were collected in 0.1M $CaCl_2$ containing 1 wt% of chitosan oligosaccharide and the MCCs were crosslinked for 30 min on ice. The MCCs were then washed 3 times with normal saline to remove excess calcium and stored in PBS. To observe growth of cells in each inner compartment, the MCCs were incubated at 37 °C in YPD broth while shaken at 250 rpm. For differential change study using antibiotic, 50 µg/ml kanamycin was added to the culture media before incubation. In studies using sodium acetate buffer and CTAB, cells in MCCs were grown for 3 hrs before the addition of 2 mL of acetate buffer or 50 µM of CTAB to the culture media.

Optical Microscopy. Brightfield images of the microcapsules were obtained using an inverted optical microscope (Zeiss Axiovert 135 TV) using a 2.5× objective.

Scanning Electron Microscopy (SEM). To prepare samples for SEM, alginate microcapsules bearing *C. albicans* were dried using a method as described by *Suvarna, et al*.[110] Briefly, microcapsules were kept in 2 wt% glutaraldehyde in PBS and kept at 4°C for 3 hrs. The capsules were then washed in a series of ethanol (50, 70, 90, 100%) for 15 min at each dilution and dried overnight at room temperature. The dried capsules were pipetted onto a double-sided carbon tape that in turn was attached on an SEM stub. The samples were coated with gold and examined on a Tescan XEIA FEG SEM with an accelerating voltage of 5 kV.

Measurement of AI-1 Production from the Encapsulated *P. aeruginosa*. Bioluminescent reporter assay was used to measure level of AI-1 produced by encapsulated *P. aeruginosa*.[111] Condition media was collected by filtering supernatant of capsules from 18 hr incubation through a 0.2 µM filter and stored at −20 °C until needed. For the AI-1 activity assay, *E. coli* luminescent reporter cells with pAL10545 plasmid were grown in LB media overnight. Next day, the cells were diluted 2500 fold in LB media with 50 µg/mL tetracycline and 50 µg/mL kanamycin. Pre-collected condition media samples were diluted in LB to be within the linear range of the assay. Samples for a standard curve of known AI-1 concentrations ranging from 0–60 nM AI-1 in LB were also prepared. 10 µL of the experimental or standard curve samples were added to 90 µL of the reporter cells. Cultures were grown at 30 °C and 250 rpm shaking, and luminescent values were recorded after 3 h using a GloMax®-Multi Jr (Promega, Madison, WI, USA). Each sample was performed in duplicate.

Growth Curve of *C. albicans* and *P. aeruginosa* with CTAB. Growth curves of the fungi and bacteria were obtained by inoculating overnight culture at 1:100 ratio in YPD. CTAB (500 µM) was added to the overnight dilution and cells were grown in incubator shaker at 37 °C and 250 rpm. The growth of the cells was recorded by measuring optical density every 30 min for 6 hrs. The growth was then plotted on a semi-log scale.

4.3 Results and Discussion

4.3.1 MCC Synthesis

The microfluidic setup shown in Figure 4.2 is used to synthesize MCCs with bacteria (*P. aeruginosa*) and fungi (*C. albicans*) in separate inner compartments. First, we make the microcapsules that will serve as inner compartments. Suspensions of the bacteria and fungi in 1% alginate solutions are fed through a 150 µm capillary at a flow rate of 10 µL/min (see Experimental Section for further details). Nitrogen gas, pulsed at 1 Hz, shears off droplets containing cells from the capillary tip. which are collected in the reservoir solution (0.1 M $CaCl_2$ + 1 wt% oligochitosan). The droplets are thereby converted to microcapsules with diameters ~ 200 µm over an incubation time of 30 min, after which they are washed and stored in phosphate-buffered saline (PBS).

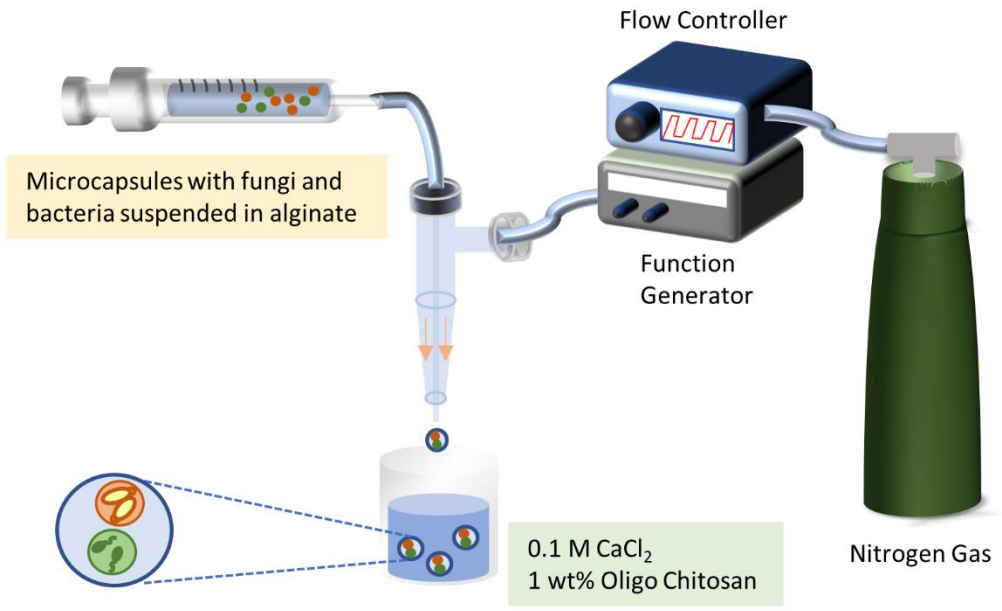

Figure 4.2. Microfluidic synthesis of MCCs with bacteria and fungi. Microcapsules containing each microbe are made first. These are mixed with alginate and used as a feed for the MCCs. The feed solution is flowed through a 400 µm capillary and droplets are sheared off the capillary tip by pulses of nitrogen gas. The droplets are collected in the reservoir, where they are converted to MCCs.

Next, we prepare the feed solution for making the MCCs. Microcapsules containing fungi and the bacteria are suspended in 1 mL of PBS in an equal ratio. The capsule suspension is added to 4 mL of a 2% alginate solution. This feed is flowed through a capillary with a diameter of 400 μm and droplets are again sheared off the capillary tip by nitrogen gas pulsed at 1 Hz (Figure 4.2). The droplets are collected in the same reservoir as above and allowed to incubate for 30 min, whereupon they are converted to MCCs. The MCCs are washed and stored in PBS on ice.

4.3.2 Growth of Fungi and Bacteria in MCCs under Various Conditions

Our MCC construct allows real-time observation of cell growth by optical microscopy. Because the fungi and bacteria are in separate compartments, their growth can each be monitored independently. If there is a change in the environment that affects either bacteria or fungi, the effect on the cells can be observed and quantified. In this regard, Figure 4.3 shows two cases where the *P. aeruginosa* are affected by chemical additives much more than *C. albicans*. In Figure 4.3A, 50 μg/mL of kanamycin is added at $t = 0$ to the growth medium around the MCCs. Kanamycin is an aminoglycoside that is known to kill bacteria by binding to ribosomes and thus blocking protein synthesis.[112] However, kanamycin is expected to be ineffective against fungi as it does not bind to fungal ribosomes.[112]

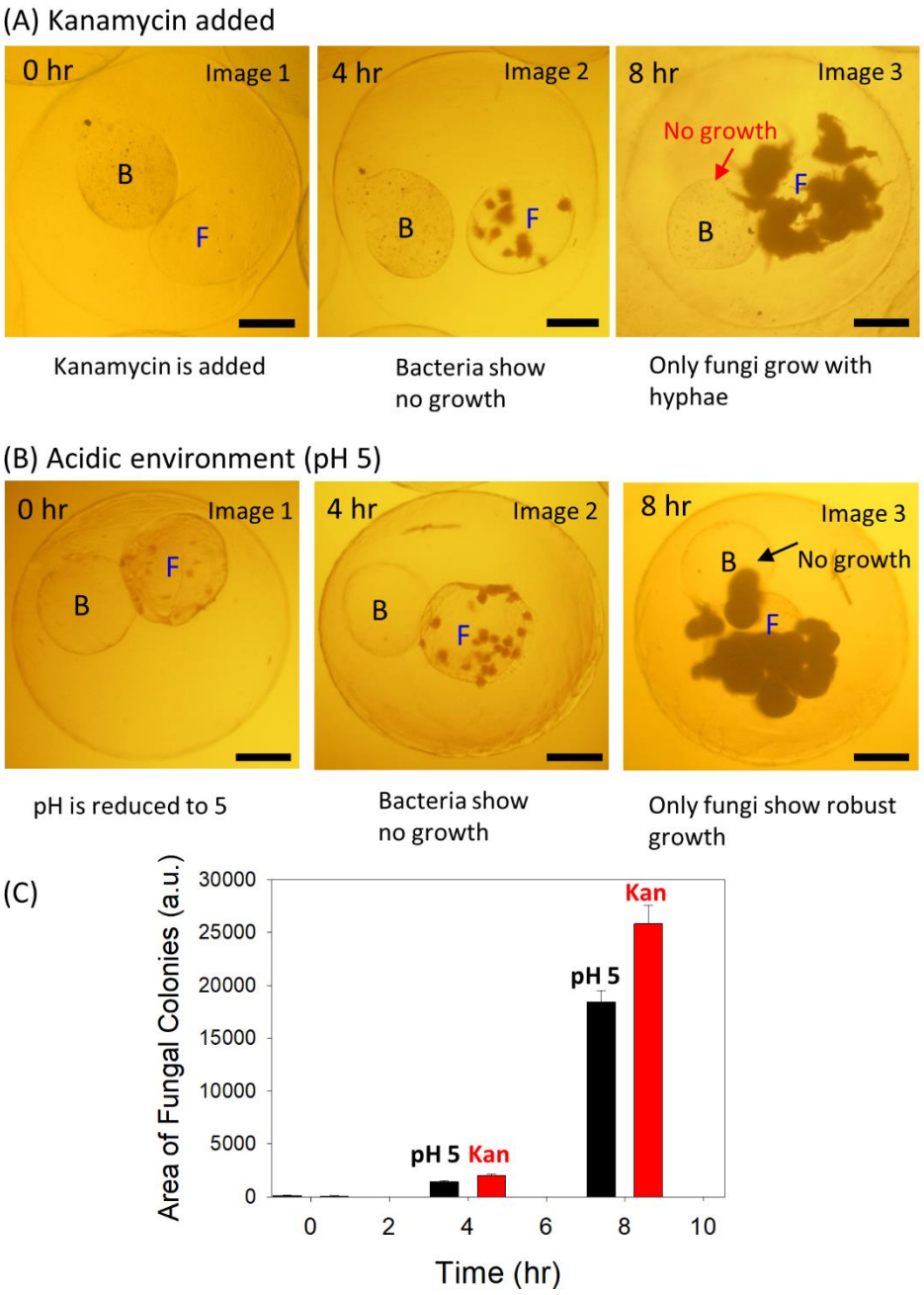

Figure 4.3. MCCs with fungi and bacteria showing preferential growth of the fungi under certain conditions. Optical micrographs at various time points of an MCC with Compartment F containing fungi (*C. albicans*) and Compartment B containing bacteria (*P. aeruginosa*). (A) The presence of 50 µg/mL kanamycin inhibits the growth of bacteria, but the fungi grow uninhibited. (B) When the pH is lowered to 5, again the fungi grow whereas the bacteria show no growth. (C) A graph showing the areas covered by fungal colonies at the 4 h and 8 h time points. The error bars correspond to standard deviations from $n = 10$ observations. (Scale bars in the images: 100 µm.)

The results in Figure 4.3A focus on a typical MCC in the culture and show images at different time points. The MCC has two inner compartments, one with *C. albicans* (Compartment F) and the other with *P. aeruginosa* (Compartment B). Carbon black (CB) nanoparticles are incorporated in trace amounts (~ 0.01%) along with the bacterial feed so that the Compartment B can be distinguished in the images; note that it has a slightly darker hue at $t = 0$ (Image 1). No cell colonies are visible in either compartment at this stage. After 4 h, colonies of fungi (mainy spheroidal) are visible in Compartment F (Image 2), indicating robust fungal growth. However, no growth is observed in Compartment B. At the 8 h mark (Image 3), the fungi have grown further, and large colonies are seen both inside and outside Compartment F. The fungal colonies also show visible hyphae, i.e., thread-like filaments at their edges. Conversely, no growth is observed in Compartment B and this can be attributed to the antibacterial effect of kanamycin.

Similar results are seen for the effects of acidic pH on cell culture (Figure 4.3B). Typical culture of MCCs is done in growth media at neutral pH (7.2 to 7.4). We incubate MCCs under these conditions for 3 h, and by this stage small colonies are visible in Compartment F (Image 1) in a typical MCC. Although not as clearly visible, the bacteria are also growing in Compartment B. At this point, which is $t = 0$ for our pH experiment, we add acetate buffer to the system, bringing the pH down to 5. Image 2, which is after 4 h at pH 5 shows growth of the fungi into colonies containing spheroidal cells, but no growth of the bacteria. Subsequently, at the 8 h mark (Image 3), there is still no growth of the bacteria in Compartment B, but the fungi have grown further and their colonies extend out of Compartment F. Interestingly, the fungal colonies at pH 5 show smooth edges with less

filamentation (indicating that the cells are mostly in yeast rather than hyphal form) compared to those grown at neutral pH in Figure 4.3A.

The pH effects observed in Figure 4.3B are consistent with the reported literature on *C. albicans* and *P. aeruginosa*. Specifically, *P. aeruginosa* cells are known to grow optimally at neutral pH.[113] Acidic pH hinders their growth because it lowers the activity of enzymes in the cells or damages proteins on cell membranes.[114] Fungi like *C. albicans* are more resilient to acidic pH because they have evolved to withstand acidic conditions from fermentation. Unlike bacteria, fungi have a built-in mechanism that allows them to pump extra H^+ ions across the cell membrane and maintain neutral pH in the cells.[115] These aspects explain why the fungi show robust growth in the MCCs whereas the bacteria do not.

Growth of fungi in both the conditions studied in Figure 4.3 can be quantified by image analysis using ImageJ. For this, we measured the areas of the fungal colonies in a given MCC at various time points, and in each case, we sampled at least $n = 10$ MCCs and computed the average. Once small colonies form in Compartment F (e.g., at the 4 h mark), the number of colonies remain the same, but each colony grows in size. When the colonies are large, they overlap on the image, making it difficult to resolve individual ones, which is why we prefer to focus on colony area (Figure 4.3C). The data show that the colonies grow more at neutral pH (in the presence of kanamycin) than at acidic pH. Also, between the 4 and 8 h mark, the fungi grow exponentially and there is a ten-fold increase in colony area in both experiments.

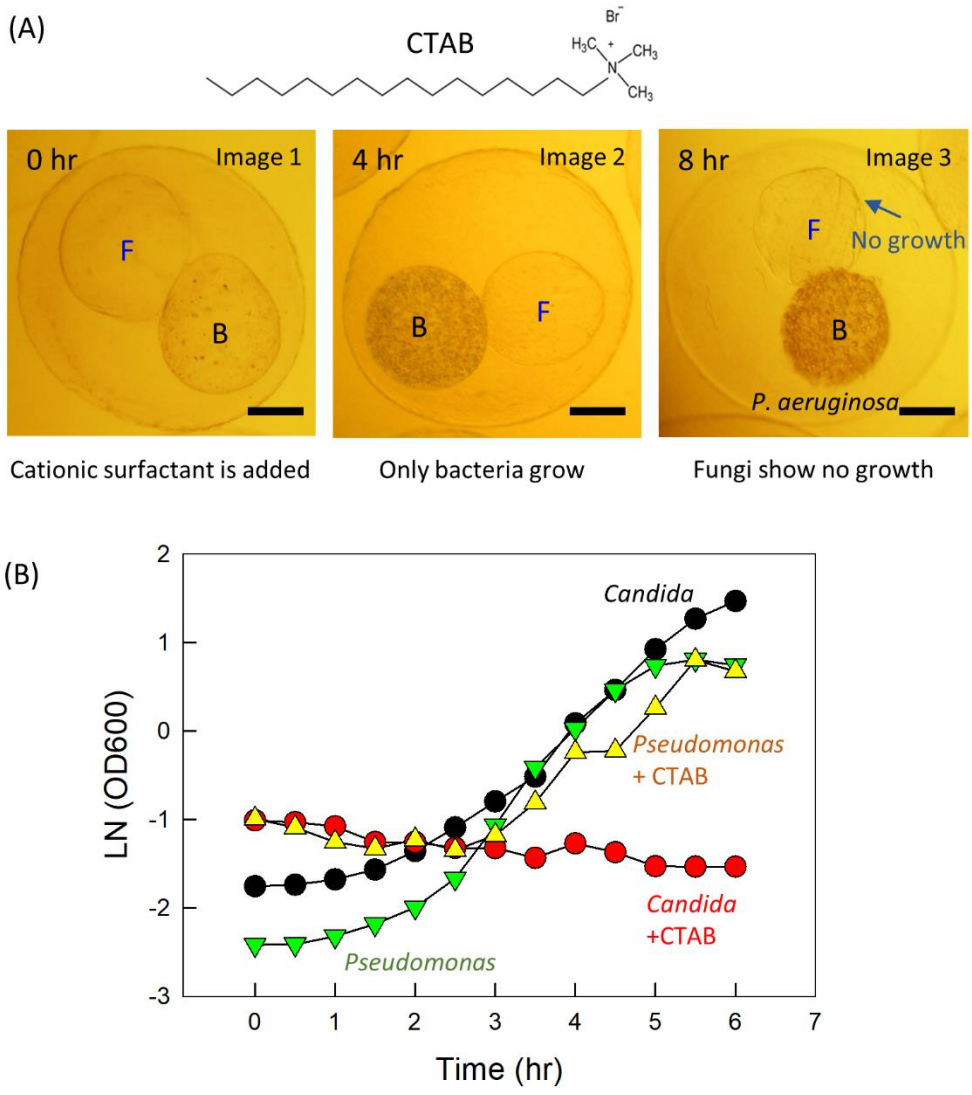

Figure 4.4. MCCs with fungi and bacteria showing preferential growth of the bacteria in the presence of a cationic surfactant. (A) Optical micrographs at various time points of an MCC with Compartment B containing bacteria (*P. aeruginosa*) and Compartment F with fungi (*C. albicans*). The MCC is cultured with 500 µM of the surfactant CTAB (structure shown). Growth is only observed in Compartment B while the fungi are killed by the surfactant. (B) Growth curves (semi-log plot of optical density (OD) vs. time) for *P. aeruginosa* and *C. albicans* cultures grown with and without 500 µM CTAB. *C. albicans* shows no growth when the surfactant is present. (Scale bars in the images: 100 µm)

Next, we demonstrate a scenario where bacteria grow, but not the fungi in the MCC (Figure 4.4). In this case, we add the cationic surfactant cetyl trimethylammonium bromide (CTAB) at a concentration of 500 μM to the culture medium at $t = 0$ and monitor cell growth. The images in Figure 4.4A focus on a typical MCC over time, and as before, the MCC has two inner compartments, one with *C. albicans* (Compartment F) and the other with *P. aeruginosa* (Compartment B). Surfactants are amphiphilic molecules with a hydrophilic head and a hydrophobic tail. In the case of CTAB (structure in Figure 4.4A), it has a C_{16} tail and a cationic head. Microbial cells are expected to have strongly anionic membranes, and as a result, cationic surfactants like CTAB will have a strong propensity to bind and embed in the membranes, thereby disrupting the membranes and causing cell lysis.[116] Indeed, CTAB is reported to have antiviral, antibacterial and antifungal properties.[117]

Interestingly, however, in our experiment we find that CTAB affects only the fungi. Comparing Images 1 to 3 over an 8 h period in Figure 4.4, we see that the *P. aeruginosa* grows undeterred in Compartment B, whereas no growth of the *C. albicans* is observed in Compartment F. Evidently, CTAB binds to fungal membranes and kills the cells whereas it has no effect on the bacteria. These differential effects of CTAB are verified with liquid cultures. Growth curves of *P. aeruginosa* with or without 500 μM CTAB are quite similar (Figure 4.4B), with the cells reaching a similar optical density (OD) over 6 h of culture at 37°C. In contrast, the growth curve of *C. albicans* in the presence of 500 μM CTAB remains flat (near-zero) whereas normal growth is seen in the absence of CTAB. Thus,

CTAB is toxic to fungal cells, but not to *P. aeruginosa*. The latter observation is consistent with studies by other research groups on these bacteria.[118,119]

4.3.3 Morphological Transition of *C. albicans*

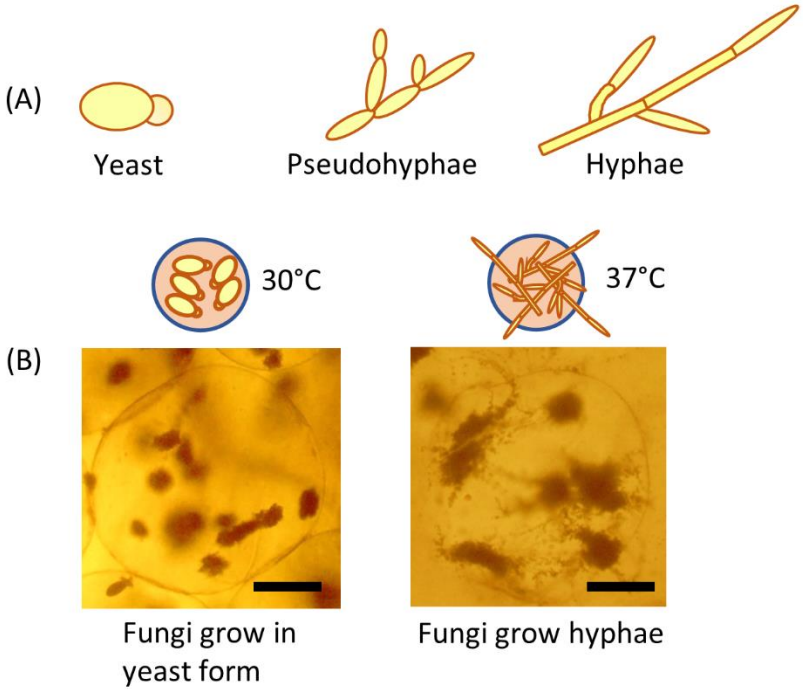

Figure 4.5. Morphology of *C. albicans* at different temperatures. (A) Schematics of the cellular morphology, showing the transition from yeast (spheroidal colonies with smooth edges) to hyphae (multicellular filaments at the edges of colonies). (B) Schematics and optical micrographs showing that *C. albicans* in capsules grown at 30°C take on the yeast form whereas they transition to hyphae at 37°C. The images are taken after 12 h of culture. (Scale bars: 100 μm)

We had previously mentioned in the Introduction that fungi like *C. albicans* can exist as yeast or hyphae, and the transition between the two is dictated by pH, temperature, and various nutrients or chemicals.[107-109] Here, we study the morphological transition as a function of temperature (Figure 4.5). When microcapsules with the fungi are incubated at 30°C, they remain in the yeast form. In this form, the cells proliferate and com together as

dense clusters (colonies) (Figure 4.5A). These colonies look spheroidal or ellipsoidal and have relatively 'smooth' edges. At 37°C, however, a significant fraction of the cells transforms into multicellular filaments, i.e., hyphae. The colonies still have a dense core, but numerous hyphae emanate from their edges, which thereby have a 'rough' appearance.

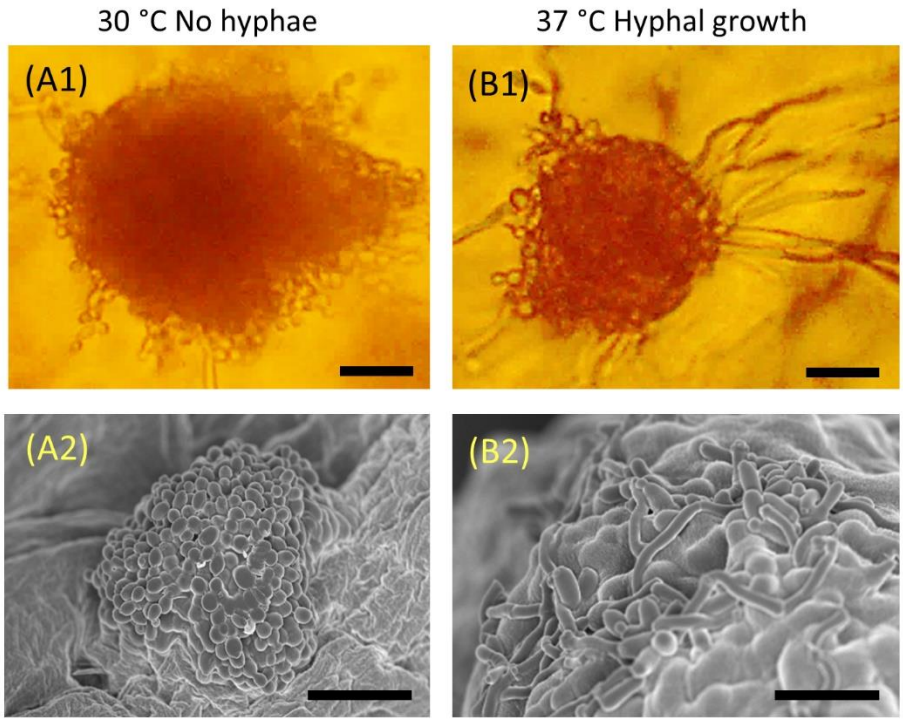

Figure 4.6. Micrographs and SEM images of a single *C. albicans* colony in yeast and hyphal forms. (A) At 30°C, the cells remain in yeast form and few filaments are seen. The SEM shows that the colony is a cluster of multiple cells, each of which is ellipsoidal. (B) At 37°C, the cells transition to hyphae and long filaments grow in random directions from the colony surface. (Scale bar: 20 µm)

To visualize these differences more clearly, Figure 4.6 shows close-up images from optical and SEM microscopy of single colonies. At 30°C (Figure 4.6A), the growing colony does have 'rough' edges, indicating that cells are adding onto the colony, but there are only a few filaments (Image A1). The SEM (Image A2) clearly shows that the colony is a cluster

of many cells, and both the individual cells as well as the colony are ellipsoidal. At 37°C (Figure 4.6B), the morphology is very different. Long filaments (i.e., hyphae) are seen to extend out of the colony in all directions (Image B1). In the SEM (Image B2), the filaments are again seen, but they are collapsed on the capsule during sample preparation for SEM.[110]

4.3.4 Inter-Kingdom Signaling between Fungi and Bacteria in an MCC

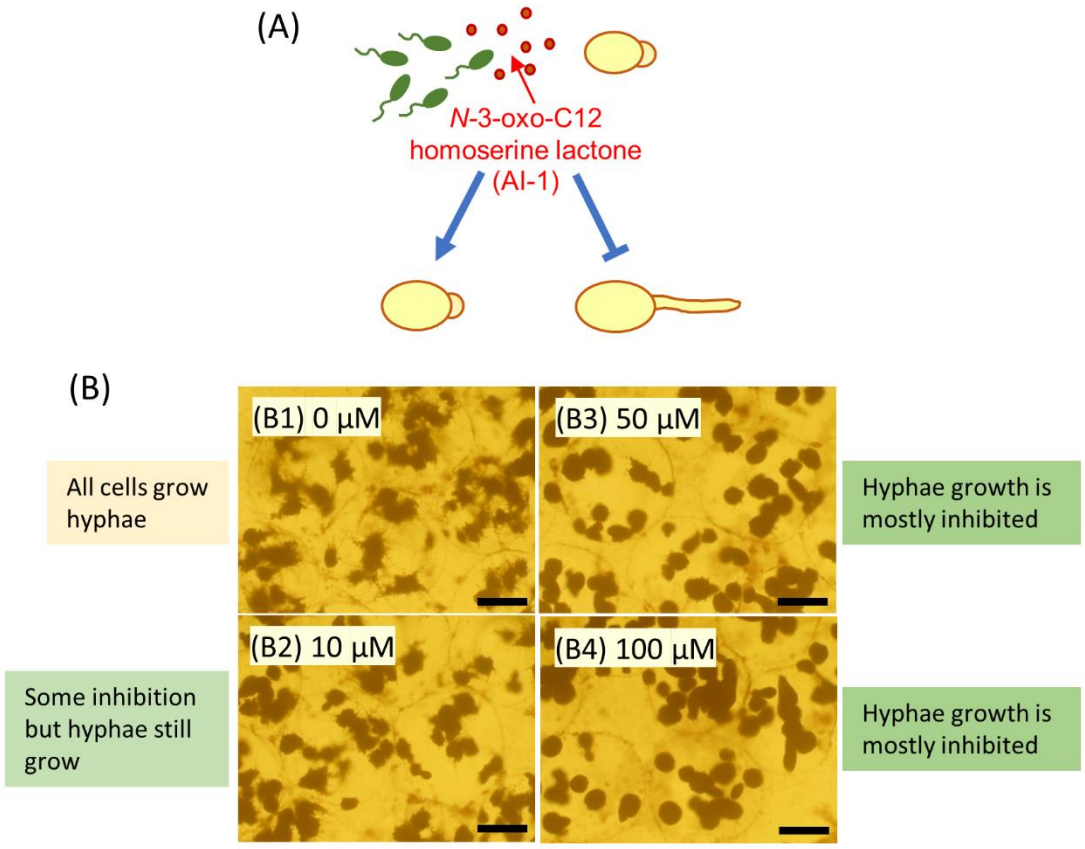

Figure 4.7. Effect of QS molecule (AI-1) produced by *P. aeruginosa* on *C. albicans*. (A) Schematics showing that as *P. aeruginosa* grow, they produce AI-1, which inhibits the transition of *C. albicans* from yeast to hyphae. (B) Morphology of encapsulated *C. albicans* at varying AI-1 concentrations. With no AI-1, hyphae are formed. With increasing AI-1, hyphae are inhibited. (Scale bars: 100 µm)

In the Introduction, we had pointed out that *P. aeruginosa* and *C. albicans* are expected to have an antagonistic relationship within biofilms. This interaction is believed to be mediated by the QS molecule, AI-1, as depicted schematically in Figure 4.7A. AI-1 is expected to inhibit the transition of *C. albicans* from yeast to hyphae.[98-101] To verify this effect, we cultured *C. albicans* in microcapsules and added synthetic AI-1 to the culture medium. Figure 4.7B shows images of capsules at 37°C after 12 h of culture (note that this temperature was found to be suitable for hyphal growth in Figures 4.5 and 4.6). When there is no AI-1 present, the cells do show robust growth with hyphae extending out from all the colonies (Image B1). With 10 μM of AI-1, the hyphae are considerably reduced compared to the control case (Image B2). Increasing the AI-1 to 50 μM (Image B3) and then to 100 μM (Image B4) further reduces the hyphae. In Image B4, the colonies mostly have a spheroidal shape with no hyphae at all around the edges. These results confirm the expected effects of AI-1 on the fungi.

Next, we demonstrate how the above interaction between *P. aeruginosa* and *C. albicans* can be studied using MCCs. We create MCCs with the above bacteria in Compartment B and the fungi in Compartment F. These are cultured at 37°C under normal growth conditions, and the images in Figure 4.8 are of a typical MCC at various time points. At $t = 0$ (Image 1), there are very few cells in both compartments, and we can differentiate Compartment B by its darker hue due to the CB nanoparticles in it. As the bacteria grow in Compartment B, they start to produce AI-1. The AI-1 molecules are small enough so that they can diffuse out of Compartment B into the adjacent Compartment F. After 6 h, colonies of cells are seen in both compartments (Image 2). The colonies are larger in Image

3 (9 h) and Image 4 (12 h). Importantly, the fungal colonies retain a spherical shape without visible hyphae around their edges, as shown also by the close-up image. This is evidently because the AI-1 produced in Compartment B inhibits the yeast-to-hyphae transition in Compartment F. Thus, the MCC experiment directly reveals the cross-talk between the two kingdoms of cells.

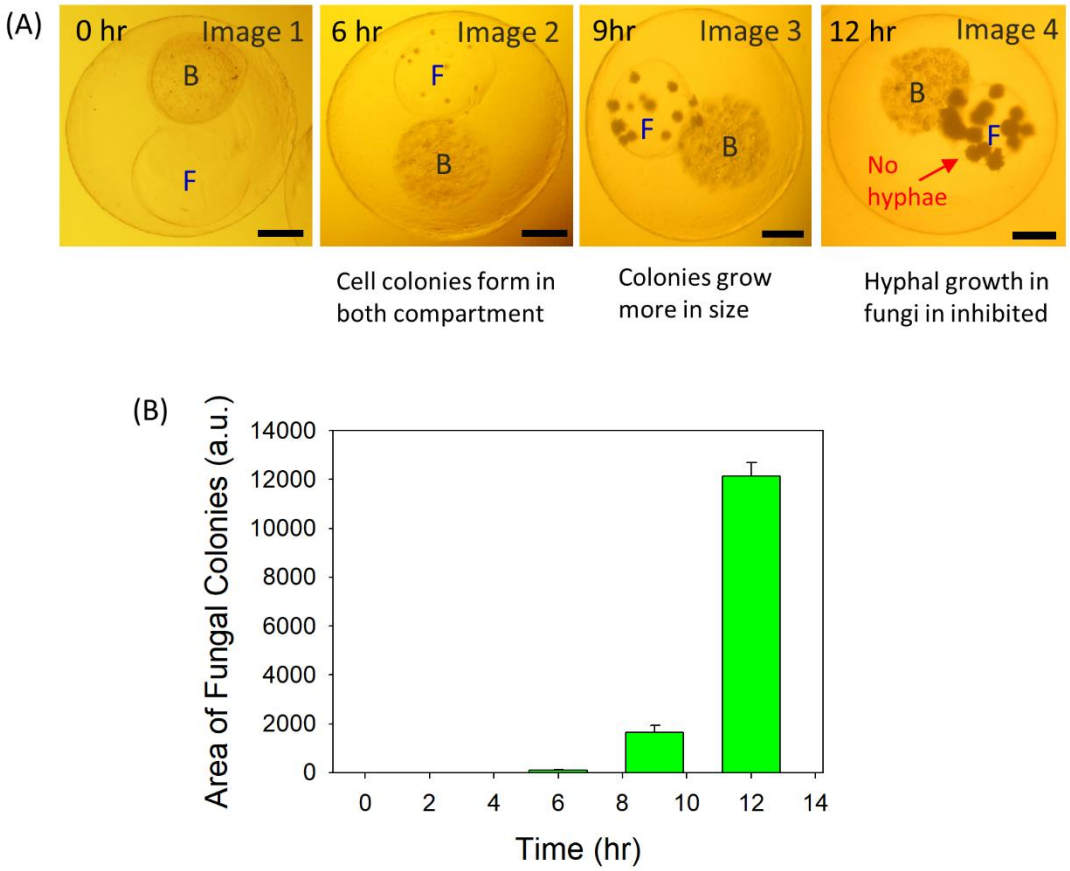

Figure 4.8. Crosstalk between *C. albicans* and *P. aeruginosa* encapsulated in distinct compartments of an MCC. (A) Optical micrographs at various time points of an MCC with Compartments B and F cultured at 37°C. Over 12 h, both cells form colonies in their individual compartments. The fungi in Compartment F do not exhibit hyphae, which is attributed to the diffusion of AI-1 from the bacteria in Compartment B. (B) A graph showing the areas covered by fungal colonies at various time points. The error bars correspond to standard deviations from n = 10 observations. (Scale bars in the images: 100 μm)

We also measured the areas of *C. albicans* colonies at various time points in Figure 4.8A using the same image-analysis procedure used previously in Figure 4.3. The results (Figure 4.8B) show a small increase in colony area from 0 to 9 h and then a sharp increase in this area from 9 to 12 h. As in Figure 4.3, once the colonies form, the number of colonies does not increase much, but each colony grows bigger. To confirm that the fungi are indeed affected by AI-1 produced by the *P. aeruginosa*, we measured how much AI-1 there was in the culture media after 12 h of culture in a sample with 50 MCCs. For this, we used a reporter strain of *E. coli* that produce bioluminescence proportional to the AI-1 concentration (see Experimental Section for details).[111] The culture media was found to contain 20 μM of AI-1. Based on Figure 4.7, this concentration of AI-1 is sufficient to inhibit hyphal growth of the encapsulated fungi.

4.4 Conclusions

In this study, we have demonstrated that multi-compartment capsules (MCCs) can be used as a convenient platform for studying microorganisms from different kingdoms in a systematic and simultaneous manner. The model microbes we chose to study were *P. aeruginosa* (bacteria) and *C. albicans* (fungi), which are known to exist together in biofilms. We created MCCs with the bacteria and fungi in distinct inner compartments. The cells mostly grew within their compartments over the 12 h culture period. We examined conditions where one of the microbes grew preferentially at the expense of the other. In the presence of kanamycin or at acidic pH, only the fungi grew. Conversely, in the presence of a cationic surfactant (CTAB), only the bacteria grew. These model studies demonstrate how our MCC platform could be used in future studies to evaluate new

antimicrobial compounds. Using optical microscopy, we can quantify whether both microbial kingdoms are equally affected by the compound or if the effects are mostly felt by one kind of microbe. In addition, we can also visualize in real-time any changes in the morphology of the fungi caused by the compound or by varying the external conditions. Under normal growth conditions, both the fungi and bacteria grew in the MCCs, but the morphological transition of *C. albicans* from yeast to hyphae was inhibited by AI-1, which is a QS molecule secreted by *P. aeruginosa* in the adjacent compartment. These model studies demonstrate how the MCCs can be used to study cross-kingdom communication between the encapsulated cells in discrete compartments.

Chapter 5
Capsules with 'Smart' Compartments

5.1 Introduction

In this Chapter, we improve the sophistication of multi-compartment capsules (MCCs) by making their inner compartments 'smart', i.e., responsive to various stimuli. As discussed previously, MCCs (also called 'artificial cells' or 'protocells') are container structures with smaller compartments in them. MCCs have been fabricated in recent years using lipids, block copolymers, proteins, and biopolymers.[12-15,24,32,73] Our design for MCCs utilizes the anionic biopolymer alginate, which is widely used in biological and biomedical applications due to its availability, low cost, and its ability to form gels/capsules under mild conditions.[34] We create capsules by complexing alginate with divalent ions like Ca^{2+} and cationic polymers like chitosan. These capsules serve as the inner compartments within an MCC, which is also made using the same scheme.

The inspiration for MCCs comes from the architecture of a eukaryotic cell, which has organelles like mitochondria, lysosomes, and peroxisomes inside them. Importantly, each organelle in a cell has distinct contents and a distinct membrane, which collectively dictate its unique function within a cell.[4,5] The whole cell, of course, is greater than its parts: life is an 'emergent' property exhibited by the cell and not its component parts. Still, within a cell, the organelles have unique chemical attributes. For example, the lysosomes have an *acidic* environment in them that facilitates degradation of proteins.[120] The peroxisomes create an *oxidative* environment within them, which facilitates the metabolism of lipids.[121,122] Another class of organelles present in plant cells are the

chloroplasts, which are involved in capturing energy from sunlight.[123,124] An important point to note here is that the organelles are chemically '*orthogonal*' to one another. For instance, the response to sunlight is unique to chloroplasts while degradation under acidic conditions is unique to lysosomes.

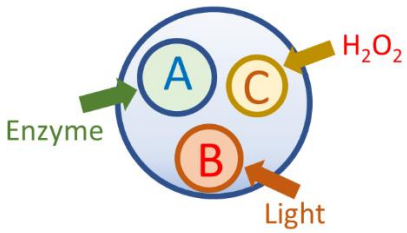

Figure 5.1. A schematic of multicompartment capsule where each inner compartment is responsive to different orthogonal stimuli. Each stimulus (enzyme, hydrogen peroxide, and light) only triggers response from one of the inner capsules which are made of different materials.

The challenge in designing MCCs is (a) to make them with a prescribed number of compartments; (b) to make each compartment distinct in terms of its contents; and (c) to achieve unique functions for each compartment. Our approach to making MCCs using biopolymers allows us to achieve (a) and (b) – for example, we have reported MCCs with two compartments composed of the same chemicals (alginate/Ca^{2+}/chitosan), but each containing a different type of nanoparticle.[23] As a step towards the larger goal of achieving unique functions, in this work, we proceed to create MCCs with *unique chemistry* for each compartment or 'organelle'. We thereby seek to achieve orthogonal responses of the compartments to distinct stimuli. This is indicated by the schematic in Figure 5.1, which shows an MCC with three distinct compartments. One compartment is responsive to an enzyme; another to hydrogen peroxide (H_2O_2); and a third to ultraviolet (UV) light. If the

responses are orthogonal, a given stimulus would only one affect one compartment while the others will remain unaffected. The simplest 'response' in this context is where the entire compartment breaks apart (degrades) upon exposure to the stimulus. Note that the stimuli we have chosen for our studies have biological relevance. We have also avoided the 'obvious' stimuli that researchers have focused on thus far, namely pH and temperature.[19,20,125]

For MCCs with distinctive 'smart' compartments to be useful to researchers for future studies, it is essential for the design to be easy to implement in the lab. Therefore, we would ideally like to make these MCCs using simple, widely available chemicals, and we would like to avoid synthesizing any complex molecules (polymers, lipids, etc.) for this purpose. This is the same philosophy that guided our original study with MCCs. In this regard, we will show that our alginate-based capsules are ideally suited to achieving the type of structure depicted in Figure 5.1. By simply changing the multivalent cations used to crosslink alginate (among Ca^{2+}, Fe^{3+}, Cu^{2+}, etc.) we can achieve unique chemical signatures for our compartments. We will show for example that alginate/Ca^{2+} compartments can be degraded by enzymes from the alginate lyase family whereas alginate/Fe^{3+} ones cannot. Conversely, chemicals such as hydrogen peroxide (H_2O_2) can degrade alginate/Fe^{3+} compartments but not alginate/Ca^{2+} ones. In addition, we will also demonstrate a sequential destruction of two compartments in an MCC that relies on a combination of enzymatic and hydrogen peroxide-induced events.

5.2 Experimental Section

Materials. The following chemicals were obtained from Sigma-Aldrich: alginate (medium viscosity alginic acid, sodium salt from brown algae), xanthan gum, acrylamide (AAm), N,N'-methylenebis(acrylamide) (BIS), sodium acetate, calcium chloride dihydrate ($CaCl_2$), ferrous chloride ($FeCl_3$), ammonium persulfate (APS), tetramethylethylene diamine (TEMED), D-glucose, 1x phosphate buffered saline (PBS), glucose oxidase from Aspergillus niger (100,000 units/g) and alginate lyase (≥10,000 units/g). Hydrogen peroxide (30% in water) was obtained from Thermo-Fisher. Sodium DL-lactate solution was purchased from Santa Cruz Biotechnology. Fluoresbrite™ Carboxy YG 3.0 Micron Microspheres (Cat# 17147-5) were obtained from Polysciences.

Synthesis of Alginate Lyase loaded Capsules. Alginate lyase powder was dissolved in PBS to make a stock solution of 100 units/mL and kept at -20 °C. Sodium alginate was dissolved in sodium acetate buffer (pH 5.2) to make 2 wt% solution. Alginate lyase stock solution was mixed with the alginate solution to reach a desired concentration (0.1, 0.25, 0.5, 0.75, 1.0 unit/mL). Alginate and enzyme mixture was then loaded on a syringe with 22G needle and dropped into 0.1 M $CaCl_2$ solution to create capsules. The capsules were incubated for 1 hr at 4°C for complete crosslinking. After incubation, capsules were washed with DI water and stored in DI water until further use.

Synthesis of Fe (III) crosslinked Alginate Capsules. Sodium alginate was dissolved in 0.9% sodium chloride to prepare 2 wt% alginate solution. The prepared solution was dropped into 0.1 M $FeCl_3$ solution using a syringe with 22G needle to make iron (III)

crosslinked capsules. After incubation, capsules were washed with DI water and stored in DI water until further use.

Synthesis of MCCs with calcium crosslinked and Fe^{3+} crosslinked inner compartments. Capsules crosslinked with $CaCl_2$ and $FeCl_3$ were mixed in equal ratio in 2 wt% alginate solution dissolved in 0.9% sodium chloride. The suspended inner capsules were dropped into 0.1 M $CaCl_2$ solution using a transfer pipette to form multi-compartment capsules (MCCs). The MCCs were incubated for 1hr, washed with DI water and stored in DI water until further use.

Synthesis of MCCs with a polymer shell. To synthesize macro-sized MCCs (~5 mm) with a polymer shell, the MCCs made from the above step was used as a core. The cores were soaked in a 15 mg/mL solution of the initiator APS for 2 min. The APS-loaded cores were transferred to a monomer solution made by dissolving 10 wt% AAm, 0.034 wt% cross-linker (BIS), 1.5 wt% accelerant (TEMED), 1.6 wt% (150 mM) of $CaCl_2$ and in 5mL DI water and 5mL of 1.5 wt% xanthan gum solution. Polymerizations were conducted at room temperature for 5 min. Synthesized MCCs were washed three times with DI water to remove residual chemicals. Capsules were then suspended in DI water for storage. To synthesize micro-sized MCCS (~ 1mm), the feed solution containing 1.5 wt% APS and equal ratio of Ca^{2+} and Fe^{3+} crosslinked microcapsules (~200 µm) suspended in 1 mL of DI water mixed in 5mL of 2 wt% alginate solution was loaded into a syringe and fed through the capillary device mentioned in Chapter 3, with the feed flow rate of 50 µL/min.

Microparticles (~3 um) with green fluorescence was added to microcapsules crosslinked with calcium for enhanced visualization of degradation behavior.

Synthesis of Glucose oxide (GOx) Loaded Capsules. Glucose oxidase (GOx) was dissolved in PBS to make stock solution of 1000 unit/mL. To make GOx loaded capsules, 10μL of the stock solution was first added to 1mL of 2wt % alginate solution dissolved in 1X PBS. This solution was then loaded onto a syringe with a 22G needle and dropped into 0.1M $CaCl_2$ solution. The capsules were crosslinked for 1hr at 4°C for complete crosslinking. After incubation, capsules were washed with DI water and stored in DI water at 4°C until further use.

Capsule Degradation Experiments using Alginate lyases. For degradation of calcium crosslinked capsules loaded with alginate lyase, capsules were placed in 1mL of 1x PBS (pH 7.4) in 24-well petri dish and kept at 37 °C incubator. The degradation of capsules loaded with different concentration of the enzyme was visually verified every 30 min. In a similar manner, for inner compartment degradation of MCCs, an MCC containing one calcium crosslinked inner compartment and one iron (III) crosslinked inner compartment was suspended in 5 mL of 1X PBS in a small vial. To the vial, 0.5 – 1.0 unit/mL of alginate lyase was added and kept at 37°C to observe degradation of the calcium crosslinked compartment.

Capsule Degradation Experiments using H_2O_2. For degradation of Fe^{3+} crosslinked capsules using hydrogen peroxide, the capsules were placed in sodium acetate buffer (pH 5) or normal saline solution. Hydrogen peroxide (1 mM) was added directly to the solution and the capsule degradation was observed at room temperature. For MCC inner compartment degradation experiment, an MCC was placed in 5 mL of sodium acetate buffer in a small vial to which 1mM of hydrogen peroxide was added. The degradation was visually checked every 30 min.

Capsule Degradation Experiments using UV light. The degradation of Fe^{3+} crosslinked capsules under UV light was done along with addition of sodium lactate to the solution capsules were suspended in. The Fe^{3+} capsules were placed in normal saline to which 20 mM of sodium DL-lactate solution was added. The capsules were placed under UV light (MINERALIGHT® LAMP, Model UVGL-58, 365 nm and the degradation of checked every 30 min. For inner compartment degradation, an MCC was placed in 5 mL of normal saline in a small vial, 50 mM of sodium lactate was added and placed under UV light. The degradation of inner compartment was visually checked every 30 min.

Degradation of Capsules using Cascade Reaction. To synthesize MCCs for cascade degradation reaction, GOx loaded capsules and Fe^{3+} crosslinked capsules were mixed with 2 wt% alginate solution and dropped into 0.1 M $CaCl_2$ solution. The MCCs were crosslinked for 1 hr on ice, washed with DI water to remove any excess calcium and stored in DI water until further use. For a degradation study, an MCC was suspended in 5 mL of PBS containing 1 wt% of β-D glucose. The reaction was carried out at room temperature.

Sequential Degradation of MCC Inner Compartments. MCCs with a AAm shell were used in a sequential degradation study. An MCC was placed in 5 mL of normal saline to which 20 mM of sodium DL-lactate solution was added. The MCC was exposed to UV light (365 nm) for 30 min. After complete degradation of a Fe^{3+} crosslinked inner compartment, the same MCC was placed in PBS buffer. 1 unit/mL of alginate lyase was added to trigger degradation of the remaining Ca^{2+} crosslinked inner compartment. Same steps were repeated using micro-scale MCCs with a polymer shell for scaled-down experiment.

Optical Microscopy. Brightfield images of the microcapsules were obtained using an inverted optical microscope (Zeiss Axiovert 135 TV) using a 2.5× objective. Images under brightfield and fluorescence of MCCs were obtained using an Olympus MVX10 microscope. Brightfield and fluorescence images are overlayed using ImageJ software.

5.3 Results and Discussion

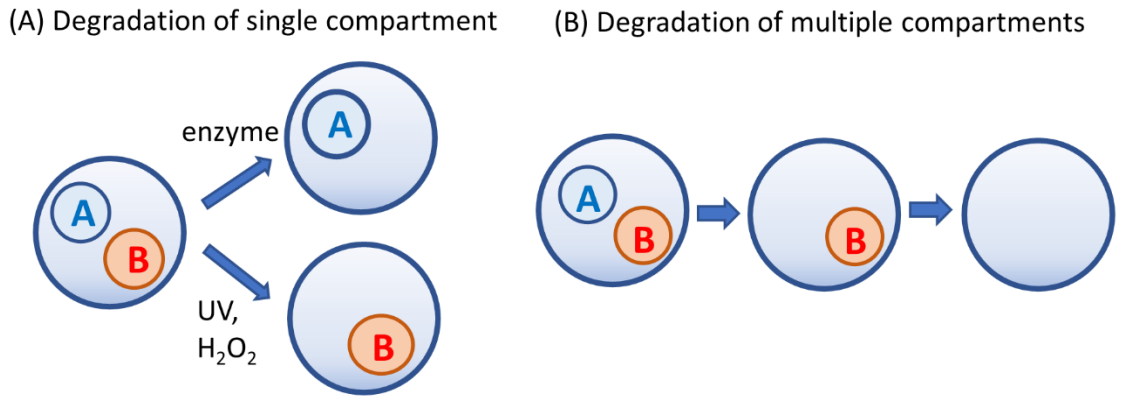

Figure 5.2. Type of degradation that can be triggered using the MCC. (A) Any one of the three stimuli can be used to achieve selective degradation of single compartment. (B) in case of multiple compartment degradation, each stimulus can be applied in series to degrade only one compartment at a time. Selective degradation is possible due to independent responsiveness of inner compartments to different stimuli.

We typically prepared the inner compartments by dropping a 2% alginate solution into 0.1 M Ca^{2+} (or other cations like Fe^{3+}) using a needle and crosslinking for 1 h (see Experimental Section for details). The resulting compartments (~ 500 µm each) are then resuspended in the same alginate solution and dropped into 0.1 M Ca^{2+} to form the multicompartment capsule (MCC) (~ 5 mm diameter). We typically create MCCs with two inner compartments (A and B) where each compartment is responsive to an orthogonal stimulus. Figure 5.2 encompasses most of the results shown in this Chapter. First, we discuss MCCs in which a stimulus (enzyme) triggers degradation of only compartment A while B remains unaffected (Figure 5.2A). Next, we show that other stimuli (hydrogen peroxide, UV light) do the reverse, i.e., degrade B but not A. Thereafter, we show that the stimuli can be applied in series to sequentially degrade one compartment and then the other (Figure 5.2B). Our design thus gives us significant versatility: we can select *which*

compartment to degrade, the *number of compartments* to degrade, as well as the *order* in which they degrade.

5.3.1 Degradation of a Compartment using Enzyme

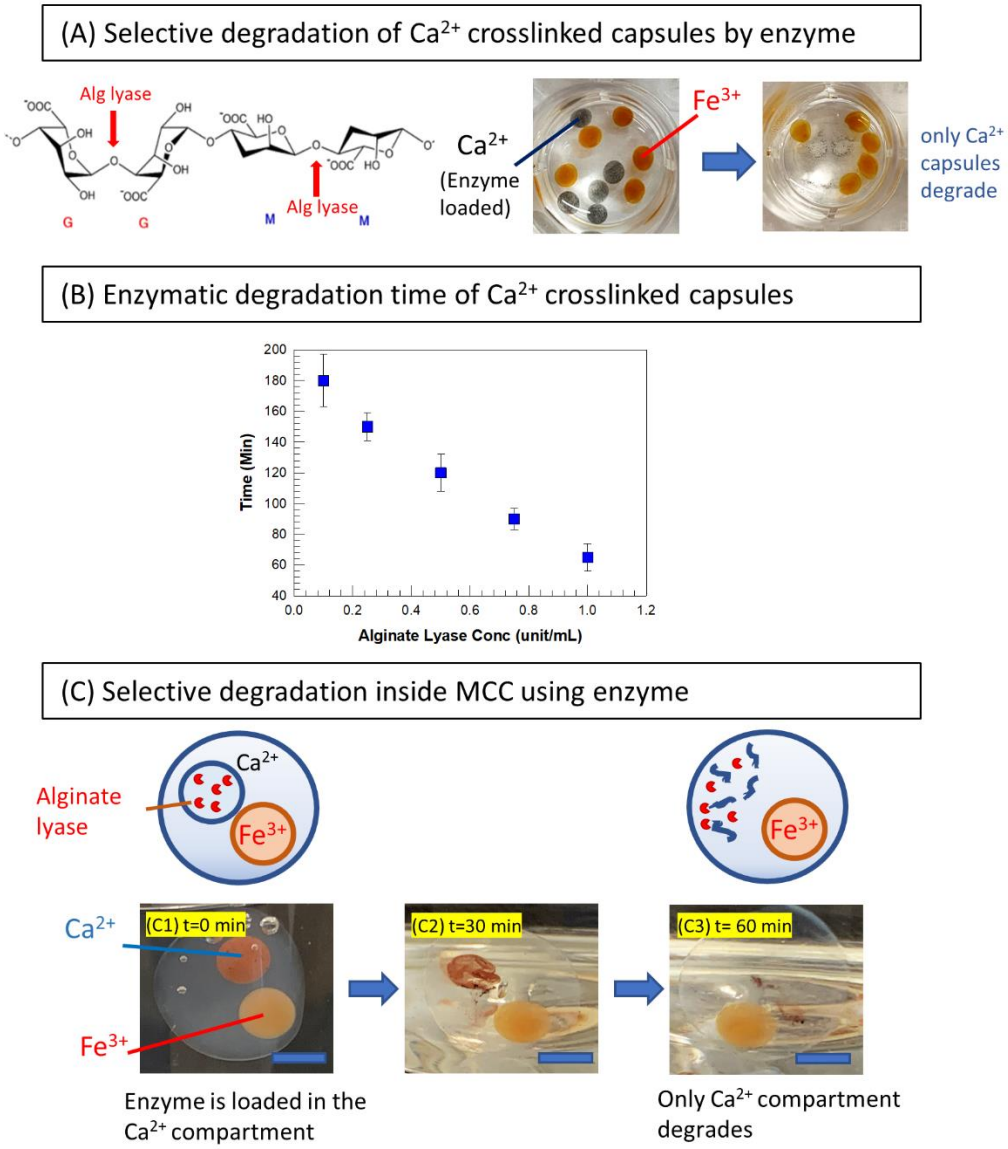

Figure 5.3. Selective degradation of one compartment in an MCC by the alginate lyase enzyme. (A) The enzyme (0.5 units/mL) degrades alginate/Ca^{2+} capsules (black) but not alginate/Fe^{3+} capsules (orange). (B) Time to completely degrade alginate/Ca^{2+} capsules as a function of the enzyme concentration. Error bars are standard deviations from n = 5 measurements. (C) Schematic and photos of an MCC with an alginate/Ca^{2+} compartment (orange) containing 0.5 units/mL of the enzyme and an alginate/Fe^{3+} compartment (yellow). Only the former is degraded over the course of 1 h. (Scale bars: 1 mm)

Alginate capsules can be degraded by enzymes from the alginate lyase family.[61] The enzyme catalyzes the cleavage of alginate chains by β-elimination, where the 4-O-glycosidic bonds between monomers are broken.[62] Thus, long alginate chains are cut into oligomers. The activity of alginate lyase depends on pH, temperature, and the nature of the cation used to crosslink alginate. We exploit the fact that alginate lyase degrades alginate/Ca^{2+} capsules but not alginate/Fe^{3+} capsules (Figure 5.3A). Here, we embedded trace amounts (~ 0.01%) of carbon black nanoparticles (CB-NPs) in the alginate/Ca^{2+} capsules and iron-oxide nanoparticles (IO-NPs) in the alginate/Fe^{3+} capsules – thus, the two capsules have a black and an orange color, respectively. In the presence of 0.5 units/mL of the enzyme, all the alginate/Ca^{2+} capsules degrade completely over the course of 1 h at 37°C. The same result was obtained in two scenarios: (a) if the enzyme was added to the solution around the capsules or (b) if the enzyme was encapsulated in one or both capsules. (Note that enzyme molecules as well as nanoparticles remain sequestered in the capsules – i.e., they do not leak out unless the capsule is degraded.) Furthermore, the time for capsule degradation can be tuned: it is inversely proportional to the concentration of encapsulated enzyme (Figure 5.3B). A linear decrease in this time (for the capsule to be completely degrade) is shown by the data: from ~180 min for 0.1 units/mL of enzyme to from ~ 60 min for 1 unit/mL.

Figure 5.3C shows selective degradation of one compartment in an MCC. The MCC contains an alginate/Ca^{2+} compartment (orange) with 0.5 units/mL of alginate lyase and an alginate/Fe^{3+} compartment (yellow). The colors are due to IO-NPs embedded in the compartments at different concentrations. At t = 0, the MCC is placed in PBS (pH 7.4) at

37°C (Image C1). Within 30 min, the IO-NPs are seen to leak out of the alginate/Ca^{2+} compartment into the solution, which is a sign that the compartment is getting degraded (Image C2). After 1 h, the degradation of the alginate/Ca^{2+} compartment is complete (Image C3), while the alginate/Fe^{3+} compartment remains intact. Incidentally, we have found that we can trigger the onset of this selective degradation. That is, if the MCC is stored in acidic conditions, such as in a sodium acetate buffer (pH 5), no degradation occurs because the alginate lyase has very low activity at pH 5.[63] When the MCC is transferred to PBS, this serves as an "on" switch to start the enzymatic degradation of the alginate/Ca^{2+} compartment.

5.3.2 Degradation of a Compartment using H_2O_2

In the previous example, the enzyme selectively degraded alginate/Ca^{2+} while alginate/Fe^{3+} was spared. Next, we present the reverse scenario, which is caused by H_2O_2. When 0.1 mM of H_2O_2 is introduced under acidic conditions (i.e., in acetate buffer) into a suspension of alginate/Ca^{2+} capsules (black due to CB-NPs) and alginate/Fe^{3+} capsules (yellow), only the latter get degraded over the course of 10 min (Figure 5.4A). This degradation occurs because Fe^{3+} ions are reduced to Fe^{2+} by the H_2O_2 (see reaction). While Fe^{3+} is an effective crosslinker of alginate chains, Fe^{2+} has only a weak affinity for alginate and is thus not a good crosslinker. [67,71] The time for capsule degradation can be tuned like in the enzyme case (Figure 5.4B), with this time decreasing with increasing H_2O_2 concentration (from 120 min for 88 μM H_2O_2 to 5 min for 1 mM).

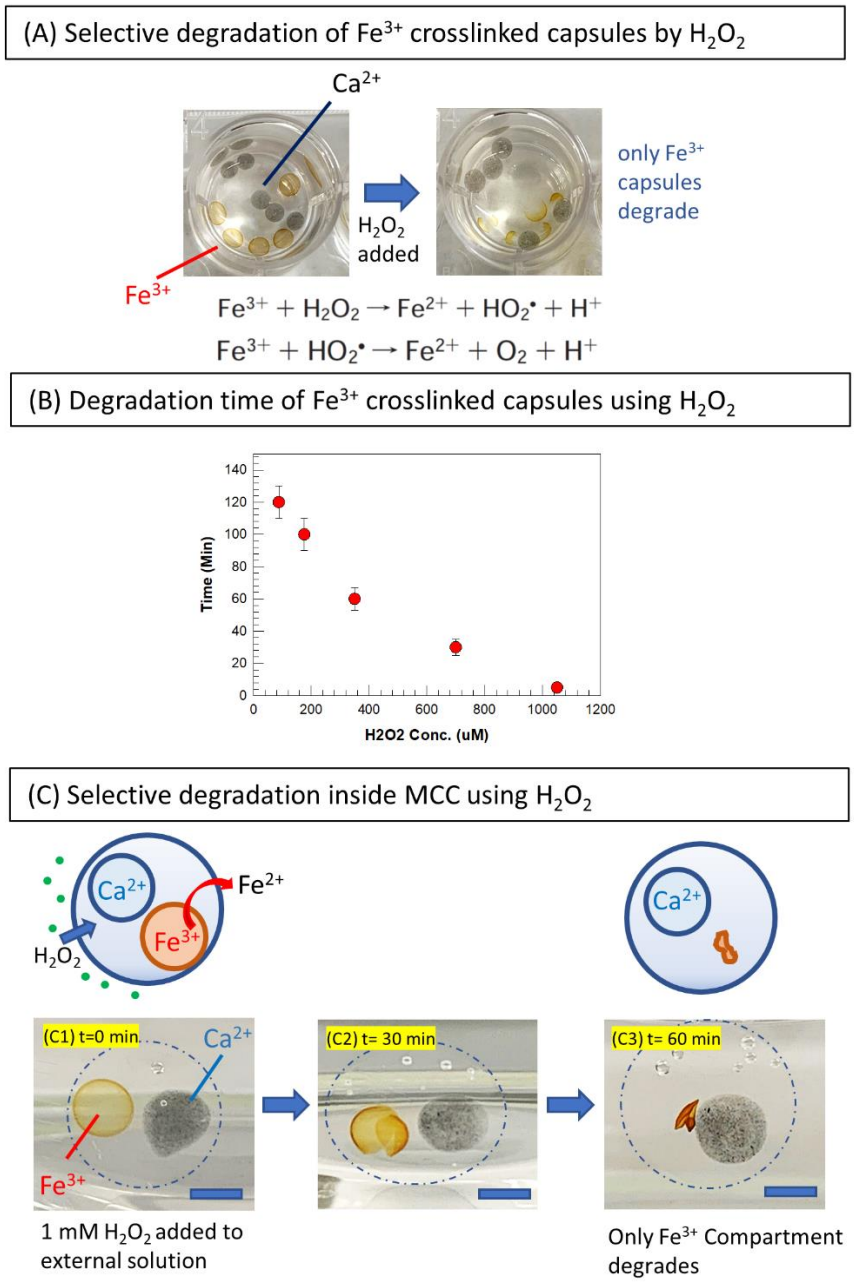

Figure 5.4. Selective degradation of one compartment in an MCC by hydrogen peroxide (H_2O_2). (A) H_2O_2 (0.1 mM) degrades alginate/Fe^{3+} capsules (yellow) but not alginate/Ca^{2+} capsules (black). This is because H_2O_2 reduces Fe^{3+} to Fe^{2+} by the reaction shown (Fe^{2+} has only a weak affinity for alginate). (B) Time to completely degrade alginate/Fe^{3+} capsules as a function of the H_2O_2 concentration. Error bars are standard deviations from n = 5 measurements. (C) Schematic and photos of an MCC with alginate/Ca^{2+} (black) and alginate/Fe^{3+} (yellow) compartments. Upon addition of 1 mM H_2O_2, only the latter is degraded over the course of 1 h. (Scale bars: 0.5 mm)

Figure 5.4C shows selective degradation of an MCC compartment. At t = 0, the MCC is placed in acetate buffer (pH 5.2) and 0.1 mM H_2O_2 is added (Image C1). Within 30 min, the yellow alginate/Fe^{3+} compartment is broken in half (Image C2) and this degradation is complete in 1 h (Image C3). The alginate/Ca^{2+} compartment (black) remains intact. Note that the bubbles in the images are O_2 generated by the H_2O_2 decomposition. The onset of this selective degradation can also be triggered. That is, if the MCC is stored at neutral pH, such as in PBS, no degradation occurs because the H_2O_2 acts a reducing agent only at low pH.[66,126] When acetate buffer is added, it serves an "on" switch for H_2O_2 to start degrading the alginate/Fe^{3+} compartment. Thus, the degradations by enzyme and H_2O_2 are complementary: the former is switched on under neutral conditions, while the latter is switched on under acidic conditions.

5.3.3 Degradation of a Compartment using UV Light

Aside from H_2O_2, Fe^{3+} ions can also be reduced photochemically.[68,69,71] In the presence of an α-hydroxy carboxylate like sodium lactate (SLac), alginate/Fe^{3+} gels can be converted to sols by UV irradiation. The mechanism involves the carboxylates (COO^-) on SLac competing with those on alginate for binding to Fe^{3+}. That Fe^{3+}-COO^- complex absorbs UV light, which induces transfer of an electron from the COO^- to the Fe^{3+} ion (Figure 5.5A).[67] The net result is that Fe^{3+} gets reduced to Fe^{2+}. Similar reduction does not occur with Ca^{2+}, and thus alginate/Ca^{2+} capsules are unaffected by UV light.

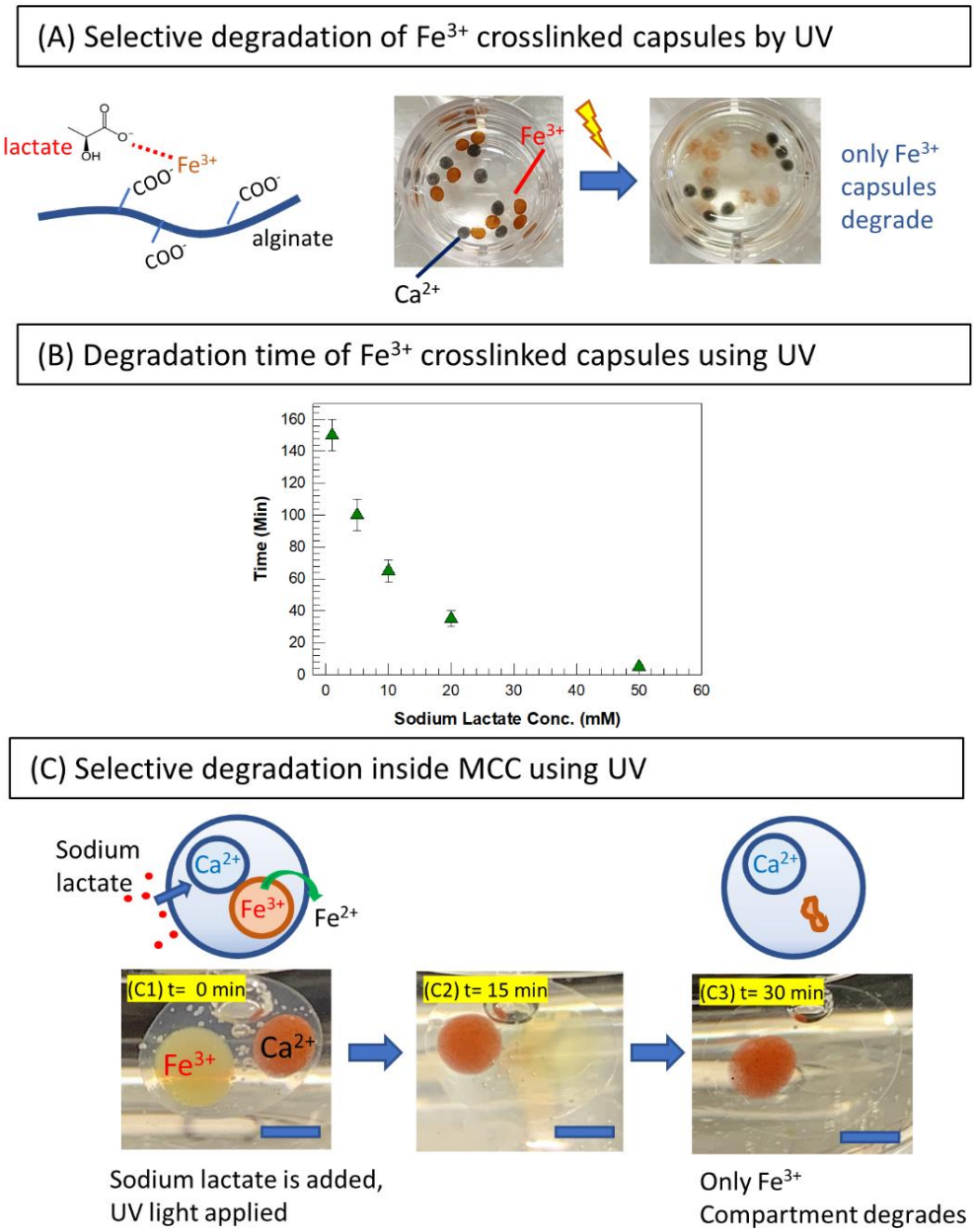

Figure 5.5. Selective degradation of one compartment in an MCC by UV light. (A) In the presence of 20 mM sodium lactate (SLac), UV irradiation degrades alginate/Fe^{3+} capsules (orange) but not alginate/Ca^{2+} capsules (black). This is because the Fe^{3+} is photoreduced to Fe^{2+} by the scheme shown (Fe^{2+} has only a weak affinity for alginate). (B) Time to completely degrade alginate/Fe^{3+} capsules by UV light as a function of the SLac concentration. Error bars are standard deviations from n = 5 measurements. (C) Schematic and photos of an MCC with alginate/Ca^{2+} (orange) and alginate/Fe^{3+} (yellow) compartments. In the presence of 20 mM SLac, only the latter is degraded over the course of 30 min. (Scale bars: 1 mm.)

We can thus explore light as another stimulus for compartment degradation. For the experiment in Figure 5.5A, we take a suspension of alginate/Ca^{2+} capsules (black due to CB-NPs) and alginate/Fe^{3+} capsules (orange due to IO-NPs) in acetate buffer containing 20 mM SLac and expose to UV light (365 nm). Only the alginate/Fe^{3+} capsules degrade over 30 min. The time for UV degradation is dictated by the SLac concentration (Figure 5.5C), and it decreases from 150 min for 1 mM SLac to 5 min for 50 mM SLac. Figure 5.5C shows selective degradation of an MCC compartment by UV light. An MCC in acetate buffer with 20 mM SLac is exposed to UV light at t = 0 (Image C1). The yellow alginate/Fe^{3+} compartment is partially degraded in 15 min (Image C2) and fully degraded in 30 min. The alginate/Ca^{2+} compartment (orange) remains intact.

5.3.4 Degradation of a MCC Compartment in Cascade Processes

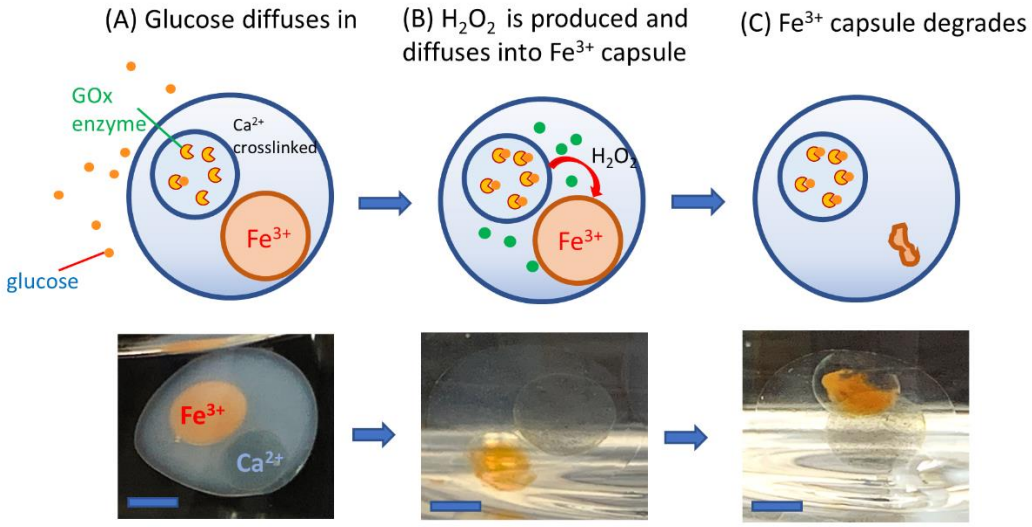

Figure 5.6. Degradation of a compartment in an MCC by a reaction in an adjacent compartment. The MCC is in PBS and has an alginate/Fe^{3+} compartment (orange) and an alginate/Ca^{2+} compartment (black) that contains 100 units/mL of GOx enzyme. At t = 0, 1% glucose is added to the solution. The glucose is catalyzed by GOx to produce H_2O_2, which degrades the alginate/Fe^{3+} compartment over 60 min. (Scale bars: 1 mm.)

Next, we demonstrate a cascade reaction in an MCC, which results in the selective degradation of one compartment. We use glucose oxidase (GOx), an enzyme that catalyzes the oxidation of glucose, with the by-product being H_2O_2 (see reaction in Figure 5.6). This H_2O_2 is then used to degrade a compartment. Cascade processes inside multicompartment capsules using GOx and glucose have been reported previously, but not to degrade a compartment.[29,30,127,128] Figure 5.6A presents the design of our MCC. It has an alginate/Fe^{3+} compartment (orange due to IO-NPs) and an alginate/Ca^{2+} compartment (black due to CB-NPs) that contains 100 units/mL of GOx. At t = 0, 1% glucose is added to the PBS solution surrounding the MCC. The glucose diffuses into the alginate/Ca^{2+} compartment where it is catalyzed by GOx to produce H_2O_2. The H_2O_2 cascades down to the alginate/Fe^{3+} compartment (Figure 5.6B), where it reduces Fe^{3+} to Fe^{2+} and hence the compartment

degrades over the course of 60 min (Figure 5.6C). Thus, we successfully employ an enzyme and its reaction product in sequence to induce selective degradation of a compartment.

5.3.5 Degradation of MCC Compartments in a Sequential Process

One limitation of the MCCs in the previous sections is that both the inner compartments (i.e., the 'organelles') as well as the MCC lumen around them (i.e., the 'cytoskeleton') are made of alginate. Typically, the lumen is a gel of alginate/Ca^{2+}. Thus, if the alginate lyase enzyme is used to degrade an alginate/Ca^{2+} compartment, it will also eventually degrade the outer matrix, and thereby the whole MCC. We wanted to explore a scenario where the MCC itself would stay intact even though the compartments inside it were degraded. For this, we used the procedure described in Chapter 3 to add a shell of covalently crosslinked polymer around an MCC. The MCC (~ 2 mm) is loaded with a free-radical initiator, then suspended in a solution of acrylamide (AAm) for 5 min (see Experimental Section for details). This results in a layer of chemically crosslinked AAm gel (~ 100 μm thick) around the entire MCC (Image 1 in Figure 5.7).

The above 'reinforced' MCC is then placed in PBS at room temperature for the degradation studies. First, we add 20 mM SLac to the solution and expose the MCC to UV light. Within 30 min, the alginate/Fe^{3+} compartment is degraded (Image 2). We then add 10 units/mL of alginate lyase and thereby the alginate/Ca^{2+} compartment is degraded over the next 30 min (Image 3). Even after the compartments are degraded, the thin AAm layer around the MCC is still visible. Because this layer is formed by covalent bonds, it makes the construct robust and allows it to survive the degradation steps.

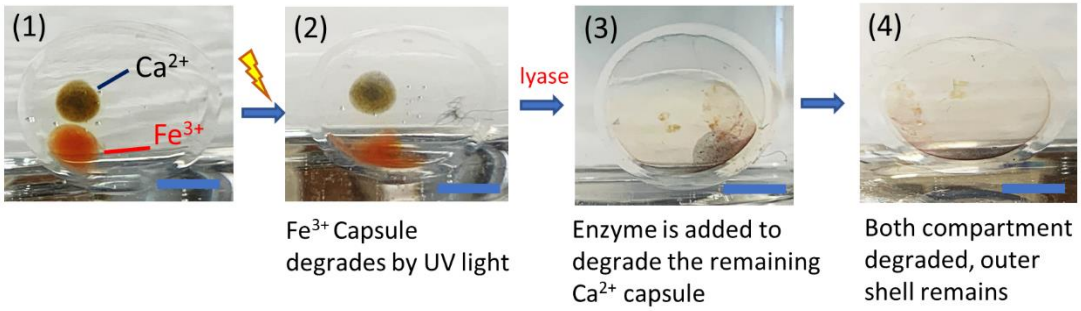

Figure 5.7 Sequential degradation of both compartments in a reinforced MCC. (1) The MCC has an alginate/Fe^{3+} compartment (orange) and an alginate/Ca^{2+} compartment (black). It also has an outer shell of acrylamide (AAm) to add stability to the structure. (2) First, the alginate/Fe^{3+} compartment is degraded by adding 20 mM sodium lactate and exposing to UV light for 30 min. (3) Next, 10 units/mL of alginate lyase are added to degrade the alginate/Ca^{2+} compartment. (4) After both compartments are degraded, the AAm shell remains, keeping the structure intact. (Scale bars: 1 mm.)

Next, we demonstrate the same sequential degradation of compartments in a reinforced MCC at a smaller (micro) scale. For this, we made the inner compartments of alginate/Fe^{3+} and alginate/Ca^{2+} with a diameter ~ 200 µm using the microfluidic device described in Chapter 3. The compartments were then encapsulated in MCCs and in that same step, we also added the AAm shell to reinforce the MCC. In a batch of such MCCs, some have two and others have three inner compartments (Panels 1 in Figure 5.8). The alginate/Fe^{3+} compartments have iron-oxide nanoparticles (IO-NPs), which allows them to be distinguished in brightfield images. To visualize the alginate/Ca^{2+} compartments, we included trace amounts (~ 0.01%) of green fluorescent nanoparticles (GF-NPs) in the feed while making them, and hence those compartments can be distinguished by fluorescence microscopy. Brightfield and fluorescence images are combined using ImageJ for the images shown in Figure 5.8.

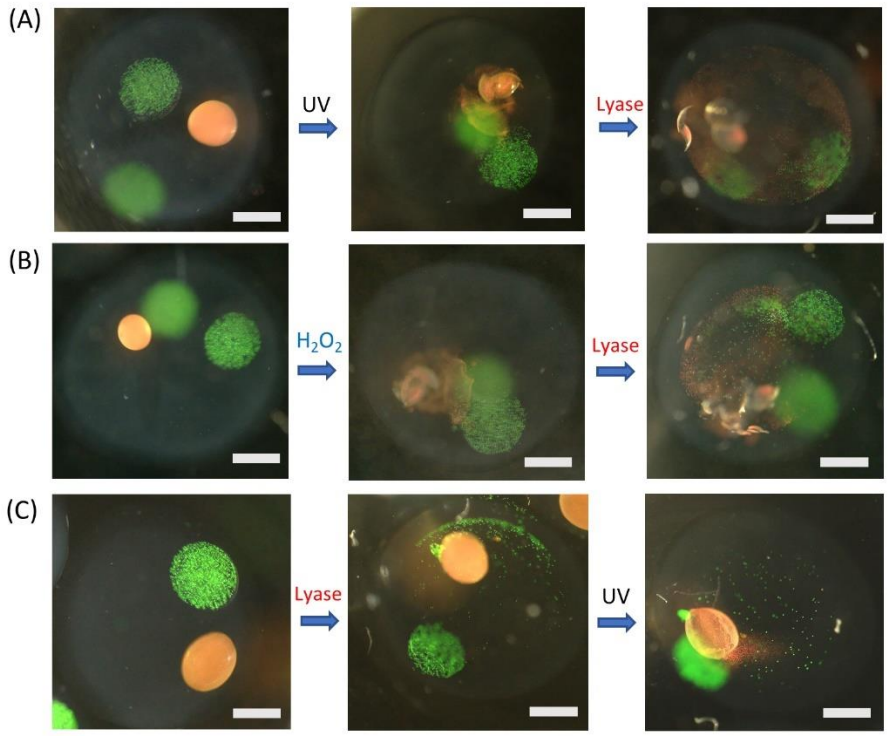

Figure 5.8 Sequential degradation of both compartments in reinforced microscale MCCs. (A) Degradation of inner micro-compartments inside MCC with a polymer shell. Inner compartments are each crosslinked with Ca^{2+} (green) and Fe^{3+} (orange) ions. Fluorescent microparticles are added to the calcium crosslinked compartment for visualization. A compartment crosslinked with iron is degraded first using photoreduction. Alginate lyase (10 units/mL) is added subsequently to degrade the remaining compartment. (B) Fe^{3+} compartment is degraded first with 1 mM hydrogen peroxide followed by 10 units/mL of alginate lyase. (C) In this case, alginate lyase is added first to degrade Ca^{2+} compartment. Remaining compartment is degraded by photoreduction of Fe^{3+} to Fe^{2+} using UV and sodium lactate. (Scale bars: 200 µm)

When 20 mM sodium lactate is added and the MCC is shone with UV light for 30 min, Fe^{3+} crosslinked inner capsule degrades (Figure 5.8A, panel 2). The remaining inner compartment crosslinked with calcium ions is degraded by addition of 10 units/mL alginate (Figure 5.8A, panel 3). The degradation of the calcium crosslinked compartment can be verified by spread of the fluorescent green particles inside the MCC. A brightfield image

and a fluorescent image of the MCC are combined using ImageJ software to better visualize the degradation.

Furthermore, different stimuli used throughout in this study can be mix and matched to achieve the same result. Hydrogen peroxide (1mM) is used in place of UV light to degrade the Fe^{3+} crosslinked inner capsule (Figure 5.8B). Upon exposure to hydrogen peroxide, cracks appear on the surface of the inner capsule and the capsule degrades in about 20 min (Figure 5.8B, panel 2). In a similar manner, 10 units/mL of alginate lyase is added next to degrade the other compartment (Figure 5.8B, panel 3). Lastly, we change the order of degradation and apply alginate lyase first to degrade the calcium crosslinked compartment. In Figure 5.8(C), 10 units/mL of alginate lyase is added to the outer solution first, indicated by the spread of fluorescent particles (panel 2). After 30 min, 20mM sodium lactate is added and the MCC is placed under UV light for 30 min to degrade the remaining Fe^{3+} crosslinked compartment (Figure 5.8C, panel 3). In all three cases, even after completing inner compartment degradation, the polymer shell lends structural integrity to the MCC allowing the outer capsule to remain intact.

5.4 Conclusions

In this chapter, we have demonstrated that we can selectively degrade inner compartments of an MCC using alginate capsules that are crosslinked by Ca^{2+} or Fe^{3+} as inner compartments. The capsules crosslinked with Ca^{2+} are degraded by an enzyme, alginate lyase, which cuts alginate chains into smaller oligomers thereby degrading the matrix forming the capsule. In case of capsules crosslinked with Fe^{3+} are degraded by

reducing Fe^{3+} to Fe^{2+} which has weaker affinity for the alginate. The reduction can be achieved by using hydrogen peroxide or employing a photoreduction by UV light and sodium lactate. We also demonstrate a cascade style degradation by encapsulating glucose oxide in one of the inner compartments which is placed next to a Fe^{3+} crosslinked inner capsule. When glucose is added, it combined with the encapsulated enzyme producing hydrogen peroxide. The produced hydrogen peroxide diffuses to the next compartment, resulting in its degradation. Finally, we show sequential degradation of the inner compartments inside an MCC with a polymer shell. By applying two different stimuli in a sequential order, we can trigger degradation of one inner capsule followed by degradation of the next compartment. The polymer shell allows the MCCs to remain intact even after complete degradation of all inner compartments. The ability to selectively degrade inner compartments may prove useful in controlled release of encapsulated payloads in an environment where multiple stimuli are present.

Chapter 6
Recommendations and Future Work

6.1 Project Summary

In this dissertation, we have presented biomimetic polymer capsules with novel designs that are inspired by structure that are found in nature. We developed a single-step synthesis method to generate core-shell microcapsules with an alginate core and a polymer shell which resembles multilayered structures such as an onion. A multi-compartment capsules that mimic a eukaryotic cell was also generated and used in studies of response and interaction of the encapsulated cells and selective degradation of inner compartments.

In Chapter 3, we introduced an adaptation of "inside-out" method of synthesizing capsules whose core is alginate and shell composed of a covalently crosslinked polymer network. We devised a new synthesis method using a microfluidic device where microcapsules (~200 μm) with an alginate core and a polymer shell were generated in a single step. Alginate solution mixed with an initiator solution was introduced into a receiving solution consisting of monomer, crosslinker and/or accelerant. The polymerization of the polymer layer on the core surface was performed both using thermal initiator and UV initiator. Bacterial and mammalian cells were encapsulated inside the core-shell microcapsules to demonstrate improved mechanical stability over alginate microcapsules as well as biocompatibility of the synthesis method.

In Chapter 4, we demonstrated that multi-compartment capsules (MCCs) could be used as a useful platform to study cell-cell signaling and changes in behavior of the encapsulated cells using microorganisms from different kingdoms. Fungi (*C. albicans*) and bacteria (*P. aeruginosa*) were encapsulated in distinct inner compartment. When exposed to chemicals, cell growth was observed only in one of the compartments containing fungi in case of kanamycin and low pH, and the bacteria compartment in case of cationic surfactants (CTAB). Cell-cell signaling behavior was also confirmed based on reduced hyphae formation of the fungi in presence of AI-1 secreted by the bacteria. The MCCs provided physical separation between the cells in each inner compartment and allowed real-time observation of any changes in cell behavior, an advantage over studies using liquid culture or agar plates.

In Chapter 5, we employed the same MCC construct to demonstrate selective degradation of the inner compartments. Microcapsules used as inner compartments were crosslinked with two different cations (Ca^{2+} and Fe^{3+}) to enable selective degradation of only one of the inner compartments under different stimuli such as enzyme, hydrogen peroxide and UV. We also showed a cascade type degradation of the inner capsule where stimulus (H_2O_2) was generated by the enzyme encapsulated in one of the compartments which was then passed onto the next compartment to trigger its degradation. Sequential degradation of both inner compartments using different stimuli was also demonstrated using an MCC with a polymer shell. We believe that our findings would serve as a useful tool in future studies where selective release of encapsulated materials are desired.

6.2 Recommendations for Future Work

6.2.1 Future Work for Polymer Shell Capsules Containing Cells

In Chapter 3, we demonstrate that we can synthesize core-shell microcapsules with various types of polymers that are compatible for cell encapsulation. We show that bacteria and mammalian cells can remain viable and functional inside the capsules, but further work where we can utilize the stability of the microcapsules may be interesting. Gut microbiome and their effects on the host's health has received increasing attention recently. Despite active research efforts, retrieval of bacteria from fecal samples remains as an inconvenient step in related studies. Our microcapsules have a protective layer of polymer shell that can keep the encapsulated bacteria inside the capsule while traveling down the GI tract (< 24 hrs) and the extra layer can provide protection against pH changes and external stresses to the encapsulated cells. In this regard, the polymer microcapsules can serve as a useful tool, allowing easy retrieval of the samples. Moreover, we have in our library various reporter strains that can detect certain chemical in the environment (e.g. hydrogen peroxide, nitric oxide, pyocyanin) which are found in high concentration around inflammation sites and report the concentration by producing fluorescent protein. If we encapsulate such reporter cells inside the polymer shell microcapsules and send it down the GI tract, it can serve as a biological sensor that can report presence and/or concentration of chemicals of interest without need for collecting and analyzing composition of microbes from fecal samples.

Additional work with encapsulated fungi in polymer shell microcapsules would be also of great interest. Studies on behavior of fungal hyphae have shown that the formation of hyphae and how it behaves (i.e. change directions, different penetration depth) are

affected by type of surfaces they encounter. Therefore, studying how the fungi form hyphae inside capsules made of different biopolymers with various modulus might be an interesting study. Preliminary studies with *C. albicans* inside polymer shell capsules using acrylamide and polymer shell demonstrated that the fungi could maintain viability and show robust growth inside the microcapsules. Synthesizing a shell with various types of polymers that exhibit different hardness and robustness will also add values to study of *C. albicans* encapsulation in hydrogel capsules.

Furthermore, encapsulation of fungi and bacteria in an MCC in Chapter 4 may prove useful in futures studies of antibacterial and antifungal agents. As multiple strains of microorganisms from different kingdoms can be encapsulated inside a single construct, effects of various agents can be tested simultaneously without having to prepare multiple samples of liquid cultures of agar plates which can be often time consuming. Growth of each encapsulated strain can be tracked real-time simply by observing the MCC under a microscope. Testing various concentrations of candidate agents can be performed easily by placing several capsules in multi-well plates. Therefore, the MCC design could be a simple yet useful tool in this regard.

6.2.2. Future Work for Capsules with Smart Inner Compartments

In Chapter 5, we show that individual inner compartment inside an MCC which are crosslinked with different multivalent cations can be used for selective degradation. We also demonstrate that the construct can be scaled down to include inner compartments whose size falls within a few hundred microns. Smaller inner compartments can be created using the same microfluidic device which are less than hundred microns or other techniques for creating microcapsules can be used for the synthesis. With further scaling down, it would be interesting to encapsulate biological payloads such as enzyme or live cells inside the MCC and show their release from the inner compartment. Alginate lyase has been demonstrated to be safe for encapsulated cells in previous studies and can be easily used in our system for future studies of cell encapsulation and their release. Furthermore, the low concentration of hydrogen peroxide that can degrade the capsules (1-10 mM) have been shown to be non-toxic to bacteria and can be used as a stimulus to degrade the inner capsule and release the cells. An MCC with multiple compartments each containing different types of enzymes can also be constructed to study more interesting enzymatic cascade reactions. Overall, any future studies on release of biological molecules or cells from the micro MCCs in a selective manner would be a very interesting work.

References

[1] Sheikhpour, M.; Barani, L.; Kasaeian, A. “Biomimetics in drug delivery systems: A critical review.” *J Control Release* **2017**, *253*, 97-109.

[2] Vincent, J. F. V. “Biomimetics — a review.” *Proc. IMechE* **2009**, *223*, 919-939.

[3] Chaffey, N. “Alberts, B., Johnson, A., Lewis, J., Raff, M., Roberts, K. and Walter, P. Molecular biology of the cell. 4th edn.” *Ann Bot* **2003**, *91*, 401-401.

[4] Chen, A. H.; Silver, P. A. “Designing biological compartmentalization.” *Trends Cell Biol* **2012**, *22*, 662-70.

[5] Yewdall, N. A.; Mason, A. F.; van Hest, J. C. M. “The hallmarks of living systems: towards creating artificial cells.” *Interface Focus* **2018**, *8*, 15.

[6] van Dongen, S. F. M.; Nallani, M.; Cornelissen, J.; Nolte, R. J. M.; van Hest, J. C. M. “A Three-Enzyme Cascade Reaction through Positional Assembly of Enzymes in a Polymersome Nanoreactor.” *Chem.-Eur. J.* **2009**, *15*, 1107-1114.

[7] Antipov, A. A.; Sukhorukov, G. B.; Mohwald, H. “Influence of the ionic strength on the polyelectrolyte multilayers' permeability.” *Langmuir* **2003**, *19*, 2444-2448.

[8] Agarwal, P.; Choi, J. K.; Huang, H. S.; Zhao, S. T.; Dumbleton, J.; Li, J. R.; He, X. M. “A Biomimetic Core-Shell Platform for Miniaturized 3D Cell and Tissue Engineering.” *Part. Part. Syst. Charact.* **2015**, *32*, 809-816.

[9] Ma, M. L.; Chiu, A.; Sahay, G.; Doloff, J. C.; Dholakia, N.; Thakrar, R.; Cohen, J.; Vegas, A.; Chen, D. L.; Bratlie, K. M.; Dang, T.; York, R. L.; Hollister-Lock, J.; Weir, G. C.; Anderson, D. G. “Core-Shell Hydrogel Microcapsules for Improved Islets Encapsulation.” *Adv. Healthc. Mater.* **2013**, *2*, 667-672.

[10] Perez, R. A.; Kim, H. W. “Core-shell designed scaffolds for drug delivery and tissue engineering.” *Acta Biomater.* **2015**, *21*, 2-19.

[11] Zhu, K. X.; Yu, Y. R.; Cheng, Y.; Tian, C. H.; Zhao, G.; Zhao, Y. J. “All-Aqueous-Phase Microfluidics for Cell Encapsulation.” *ACS Appl. Mater. Interfaces* **2019**, *11*, 4826-4832.

[12] Li, S. B.; Wang, X. J.; Mu, W.; Han, X. J. “Chemical Signal Communication between Two Protoorganelles in a Lipid-Based Artificial Cell.” *Anal. Chem.* **2019**, *91*, 6859-6864.

[13] Tiourina, O. P.; Radtchenko, I.; Sukhorukov, G. B.; Mohwald, H. "Artificial cell based on lipid hollow polyelectrolyte microcapsules: Channel reconstruction and membrane potential measurement." *J. Membr. Biol.* **2002**, *190*, 9-16.

[14] Martino, C.; Kim, S. H.; Horsfall, L.; Abbaspourrad, A.; Rosser, S. J.; Cooper, J.; Weitz, D. A. "Protein Expression, Aggregation, and Triggered Release from Polymersomes as Artificial Cell-like Structures." *Angew. Chem.-Int. Edit.* **2012**, *51*, 6416-6420.

[15] Meng, F. H.; Engbers, G. H. M.; Feijen, J. "Biodegradable polymersomes as a basis for artificial cells: encapsulation, release and targeting." *J. Control. Release* **2005**, *101*, 187-198.

[16] Yi, Q. Y.; Sukhorukov, G. B. "UV light stimulated encapsulation and release by polyelectrolyte microcapsules." *Adv. Colloid Interface Sci.* **2014**, *207*, 280-289.

[17] Kolesnikova, T. A.; Gorin, D. A.; Fernandes, P.; Kessel, S.; Khomutov, G. B.; Fery, A.; Shchukin, D. C.; Mohwald, H. "Nanocomposite Microcontainers with High Ultrasound Sensitivity." *Adv. Funct. Mater.* **2010**, *20*, 1189-1195.

[18] Huang, X. N.; Du, F. S.; Ju, R.; Li, Z. C. "Novel acid-labile, thermoresponsive poly(methacrylamide)s with pendent ortho ester moieties." *Macromol. Rapid Commun.* **2007**, *28*, 597-603.

[19] Lvov, Y.; Antipov, A. A.; Mamedov, A.; Mohwald, H.; Sukhorukov, G. B. "Urease encapsulation in nanoorganized microshells." *Nano Lett.* **2001**, *1*, 125-128.

[20] Dejugnat, C.; Sukhorukov, G. B. "PH-responsive properties of hollow polyelectrolyte microcapsules templated on various cores." *Langmuir* **2004**, *20*, 7265-7269.

[21] Marguet, M.; Bonduelle, C.; Lecommandoux, S. "Multicompartmentalized polymeric systems: towards biomimetic cellular structure and function." *Chem Soc Rev* **2013**, *42*, 512-29.

[22] Huang, X.; Voit, B. "Progress on multi-compartment polymeric capsules." *Polym. Chem.* **2013**, *4*, 435-443.

[23] Lu, A. X.; Oh, H.; Terrell, J. L.; Bentley, W. E.; Raghavan, S. R. "A new design for an artificial cell: polymer microcapsules with addressable inner compartments that can harbor biomolecules, colloids or microbial species." *Chem. Sci.* **2017**, *8*, 6893-6903.

[24] Deng, N. N.; Yelleswarapu, M.; Zheng, L. F.; Huck, W. T. S. "Microfluidic Assembly of Monodisperse Vesosomes as Artificial Cell Models." *J. Am. Chem. Soc.* **2017**, *139*, 587-590.

[25] Peters, R.; Marguet, M.; Marais, S.; Fraaije, M. W.; van Hest, J. C. M.; Lecommandoux, S. "Cascade Reactions in Multicompartmentalized Polymersomes." *Angew. Chem.-Int. Edit.* **2014**, *53*, 146-150.

[26] Hindley, J. W.; Elani, Y.; McGilvery, C. M.; Ali, S.; Bevan, C. L.; Law, R. V.; Ces, O. "Light-triggered enzymatic reactions in nested vesicle reactors." *Nat Commun* **2018**, *9*, 1093.

[27] Hu, J.; Liu, S. S.; Deng, W. J. "Dual responsive linalool capsules with high loading ratio for excellent antioxidant and antibacterial efficiency." *Colloid Surf. B-Biointerfaces* **2020**, *190*, 10.

[28] Kreft, O.; Skirtach, A. G.; Sukhorukov, G. B.; Mohwald, H. "Remote control of bioreactions in multicompartment capsules." *Adv. Mater.* **2007**, *19*, 3142-+.

[29] Godoy-Gallardo, M.; Labay, C.; Trikalitis, V. D.; Kempen, P. J.; Larsen, J. B.; Andresen, T. L.; Hosta-Rigau, L. "Multicompartment Artificial Organelles Conducting Enzymatic Cascade Reactions inside Cells." *ACS Appl. Mater. Interfaces* **2017**, *9*, 15907-15921.

[30] Delcea, M.; Yashchenok, A.; Videnova, K.; Kreft, O.; Mohwald, H.; Skirtach, A. G. "Multicompartmental micro- and nanocapsules: hierarchy and applications in biosciences." *Macromol Biosci* **2010**, *10*, 465-74.

[31] Dowling, M. B.; Bagal, A. S.; Raghavan, S. R. "Self-Destructing "Mothership" Capsules for Timed Release of Encapsulated Contents." *Langmuir* **2013**, *29*, 7993-7998.

[32] Wei, O. Y.; Chen, H. M.; Jones, M. L.; Metz, T.; Haque, T.; Martoni, C.; Prakash, S. "Artificial cell microcapsule for oral delivery of live bacterial cells for therapy: design, preparation, and in-vitro characterization." *J. Pharm. Pharm. Sci.* **2004**, *7*, 315-324.

[33] Zarket, B. C.; Raghavan, S. R. "Onion-like multilayered polymer capsules synthesized by a bioinspired inside-out technique." *Nat. Commun.* **2017**, *8*.

[34] Lee, K. Y.; Mooney, D. J. "Alginate: Properties and biomedical applications." *Prog. Polym. Sci.* **2012**, *37*, 106-126.

[35] Jen, A. C.; Wake, M. C.; Mikos, A. G. "Review: Hydrogels for cell immobilization." *Biotechnol. Bioeng.* **1996**, *50*, 357-364.

[36] Gasperini, L.; Mano, J. F.; Reis, R. L. "Natural polymers for the microencapsulation of cells." *J. Royal Soc. Interface* **2014**, *11*, 20140817.

[37] Rinaudo, M. “Main properties and current applications of some polysaccharides as biomaterials.” *Polym. Int.* **2008**, *57*, 397-430.

[38] Gupta, A.; Terrell, J. L.; Fernandes, R.; Dowling, M. B.; Payne, G. F.; Raghavan, S. R.; Bentley, W. E. “Encapsulated fusion protein confers "sense and respond" activity to chitosan-alginate capsules to manipulate bacterial quorum sensing.” *Biotechnol. Bioeng.* **2013**, *110*, 552-562.

[39] Banerjee, A.; Arha, M.; Choudhary, S.; Ashton, R. S.; Bhatia, S. R.; Schaffer, D. V.; Kane, R. S. “The influence of hydrogel modulus on the proliferation and differentiation of encapsulated neural stem cells.” *Biomaterials* **2009**, *30*, 4695-4699.

[40] Bashan, Y.; Hernandez, J. P.; Leyva, L. A.; Bacilio, M. “Alginate microbeads as inoculant carriers for plant growth-promoting bacteria.” *Biol. Fertil. Soils* **2002**, *35*, 359-368.

[41] Haque, T.; Chen, H.; Ouyang, W.; Martoni, C.; Lawuyi, B.; Urbanska, A. M.; Prakash, S. “In vitro study of alginate-chitosan microcapsules: an alternative to liver cell transplants for the treatment of liver failure.” *Biotechnol. Lett.* **2005**, *27*, 317-322.

[42] Lim, F.; Sun, A. M. “Microencapsulated islets as bioartificial endocrine pancreas.” *Science* **1980**, *210*, 908-910.

[43] Prakash, S.; Chang, T. M. S. “Microencapsulated genetically engineered live E-coli DH5 cells administered orally to maintain normal plasma urea level in uremic rats.” *Nat. Med.* **1996**, *2*, 883-887.

[44] Sarker, B.; Rompf, J.; Silva, R.; Lang, N.; Detsch, R.; Kaschta, J.; Fabry, B.; Boccaccini, A. R. “Alginate-based hydrogels with improved adhesive properties for cell encapsulation.” *Int. J. Biol. Macromol.* **2015**, *78*, 72-78.

[45] Tan, W. H.; Takeuchi, S. “Monodisperse alginate hydrogel microbeads for cell encapsulation.” *Adv. Mater.* **2007**, *19*, 2696-2701.

[46] Yoo, I. K.; Seong, G. H.; Chang, H. N.; Park, J. K. “Encapsulation of Lactobacillus casei cells in liquid-core alginate capsules for lactic acid production.” *Enzyme Microb. Technol.* **1996**, *19*, 428-433.

[47] Ma, Y. J.; Dong, W. F.; Hempenius, M. A.; Mohwald, H.; Vancso, G. J. “Redox-controlled molecular permeability of composite-wall microcapsules.” *Nat. Mater.* **2006**, *5*, 724-729.

[48] Leslie, S. K.; Cohen, D. J.; Sedlaczek, J.; Pinsker, E. J.; Boyan, B. D.; Schwartz, Z. "Controlled release of rat adipose-derived stem cells from alginate microbeads." *Biomaterials* **2013**, *34*, 8172-84.

[49] Ashton, R. S.; Banerjee, A.; Punyani, S.; Schaffer, D. V.; Kane, R. S. "Scaffolds based on degradable alginate hydrogels and poly(lactide-co-glycolide) microspheres for stem cell culture." *Biomaterials* **2007**, *28*, 5518-25.

[50] Orive, G.; Hernandez, R. M.; Gascon, A. R.; Calafiore, R.; Chang, T. M. S.; De Vos, P.; Hortelano, G.; Hunkeler, D.; Lacik, I.; Shapiro, A. M. J.; Pedraz, J. L. "Cell encapsulation: Promise and progress." *Nat. Med.* **2003**, *9*, 104-107.

[51] Nicodemus, G. D.; Bryant, S. J. "Cell encapsulation in biodegradable hydrogels for tissue engineering applications." *Tissue Eng. B-Rev.* **2008**, *14*, 149-165.

[52] Rana, D.; Tabasum, A.; Ramalingam, M. "Cell-laden alginate/polyacrylamide beads as carriers for stem cell delivery: preparation and characterization." *RSC Adv.* **2016**, *6*, 20475-20484.

[53] Darnell, M. C.; Sun, J. Y.; Mehta, M.; Johnson, C.; Arany, P. R.; Suo, Z. G.; Mooney, D. J. "Performance and biocompatibility of extremely tough alginate/polyacrylamide hydrogels." *Biomaterials* **2013**, *34*, 8042-8048.

[54] Orive, G.; Hernandez, R. M.; Gascon, A. R.; Igartua, M.; Pedraz, J. L. "Survival of different cell lines in alginate-agarose microcapsules." *Eur. J. Pharm. Sci.* **2003**, *18*, 23-30.

[55] Yao, R.; Zhang, R. J.; Luan, J.; Lin, F. "Alginate and alginate/gelatin microspheres for human adipose-derived stem cell encapsulation and differentiation." *Biofabrication* **2012**, *4*, 025007.

[56] De Castro, M.; Orive, G.; Hernandez, R. M.; Gascon, A. R.; Pedraz, J. L. "Comparative study of microcapsules elaborated with three polycations (PLL, PDL, PLO) for cell immobilization." *J. Microencapsul.* **2005**, *22*, 303-315.

[57] Lee, K. G.; Park, T. J.; Soo, S. Y.; Wang, K. W.; Kim, B. H.; Park, J. H.; Lee, C. S.; Kim, D. H.; Lee, S. J. "Synthesis and utilization of E. coli-encapsulated PEG-based microdroplet using a microfluidic chip for biological application." *Biotechnol. Bioeng.* **2010**, *107*, 747-751.

[58] Hunt, N. C.; Smith, A. M.; Gbureck, U.; Shelton, R. M.; Grover, L. M. "Encapsulation of fibroblasts causes accelerated alginate hydrogel degradation." *Acta Biomater.* **2010**, *6*, 3649-3656.

[59] Shoichet, M. S.; Li, R. H.; White, M. L.; Winn, S. R. "Stability of hydrogels used in cell encapsulation: An in vitro comparison of alginate and agarose." *Biotechnol. Bioeng.* **1996**, *50*, 374-381.

[60] Martinez, C. J.; Kim, J. W.; Ye, C. W.; Ortiz, I.; Rowat, A. C.; Marquez, M.; Weitz, D. "A microfluidic approach to encapsulate living cells in uniform alginate hydrogel microparticles." *Macromol. Biosci.* **2012**, *12*, 946-951.

[61] Blanco-Cabra, N.; Paetzold, B.; Ferrar, T.; Mazzolini, R.; Torrents, E.; Serrano, L.; M, L. L.-S. "Characterization of different alginate lyases for dissolving Pseudomonas aeruginosa biofilms." *Sci Rep* **2020**, *10*, 9390.

[62] Zhu, Y.; Wu, L.; Chen, Y.; Ni, H.; Xiao, A.; Cai, H. "Characterization of an extracellular biofunctional alginate lyase from marine Microbulbifer sp. ALW1 and antioxidant activity of enzymatic hydrolysates." *Microbiol Res* **2016**, *182*, 49-58.

[63] Huang, G.; Wang, Q.; Lu, M.; Xu, C.; Li, F.; Zhang, R.; Liao, W.; Huang, S. "AlgM4: A New Salt-Activated Alginate Lyase of the PL7 Family with Endolytic Activity." *Mar Drugs* **2018**, *16*.

[64] Campbell, K. T.; Stilhano, R. S.; Silva, E. A. "Enzymatically degradable alginate hydrogel systems to deliver endothelial progenitor cells for potential revasculature applications." *Biomaterials* **2018**, *179*, 109-121.

[65] Liu, X.; Zuo, Y.; Sun, J.; Guo, Z.; Fan, H.; Zhang, X. "Degradation regulated bioactive hydrogel as the bioink with desirable moldability for microfluidic biofabrication." *Carbohydr Polym* **2017**, *178*, 8-17.

[66] De Laat, J.; Gallard, H. "Catalytic decomposition of hydrogen peroxide by Fe(III) in homogeneous aqueous solution: Mechanism and kinetic modeling." *Environ. Sci. Technol.* **1999**, *33*, 2726-2732.

[67] Narayanan, R. P.; Melman, G.; Letourneau, N. J.; Mendelson, N. L.; Melman, A. "Photodegradable iron(III) cross-linked alginate gels." *Biomacromolecules* **2012**, *13*, 2465-71.

[68] Chakraborty, I. "Fe (III)-Coordinated Hydrogel and Photo-Induced Sol-Gel Process—A Case Study." *Int. J. Eng. Sci. Math* **2018**, *7*, 1-11.

[69] Bruchet, M.; Mendelson, N.; Melman, A. "Photochemical Patterning of Ionically Cross-Linked Hydrogels." *Processes* **2013**, *1*, 153-166.

[70] Veres, P.; Sebok, D.; Dekany, I.; Gurikov, P.; Smirnova, I.; Fabian, I.; Kalmar, J. "A redox strategy to tailor the release properties of Fe(III)-alginate aerogels for oral drug delivery." *Carbohydr Polym* **2018**, *188*, 159-167.

[71] Giammanco, G. E.; Sosnofsky, C. T.; Ostrowski, A. D. “Light-Responsive Iron(III)-Polysaccharide Coordination Hydrogels for Controlled Delivery.” *ACS Appl. Mater. Interfaces* **2015**, *7*, 3068-3076.

[72] Delcea, M.; Mohwald, H.; Skirtach, A. G. “Stimuli-responsive LbL capsules and nanoshells for drug delivery.” *Adv Drug Deliv Rev* **2011**, *63*, 730-47.

[73] Peters, R. J.; Marguet, M.; Marais, S.; Fraaije, M. W.; van Hest, J. C.; Lecommandoux, S. “Cascade reactions in multicompartmentalized polymersomes.” *Angew Chem Int Ed Engl* **2014**, *53*, 146-50.

[74] Whitesides, G. M. “The origins and the future of microfluidics.” *Nature* **2006**, *442*, 368-373.

[75] Fontana, F.; Ferreira, M. P. A.; Correia, A.; Hirvonen, J.; Santos, H. A. “Microfluidics as a cutting-edge technique for drug delivery applications.” *J. Drug Deliv. Sci. Technol.* **2016**, *34*, 76-87.

[76] Teh, S. Y.; Lin, R.; Hung, L. H.; Lee, A. P. “Droplet microfluidics.” *Lab Chip* **2008**, *8*, 198-220.

[77] Wang, J. T.; Wang, J.; Han, J. J. “Fabrication of Advanced Particles and Particle-Based Materials Assisted by Droplet-Based Microfluidics.” *Small* **2011**, *7*, 1728-1754.

[78] Chen, P. W.; Erb, R. M.; Studart, A. R. “Designer Polymer-Based Microcapsules Made Using Microfluidics.” *Langmuir* **2012**, *28*, 144-152.

[79] Chou, W. L.; Lee, P. Y.; Yang, C. L.; Huang, W. Y.; Lin, Y. S. “Recent Advances in Applications of Droplet Microfluidics.” *Micromachines* **2015**, *6*, 1249-1271.

[80] Breger, J. C.; Fisher, B.; Samy, R.; Pollack, S.; Wang, N. S.; Isayeva, I. “Synthesis of "click" alginate hydrogel capsules and comparison of their stability, water swelling, and diffusion properties with that of Ca+2 crosslinked alginate capsules.” *J. Biomed. Mater. Res. Part B* **2015**, *103*, 1120-1132.

[81] Szabo, L.; Gonelle-Gisper, C.; Montanari, E.; Noverraz, F.; Bornet, A.; Buhler, L. H.; Gerber-Lemaire, S. “Cross-Reactive Alginate Derivatives for the Production of Dual Ionic-Covalent Hydrogel Microspheres Presenting Tunable Properties for Cell Microencapsulation.” *ACS Appl. Polym. Mater.* **2019**, *1*, 1326-1333.

[82] Liu, J. W.; Zhang, Y.; Yang, T.; Ge, Y. Q.; Zhang, S.; Chen, Z. P.; Gu, N. “Synthesis, Characterization, and Application of Composite Alginate Microspheres with Magnetic and Fluorescent Functionalities.” *J. Appl. Polym. Sci.* **2009**, *113*, 4042-4051.

[83] Cheng, Y.; Luo, X. L.; Tsao, C. Y.; Wu, H. C.; Betz, J.; Payne, G. F.; Bentley, W. E.; Rubloff, G. W. "Biocompatible multi-address 3D cell assembly in microfluidic devices using spatially programmable gel formation." *Lab Chip* **2011**, *11*, 2316-2318.

[84] Cheng, Y.; Tsao, C. Y.; Wu, H. C.; Luo, X. L.; Terrell, J. L.; Betz, J.; Payne, G. F.; Bentley, W. E.; Rubloff, G. W. "Electroaddressing Functionalized Polysaccharides as Model Biofilms for Interrogating Cell Signaling." *Adv. Funct. Mater.* **2012**, *22*, 519-528.

[85] Fairbanks, B. D.; Schwartz, M. P.; Bowman, C. N.; Anseth, K. S. "Photoinitiated polymerization of PEG-diacrylate with lithium phenyl-2,4,6-trimethylbenzoylphosphinate: polymerization rate and cytocompatibility." *Biomaterials* **2009**, *30*, 6702-6707.

[86] Xu, H. Q.; Casillas, J.; Krishnamoorthy, S.; Xu, C. X. "Effects of Irgacure 2959 and lithium phenyl-2,4,6-trimethylbenzoylphosphinate on cell viability, physical properties, and microstructure in 3D bioprinting of vascular-like constructs." *Biomed. Mater.* **2020**, *15*.

[87] Sasaki, E.; Kurayama, F.; Ida, J. I.; Matsuyama, T.; Yamamoto, H. "Preparation of microcapsules by electrostatic atomization." *J. Electrost.* **2008**, *66*, 312-318.

[88] Nussinovitch, A.; Gershon, Z.; Nussinovitch, M. "Liquid-core hydrocolloid capsules." *Food Hydrocolloids* **1996**, *10*, 21-26.

[89] Chang, H. N.; Seong, G. H.; Yoo, I.-K.; Park, J. K.; Seo, J.-H. "Microencapsulation of recombinant Saccharomyces cerevisiae cells with invertase activity in liquidcore alginate capsules." *Biotechnol. Bioeng.* **1996**, *51*, 157-162.

[90] Gao, M.; Song, H.; Liu, X.; Yu, W.; Ma, X. "Improved quorum sensing capacity by culturing Vibrio harveyi in microcapsules." *J Biosci Bioeng* **2016**, *121*, 406-12.

[91] Bassler, B. L. "Small talk: Cell-to-cell communication in bacteria." *Cell* **2002**, *109*, 421-424.

[92] Jarosz, L. M.; Ovchinnikova, E. S.; Meijler, M. M.; Krom, B. P. "Microbial spy games and host response: roles of a Pseudomonas aeruginosa small molecule in communication with other species." *PLoS Pathog* **2011**, *7*, e1002312.

[93] Williams, P. "Quorum sensing, communication and cross-kingdom signalling in the bacterial world." *Microbiology (Reading)* **2007**, *153*, 3923-3938.

[94] Peleg, A. Y.; Hogan, D. A.; Mylonakis, E. "Medically important bacterial-fungal interactions." *Nat Rev Microbiol* **2010**, *8*, 340-9.

[95] Dhamgaye, S.; Qu, Y.; Peleg, A. Y. “Polymicrobial infections involving clinically relevant Gram-negative bacteria and fungi.” *Cell Microbiol* **2016**, *18*, 1716-1722.

[96] Flemming, H. C.; Wingender, J.; Szewzyk, U.; Steinberg, P.; Rice, S. A.; Kjelleberg, S. “Biofilms: an emergent form of bacterial life.” *Nat Rev Microbiol* **2016**, *14*, 563-75.

[97] Lohse, M. B.; Gulati, M.; Johnson, A. D.; Nobile, C. J. “Development and regulation of single- and multi-species Candida albicans biofilms.” *Nat Rev Microbiol* **2018**, *16*, 19-31.

[98] De Sordi, L.; Muhlschlegel, F. A. “Quorum sensing and fungal-bacterial interactions in Candida albicans: a communicative network regulating microbial coexistence and virulence.” *FEMS Yeast Res* **2009**, *9*, 990-9.

[99] Fourie, R.; Ells, R.; Swart, C. W.; Sebolai, O. M.; Albertyn, J.; Pohl, C. H. “Candida albicans and Pseudomonas aeruginosa Interaction, with Focus on the Role of Eicosanoids.” *Front Physiol* **2016**, *7*, 64.

[100] Holcombe, L. J.; McAlester, G.; Munro, C. A.; Enjalbert, B.; Brown, A. J. P.; Gow, N. A. R.; Ding, C.; Butler, G.; O'Gara, F.; Morrissey, J. P. “Pseudomonas aeruginosa secreted factors impair biofilm development in Candida albicans.” *Microbiology (Reading)* **2010**, *156*, 1476-1486.

[101] Lindsay, A. K.; Hogan, D. A. “Candida albicans: Molecular interactions with Pseudomonas aeruginosa and Staphylococcus aureus.” *Fungal Biol. Rev.* **2014**, *28*, 85-96.

[102] Trejo-Hernandez, A.; Andrade-Dominguez, A.; Hernandez, M.; Encarnacion, S. “Interspecies competition triggers virulence and mutability in Candida albicans-Pseudomonas aeruginosa mixed biofilms.” *ISME J* **2014**, *8*, 1974-88.

[103] Tscherner, M.; Giessen, T. W.; Markey, L.; Kumamoto, C. A.; Silver, P. A. “A Synthetic System That Senses Candida albicans and Inhibits Virulence Factors.” *ACS Synth Biol* **2019**, *8*, 434-444.

[104] Moussa, M.; Ebrahim, W.; Kalscheuer, R.; Liu, Z.; Proksch, P. “Co-culture of the bacterium Pseudomonas aeruginosa with the fungus Fusarium tricinctum induces bacterial antifungal and quorum sensing signaling molecules.” *Phytochem. Lett.* **2020**, *36*, 37-41.

[105] Mountcastle, S. E.; Cox, S. C.; Sammons, R. L.; Jabbari, S.; Shelton, R. M.; Kuehne, S. A. “A review of co-culture models to study the oral microenvironment and disease.” *J. Oral Microbiology* **2020**, *12*, 12.

[106] Ranjan, A.; Dongari-Bagtzoglou, A. “Tipping the Balance: C. albicans Adaptation in Polymicrobial Environments.” *J Fungi (Basel)* **2018**, *4*.

[107] Hall, R. A.; Turner, K. J.; Chaloupka, J.; Cottier, F.; De Sordi, L.; Sanglard, D.; Levin, L. R.; Buck, J.; Muhlschlegel, F. A. “The quorum-sensing molecules farnesol/homoserine lactone and dodecanol operate via distinct modes of action in Candida albicans.” *Eukaryot Cell* **2011**, *10*, 1034-42.

[108] Hogan, D. A.; Vik, A.; Kolter, R. “A Pseudomonas aeruginosa quorum-sensing molecule influences Candida albicans morphology.” *Mol Microbiol* **2004**, *54*, 1212-23.

[109] Sudbery, P. E. “Growth of Candida albicans hyphae.” *Nat Rev Microbiol* **2011**, *9*, 737-48.

[110] Suvarna, S.; Dsouza, J.; Ragavan, M. L.; Das, N. “Potential probiotic characterization and effect of encapsulation of probiotic yeast strains on survival in simulated gastrointestinal tract condition.” *Food Sci Biotechnol* **2018**, *27*, 745-753.

[111] Rhoads, M. K.; Hauk, P.; Gupta, V.; Bookstaver, M. L.; Stephens, K.; Payne, G. F.; Bentley, W. E. “Modification and Assembly of a Versatile Lactonase for Bacterial Quorum Quenching.” *Molecules* **2018**, *23*.

[112] Recht, M. I.; Douthwaite, S.; Puglisi, J. D. “Basis for prokaryotic specificity of action of aminoglycoside antibiotics.” *Embo J.* **1999**, *18*, 3133-3138.

[113] Lund, P.; Tramonti, A.; De Biase, D. “Coping with low pH: molecular strategies in neutralophilic bacteria.” *FEMS Microbiol Rev* **2014**, *38*, 1091-125.

[114] Tanner, R. S.; James, S. A. “Rapid bacterialside effect of low pH against Pseudomonas-Aeruginosa.” *J. Indust. Microbiol.* **1992**, *10*, 229-232.

[115] Ullah, A.; Chandrasekaran, G.; Brul, S.; Smits, G. J. “Yeast adaptation to weak acids prevents futile energy expenditure.” *Front Microbiol* **2013**, *4*, 142.

[116] Falk, N. A. “Surfactants as Antimicrobials: A Brief Overview of Microbial Interfacial Chemistry and Surfactant Antimicrobial Activity.” *J Surfactants Deterg* **2019**, *22*, 1119-1127.

[117] Lyon, J. P.; dos Santos, F. V.; de Moraes, P. C.; Moreira, L. M. “Inhibition of virulence factors of Candida spp. by different surfactants.” *Mycopathologia* **2011**, *171*, 93-101.

[118] Pietsch, F.; Heidrich, G.; Nordholt, N.; Schreiber, F. “Prevalent Synergy and Antagonism Among Antibiotics and Biocides in Pseudomonas aeruginosa.” *Front Microbiol* **2020**, *11*, 615618.

[119] Anaukwu, C. G.; Ezemba, C. C.; Anakwenze, V. N.; Agu, K. C.; Nwankwegu, A. S.; Okeke, B. C.; Awah, N. S. “Influence of anionic, cationic and non-ionic surfactants on growth of hydrocarbon utilizing bacteria.” *AJCMicrob* **2016**, *4*.

[120] Eskelinen, E. L.; Tanaka, Y.; Saftig, P. “At the acidic edge: emerging functions for lysosomal membrane proteins.” *Trends Cell Biol.* **2003**, *13*, 137-145.

[121] Islinger, M.; Grille, S.; Fahimi, H. D.; Schrader, M. “The peroxisome: an update on mysteries.” *Histochem. Cell Biol.* **2012**, *137*, 547-574.

[122] Titorenko, V. I.; Rachubinski, R. A. “The life cycle of the peroxisome.” *Nat. Rev. Mol. Cell Biol.* **2001**, *2*, 357-368.

[123] Bakkergrunwald, T.; Vandam, K. “Mechanism of activation of ATPase in chloroplasts.” *Biochim. Biophys. Acta* **1974**, *347*, 290-298.

[124] Buchanan, B. B. “Role of light in the regulation of chloroplast enzymes.” *Annu. Rev. Plant Physiol. Plant Molec. Biol.* **1980**, *31*, 341-374.

[125] Mou, C. L.; Wang, W.; Li, Z. L.; Ju, X. J.; Xie, R.; Deng, N. N.; Wei, J.; Liu, Z.; Chu, L. Y. “Trojan-Horse-Like Stimuli-Responsive Microcapsules.” *Adv Sci* **2018**, *5*, 1700960.

[126] Barb, W. G.; Baxendale, J. H.; George, P.; Hargrave, K. R. “Reactions of Ferrous and Ferric Ions With Hydrogen Peroxide.” *Nature* **1949**, *163*, 692-694.

[127] Scheja, S.; Domanskyi, S.; Gamella, M.; Wormwood, K. L.; Darie, C. C.; Poghossian, A.; Schoning, M. J.; Melman, A.; Privman, V.; Katz, E. “Glucose-Triggered Insulin Release from Fe3+-Cross-linked Alginate Hydrogel: Experimental Study and Theoretical Modeling.” *ChemPhysChem* **2017**, *18*, 1541-1551.

[128] Arya, C.; Oh, H.; Raghavan, S. R. “"Killer" Microcapsules That Can Selectively Destroy Target Microparticles in Their Vicinity.” *ACS Appl. Mater. Interfaces* **2016**, *8*, 29688-29695.

List of Publications

Publications:

1. Ahn, S. H.; Rath, M.; Tsao, C. Y.; Bentley, W. E.; Raghavan, S. R. "Single-Step Synthesis of Alginate Microgels Enveloped with a Covalent Polymeric Shell: A Simple Way to Protect Encapsulated Cells." *ACS Appl. Mater. Interfaces* **2021**, *13*, 18432-18442.

2. Gargava, A.; Ahn, S.; Bentley, W. E.; Raghavan, S. R. "Rapid Electroformation of Biopolymer Gels in Prescribed Shapes and Patterns: A Simpler Alternative to 3-D Printing." *ACS Appl. Mater. Interfaces* **2019**, *11*, 37103-37111.

Manuscripts in Preparation:

1. Ahn S. H.; Karlsson A. J.; Bentley W. E.; and Raghavan S. R. "Capsules with Bacteria and Fungi in Distinct Organelles: A Platform for Studying Microbes from Different Kingdoms and their Crosstalk." *Manuscript in preparation* (2021)

2. Ahn S. H.; Subraveti N.S.; Bentley W. E.; and Raghavan S. R. "Multicompartment Capsules with Individual Compartments Sensitive to Distinct Stimuli (enzyme, hydrogen peroxide, light)." *Manuscript in preparation* (2021)

List of Presentations

1. Ahn S. H.; Karlsson A. J.; Bentley W. E.; and Raghavan S. R. "Multi-compartment capsules (MCCs) with bacteria and fungi in distinct compartments: A platform for studying cross-kingdom signaling," 95th Colloid and Surface Science Symposium, June 14-16, 2021.

2. Ahn S. H.; Bentley W. E.; and Raghavan S. R. “Synthesis of alginate microgels with a polymer shell: A simple way to protect encapsulated cells,” 2020 Virtual MRS Spring/Fall Meeting & Exhibit

3. Ahn S. H.; Bentley W. E.; and Raghavan S. R. “A clock like hydrogel that visually indicates time,” 2020 Virtual MRS Spring/Fall Meeting & Exhibit

4. Ahn S. H.; Bentley W. E.; and Raghavan S. R. “Single-step Synthesis of Alginate Microbeads with Polymer Shell,” Mid-Atlantic Soft Matter Workshop (MASM 21), February 2019, Rockville, MD, USA

5. Ahn S. H.; Bentley W. E.; and Raghavan S. R. “Single-step synthesis of alginate capsules coated with a polymer shell: improved mechanical stability and protection of encapsulated cells,” American Chemical Society Annual Conference, March 2019, FL, USA